UNIVERSITY OF CALIFORNIA SAN DIEGO

Some Like It Cool: A study of odontocete ecology in the Hawaiian Islands using passive acoustic monitoring

A dissertation submitted in partial satisfaction of the requirements for the degree Doctor of Philosophy

in

Marine Biology

by

Morgan Adair Ziegenhorn

Committee in charge:

Simone Baumann-Pickering
John Hildebrand
Andrew Barton
Kaitlin Frasier
Jennifer MacKinnon
James Nieh

2022

The Dissertation of Morgan Adair Ziegenhorn is approved, and it is accepted in quality and form for publication on microfilm and electronically:

University of California San Diego

2022

DEDICATION

to my family and friends, and everyone else who has helped along the way

EPIGRAPH

All information looks like noise until you break the code.

-- Neal Stephenson

Doors are very powerful things. Things are different on either side of them.

-- Dianna Wynne Jones

TABLE OF CONTENTS

LIST OF SUPPLEMENTAL FILES

Chapter 2

S2 Table. Recording Schedule. Recording schedule for all deployments. For one deployment, duty cycle was inconsistent due to a system malfunction (noted by '*'). Depth given as seafloor depth at deployment location, to nearest 10 meters. Deployments with 25 kHz crossover between low and high frequency hydrophones are bolded.

S2 File. Supporting Information for Click Type Validation. Information from relevant previous studies used to validate the attribution of click types in this study to known species or species groups.

Chapter 3

S3 File. Supplementary Information. File of all supplementary information for chapter 3, including

- **Appendix S3.1:** Recording schedule for deployments from all sites
- **Appendix S3.2:** Seasonal species composition for each site
- **Appendix S3.3:** Full timeseries of presence at each site

Chapter 4

S4 Table. Recording schedule. Recording schedule for deployments from all sites. Deployments with a 25 kHz crossover between the low and high frequency hydrophones have been bolded. Lines in-between rows represent different sites, including Manawai subsites 1-2.

LIST OF FIGURES

LIST OF TABLES

ACKNOWLEDGEMENTS

I would not have made it here without the help of so many friends, family, mentors, collaborators, funders, fellow SIO students, and dogs. I would like to thank especially my unofficial committee members Erin Oleson and Robin Baird, who were coauthors on my dissertation work and provided endless valuable insights into doing science and the Hawaiian Islands. Thank you to the entire science crew of the 2020 WHICEAS Cruise, and especially to Jennifer McCullough, Erik Norris, and Pina Gruden for providing awesome scientific role models at a truly pivotal point during my PhD research. Thank you to the members of the SeaTech program, with whom I've had so much fun these past couple of years. I would also like to thank the teachers (formal and otherwise) that I've had throughout my life, especially in my formative years, who taught me to love both science and writing, and always encouraged me to think for myself, work hard, and to have fun doing it whenever possible. I would also like to thank my family, especially my parents, siblings, and my grandma who have been my most vocal cheerleaders for my entire life. Special thanks to my mom for many discussions about my work during runs, hikes, and kayak trips, and to Alyssa for sitting through many, many phone calls. I love all of you.

Friends from elementary school, high school, college, and graduate school have also been a huge part of my support system throughout this journey. Huge thanks to all of you, and especially to my cohort of Biological Oceanography students at SIO—I love you so much, and I hope we can celebrate soon. I would not have made it to graduate school at all without the UC Berkeley Mo'orea class of 2015, where I learned so much and made so

many memories, published my first scientific paper, and met my best friends and the love of my life. Kyle, you (and Kodiak) deserve an honorary PhD for keeping me afloat for the past five years. I can't wait to marry you.

This work would also not have been possible without my many friends and mentors within the Scripps Whale Acoustic Lab, Scripps Acoustic Ecology Lab, and Scripps Machine Listening Lab. Our lab group is full of some of the best scientists I think anyone could possibly hope to work with. Thank you to everyone who keeps the data coming in and going out, and especially to Bruce, Hurwitz, Ally, Jenny, Erin, Shelby, Sean, Kieran, Nic, Beve, Macey, and so many others!!! Thank you to my advisors John and Simone for supporting me in so many ways and teaching me about being a scientist and an adult on many occasions. Thank you to my mentor and friend Kait Frasier for everything you've done for me so far, for your patience and understanding, and for always being a listening ear. You absolutely rock. Finally, thank you to the many wonderful graduate students and postdocs (past and present) in our lab group who kept me going day-to-day, asked and answered so many interesting questions, pushed me to be my best, and forgave me when I wasn't. I would also like to thank my summer 2022 intern Renea Briner, whose work did not contribute to my dissertation, but whose attitude and spirit really kept me going in the final months of this program. I want to send a special thanks, and much love, to Natalie Posdaljian and Vanessa ZoBell for keeping the vibe up over Slack for the past two years, and for being such wonderful friends. Lastly, I want to thank Rebecca Cohen for her mentorship, encouragement, friendship, and collaboration on projects for basically my whole PhD. This work is so much better for your influence. That goes for all of you. ☺

Chapter 2, in full, is a reprint of the material as it appears in PLOS One, Ziegenhorn, Morgan A., Kaitlin E. Frasier, John A. Hildebrand, Erin M. Oleson, Robin W. Baird, Sean M. Wiggins, and Simone Baumann-Pickering. "Discriminating and classifying odontocete echolocation clicks in the Hawaiian Islands using machine learning methods." *PloS one* 17, no. 4 (2022): e0266424. The dissertation author was primarily responsible for the investigation and writing of this material.

Chapter 3, in full, is in preparation for publication of the material (Global Ecology and Biogeography). Ziegenhorn, Morgan A., John A. Hildebrand, Erin M. Oleson, Robin W. Baird, Sean M. Wiggins, and Simone Baumann-Pickering. "Odontocete spatial patterns and temporal drivers of detection at sites in the Hawaiian Islands." The dissertation author was primarily responsible for the investigation and writing of this material.

Chapter 4, in full, is in preparation for publication of the material. Ziegenhorn, Morgan A., John A. Hildebrand, Erin M. Oleson, Robin W. Baird, and Simone Baumann-Pickering. "Oceanographic conditions as indicators of odontocete detection in the Hawaiian Archipelago." The dissertation author was primarily responsible for the investigation and writing of this material.

VITA

2016 Bachelor of Arts, University of California, Berkeley

Major: Integrative Biology
Minor: Creative Writing

2020 Master of Science, University of California San Diego

2022 Doctor of Philosophy, University of California San Diego

SELECTED PUBLICATIONS

Ziegenhorn, M.A., Frasier, K.E., Hildebrand, J.A., Oleson, E.M., Baird, R.W., Wiggins, S.M., Baumann-Pickering, S. 2022. "Discriminating and classifying odontocete echolocation clicks in the Hawaiian Islands using machine learning methods". *PLoS ONE*

Merkens, K., Baumann-Pickering, S., **Ziegenhorn, M. A.,** Trickey, J. S., Allen, A. N., & Oleson, E. M. (2021). "Characterizing the Long-Term, Wide-Band and Deep-Water Soundscape Off Hawai'i ." *Frontiers in Marine Science*

FIELDS OF STUDY

Major Field: Biological Oceanography

Studies in Marine Bioacoustics
Professors Simone Baumann-Pickering and John Hildebrand

ABSTRACT OF THE DISSERTATION

Some Like It Cool: A study of odontocete ecology in the Hawaiian Islands using passive acoustic monitoring

by

Morgan Adair Ziegenhorn

Doctor of Philosophy in Marine Biology

University of California San Diego, 2022

Professor Simone Baumann-Pickering, Co-Chair
Professor John Hildebrand, Co-Chair

Studies of marine mammals using passive acoustic monitoring (PAM) tools are becoming more and more common. This methodology allows for documentation of biologically relevant factors such as movement patterns or animal behaviors while remaining largely non-invasive and cost effective. In the Hawaiian Islands, a set of PAM recordings covering the frequency band of most toothed whale (odontocete) echolocation

clicks were collected from 2008-2019 at sites off the islands of Hawai‘i, Kaua‘i, and Pearl and Hermes Reef (otherwise known as ‘Manawai’). However, due to the size of this dataset and the complexity of species-level acoustic classification, multi-year, multi-species analyses had not yet been completed. In this dissertation, a machine learning toolkit was used to effectively mitigate this problem by detecting and classifying echolocation clicks using a combination of unsupervised clustering methods and human-mediated analyses. Classified clicks were distilled into timeseries of species’ presence in order to document, and propose reasons for, observed patterns. Habitat modelling employing Generalized Additive Models (GAMs) with and without Generalized Estimating Equations (GEEs) was used to elucidate these trends in combination with oceanographic variables. The machine learning pipeline used distilled eight unique echolocation click types, attributable to eight or more species of odontocetes. Species composition differed amongst considered sites, and this difference was robust to seasonal movement patterns. Temporally, hour of day was the most significant predictor of detection across species and sites, followed by season. When considered in conjunction with sea surface variables, temperature had the strongest relationship to detections. Of the climate indices considered, El Niño Southern Oscillation (ENSO) may have the most effect on species detections at monitored sites. This study demonstrates that PAM is an invaluable tool in studies of oceanic top predators, and that machine learning tools can mitigate issues related to the size and complexity of PAM datasets. Using these tools and habitat modelling analyses, we can gain valuable insights into top predator behavior in relation to temporal variables, surface conditions, and long-term climate indicators.

Chapter 1: Introduction

1.1 Overview

The Hawaiian Island archipelago serves as a regional oasis in the generally unproductive waters of the North Pacific Subtropical Gyre (1,2). As such, the region can be an attractive habitat for many large ocean predators including odontocetes, or toothed whales. At least 18 unique species of odontocetes reside in the region (3), several stocks of which are island-associated (i.e., remaining close to one or a few closely located islands) (4). Such stocks have a limited geographic range and may be particularly vulnerable to environmental perturbations. Continuous temporal data is crucial in both detailing patterns in these movements as well as understanding drivers of said patterns. However, many previous studies of regional odontocetes have been limited by virtue of their methodology: visual efforts by time of year, temporal constraints, and sighting conditions; acoustic efforts by the recording capabilities of equipment, spatial limitations, and an inability to distinguish species. For the past decade at three Hawaiian sites, a passive acoustic monitoring dataset with recordings covering the frequency band of most odontocete echolocation clicks has been collected by the NOAA Pacific Islands Fisheries Science Center (PIFSC). While some studies have incorporated pieces of this dataset (5–7), the full dataset has not been analyzed in detail for all species present. In this study, we process this data for all recorded echolocation clicks, defining acoustic signals including a novel type description for the echolocation clicks of the rough-toothed dolphin, *Steno bredanensis*. Using defined signals, we create a labelled timeseries that is in turn used to document

patterns of odontocete acoustic presence in space and at a variety of temporal scales. We also employ these timeseries in habitat modeling, which enables comprehension of the relationship of odontocete species to environmental factors that affect primary productivity and eventually odontocete prey. Documenting long-term patterns of odontocete movement and understanding the behavioral, biological, and environmental drivers of these patterns is instrumental for successful stock management and conservation efforts, giving managers a more complete picture of the region and a deeper understanding of the species therein.

1.2 Oceanographic background

A variety of oceanic processes contribute to the high productivity in the vicinity of the Hawaiian Islands that is exploited by odontocetes. In the Main Hawaiian Island chain, high nearshore upwelling (8), regional fronts and leeward eddies (1,9–12), and increased mixing and turbulence in channels between islands encourage primary productivity (8) and subsequently provide rich foraging and reproductive grounds for many odontocete prey species. Nutrient input along coastal areas from frequent rainfall and steep island slopes also promotes the flourishing of odontocete prey; this effect is concentrated nearshore on the windward side of the islands but more dispersed and diluted in the islands' lees due to westerly winds (13). In the Northwestern Hawaiian Islands, the contrast between inshore and offshore production is less marked because of a lack of high islands and eddies, as well as proximity to the Subtropical Convergence Zone (3). However, proximity to the transition zone chlorophyll front near this convergence zone also results in higher productivity and increased abundance of odontocete prey species compared to the

surrounding gyre (14). The heightened production supported by these processes provides prime habitat for odontocete species and causes many species to stick close to the islands. Understanding the oceanographic and climatological base for odontocete presence in the islands aids in the comprehension of their movement patterns over a variety of timescales.

1.3 Passive acoustic monitoring

While visual observations and satellite tagging of odontocetes at sea may readily provide species identification and key behavioral information, studying distributions and movements using such methods can be labor intensive, invasive, and costly. Including passive acoustic monitoring (PAM) in odontocete study and conservation efforts can provide long-term, non-invasive, and cost-effective continuous monitoring of various odontocete species. PAM additionally is not subject to constraints such as variations in sea state, time of day, or weighted towards more conspicuous animals, though stationary PAM recorders have limited spatial range, which requires strategic placement and can be problematic when small-scale movements take animals outside of this range. Echolocation clicks, which are produced by odontocetes for foraging and navigational purposes, are particularly useful in PAM efforts in that certain click types are produced exclusively by a single species and under a wide variety of behavioral states, leading to reliable detection of certain species present within the detection range of the recorder. For this purpose, feature vectors of echolocation clicks are used to discriminate between species, such as the timing between successive clicks in an echolocation click 'train' (inter-click-interval, or ICI), spectral properties including peak frequency and spectral shape, and properties of the

waveform such as number of oscillations, waveform envelope and overall duration. Long-term PAM data has been used in recent years to determine distributions and densities of odontocetes as well as provide crucial information on behaviors from diving and diel foraging patterns to larger patterns of animal movement (15–18). PAM data has also been shown to be sufficient for habitat modeling of a variety of cetacean species (e.g., 17).

Passive acoustic data was collected in the Hawaiian Islands using High Frequency Acoustic Recording Packages (HARPs) (19,20). Deployments used for this study spanned the years 2008-2019 (see S2 Table). Sites for data collection were off the west coast of Hawai‘i Island (henceforth, ‘Hawai‘i’ or ‘Kona’), west of Kaua‘i, and in the vicinity of Manawai (see Fig. 3.1). Data from these sites were recorded at a 200 kHz or 320 kHz sampling frequency (16-bit quantization) at depths ranging from 550-1150 meters (see S2 Table). The data from the three sites combined represents approximately 15 instrument years of recordings. Manual identification of species of interest within such datasets is possible but the significant time investment required puts constraints on the data analysis process. However, in recent years, automated detection and classification of echolocation clicks has facilitated analysis of similar datasets from other regions, resulting in distillation of echolocation click types that can often be attributed to species (e.g., 21–23). These types can then be used to train unsupervised click classifiers, enabling classification of acoustic data at a much faster rate.

1.4 Dissertation outline

The purpose of this study was to identify Hawaiian toothed whale species in acoustic recordings using unsupervised learning algorithms and to use the resulting classifications to explore spatial, temporal, and environmental drivers for observed patterns of species presence. Chapters 2-4 are intended to be stand-alone, publishable scientific papers and as such may contain introductory and methodological redundancies.

In Chapter 1, I introduce the contents of the dissertation with information about the study region. This chapter includes oceanographic background, an introduction to passive acoustic monitoring, and an outline of the dissertation.

In Chapter 2, I establish the predominant types of echolocation clicks found in the dataset, attribute them to species or species groups, and train and test a neural network using these types as input classes. Ten distinct types of echolocation clicks were found, representing 10+ species of odontocetes. These distinctions included a novel type characterization for the rough-toothed dolphin, *Steno bredanensis,* which was validated using additional acoustic and sighting data provided by co-authors. Click types are characterized using spectral peaks and modal inter-click interval values. Neural network performance is evaluated on novel data and discussed in detail.

In Chapter 3, I use the neural-network based classifier developed in Chapter 2 to classify all data as one of the determined click types. I incorporate error rates from the classifier and duty-cycle regimes to develop a timeseries of presence for each existing type. Species composition amongst sites is variable, but markedly consistent across seasons. Stenellid dolphins (i.e., striped dolphin, *Stenella attenuata,* spinner dolphin, *S. longirostris,* and Pantropical spotted dolphin, *S. coreabuloabla)* are most common at Hawai‘i, rough-

toothed dolphins at Kaua‘i, and beaked whales (i.e., Blainville’s beaked whale, *Mesoplodon densirostris,* and Cuvier’s beaked whale, *Ziphius cavirostris*) are most common at Manawai subsites. Generalized Additive Models with Generalized Estimating Equations (GAMs with GEEs) are used to examine temporal trends in presence. Diel patterning is the most important temporal predictor across species and sites, followed by season. Long-term (i.e., multi-year) patterns at Hawai‘i are notably similar for a number of species.

In Chapter 4, I investigate relationships between the established timeseries of species acoustic presence and variation in environmental parameters. Variables include surface conditions (i.e., high-frequency fluctuations) of temperature and salinity, height anomaly, and climate indices (i.e., low-frequency fluctuations) of the North Pacific Gyre Oscillation (NPGO), Pacific Decadal Oscillation (PDO), and El Niño Southern Oscillation (ENSO). Patterns of acoustic presence in relation to these variables are considered at a daily level for all species at each site with sufficient presence of that species. Of the surface conditions considered, sea surface temperature has the most impact on species’ patterns, and the directionality of this impact (e.g., higher presence with warmer temperatures or colder temperatures) varies with species and site. Of the climate indices considered, variations in ENSO are the most common relationship. In most cases, presence is higher at the monitoring sites during the negative ENSO phase (i.e., cold phase or La Niña).

Chapter 2: Discriminating and classifying odontocete echolocation clicks in the Hawaiian Islands using machine learning methods

Morgan A. Ziegenhorn[1*], Kaitlin E. Frasier[1], John A. Hildebrand[1], Erin M. Oleson[2], Robin W. Baird[3], Sean M. Wiggins[1], Simone Baumann-Pickering[1]

[1] Scripps Institution of Oceanography, University of California San Diego, La Jolla, CA, USA

[2] NOAA Fisheries Pacific Islands Fisheries Science Center, Honolulu, HI, USA

[3]Cascadia Research Collective, Olympia, WA, USA

2.1 Abstract

Passive acoustic monitoring (PAM) has proven a powerful tool for the study of marine mammals, allowing for documentation of biologically relevant factors such as movement patterns or animal behaviors while remaining largely non-invasive and cost effective. From 2008-2019, a set of PAM recordings covering the frequency band of most toothed whale (odontocete) echolocation clicks were collected at sites off the islands of Hawai‘i, Kaua‘i, and Pearl and Hermes Reef. However, due to the size of this dataset and the complexity of species-level acoustic classification, multi-year, multi-species analyses had not yet been completed. This study shows how a machine learning toolkit can effectively mitigate this problem by detecting and classifying echolocation clicks using a combination of unsupervised clustering methods and human-mediated analyses. Using these methods, it was possible to distill ten unique echolocation click ‘types’ attributable to regional odontocetes at the genus or species level. In one case, auxiliary sightings and recordings were used to attribute a new click type to the rough-toothed dolphin, *Steno bredanensis*. Types defined by clustering were then used as input classes in a neural-network based classifier, which was trained, tested, and evaluated on 5-minute binned data segments. Network precision was variable, with lower precision occurring most notably for false killer whales, *Pseudorca crassidens*, across all sites (35-76%). However, accuracy and recall were high (>96% and >75%, respectively) in all cases except for one type of short-finned pilot whale, *Globicephala macrorhynchus*, call class at Kaua‘i and Pearl and Hermes Reef (recall >66%). These results emphasize the utility of machine learning in analysis of large PAM datasets. The classifier and timeseries developed here will facilitate

further analyses of spatiotemporal patterns of included toothed whales. Broader application of these methods may improve the efficiency of global multi-species PAM data processing for echolocation clicks, which is needed as these datasets continue to grow.

2.2 Introduction

The Hawaiian archipelago creates a regional oasis in the oligotrophic waters of the North Pacific Subtropical Gyre (1,2,24). The area is an attractive habitat for large ocean predators including odontocetes, or toothed whales. At least 18 species of odontocetes reside in the region (3), several of which have island-associated stocks (25). These stocks in particular have limited geographic ranges and may be especially vulnerable to environmental perturbations and anthropogenic impacts (e.g. (25)).

Passive acoustic monitoring (PAM) in odontocete study and conservation efforts can provide long-term, non-invasive, and cost-effective continuous monitoring of these species (e.g., (26–28)). Scientists employ a variety of acoustic recording schemes for PAM monitoring, including various bottom-moored hydrophones systems (26,29) and shipboard studies using towed acoustic arrays with combined visual observations (30,31). Bottom-moored equipment has the advantage of continuous recording over long time periods, but can suffer from difficulties in distinguishing species, resulting in few multi-species analyses. Towed array studies can cover a spatially diverse range, often with species verification, but are usually temporally limited due to factors including weather and the cost of ship time. These efforts can include analyses of a variety of animal signals

including tonal vocalizations (e.g., whistles (26,32)) and echolocation clicks, which are produced by odontocetes for foraging and navigational purposes (23,33).

Echolocation clicks are particularly useful in PAM as certain click types are produced exclusively by a single species and under a wide variety of behavioral states, resulting in a useable proxy for animal presence. PAM data can be utilized for reliable detection of species for which species-specific echolocation click types have been identified (e.g., (34,35)). For this purpose, feature vectors of echolocation clicks, typically including the timing between successive clicks in an echolocation click 'train' (inter-click-interval, or ICI), spectral properties including peak frequency and spectral shape, and properties of the waveform (e.g., number of oscillations, waveform envelope and overall duration), are used to discriminate between odontocete species using automated algorithms (21).

Long-term PAM data has been used in recent years to determine distributions and densities of odontocetes as well as provide information on behaviors from diving and diel foraging patterns to larger patterns of animal movement (18,26,27,36,37). PAM data has also been shown to be valuable and well-suited for habitat modeling of a variety of cetacean species (38–40). The NOAA Pacific Islands Fisheries Science Center (PIFSC) has been collecting passive acoustic monitoring data with recordings covering the dominant frequency band of most odontocete echolocation clicks (i.e., 5-100 kHz) for the past decade at three Hawaiian sites. While some studies have utilized portions of this dataset (e.g., (5,7)), the full dataset has not been analyzed to identify the full suite of species present.

The ability to detect and classify echolocation clicks within such a large dataset has been limited by the time-intensive nature of the manual classification approaches previously required to derive time series of acoustic presence for a given species. In recent years, machine learning tools have been successfully used in detection and discrimination tasks for a variety of species and ocean basins (e.g., (26,41,42)). Deep neural networks (e.g., (43,44)), random forests (e.g., (45,46)), and clustering algorithms (e.g., (47,48)), as well as a variety of other classification regimes, have all been used for these purposes. Amongst these techniques, unsupervised clustering (e.g., (21,23)) in particular can expedite the processing of echolocation clicks in large PAM datasets by allowing for the automated distillation of dominant signal types. These methods make use of click features to cluster similar clicks and present an opportunity to identify both known and novel signals. These signals can then be attributed to species using literature records of echolocation clicks and auxiliary data such as sighting records, tag data locations, or towed acoustic array data with concurrent visual observations (22). Attribution of echolocation clicks to species in this way facilitates development of large training sets for species identification. This method has been used successfully to analyze data from the Gulf of Mexico (21) for a variety of species but has not yet been applied to the Hawaiian Islands region. Once derived, these types can be used as input classes to build a neural-network based classifier that can be run on novel data and hence expedite analyses of large acoustic datasets (49).

Some species of odontocetes present in the Hawaiian Islands region, such as Cuvier's beaked whale, *Ziphius cavirostris,* and Blainville's beaked whale, *Mesoplodon*

densirostris, produce echolocation clicks which have already been described in the literature (35), while others remain acoustically uncharacterized. Even when clicks have been described, limitations of available classification methods in correctly identifying the whole suite of species' clicks hinders processing of datasets for the full repertoire of local species at once, especially when signals are highly similar. For some species or species groups, such as beaked whales and *Kogia* spp., disparate detectors have been used to successfully identify and study target species (e.g., (50,51)). In this study, machine learning methods were used for signal discovery, detection, and classification of Hawaiian Islands regional PAM data, resulting in a comprehensive library of the dominant echolocation click types present at three monitoring sites. A neural network-based classifier was then developed and used to classify clicks across the entirety of this dataset, facilitating future regional studies of included species. The tools used here improve upon previous methodologies by allowing for a single detection step and classification workflow for all included species, expediting data processing. Additionally, the methodology employed is malleable in that the classifier learns from the data itself instead of using heuristics defined by other researchers, often in differing ocean basins, to define types.

2.3 Methods

2.3.1 Data collection

Passive acoustic data were collected using bottom-moored High-frequency Acoustic Recording Packages (HARPs) (19) consisting of one or more hydrophones, logging equipment, batteries, and flotation. The majority of the deployments used in this

study utilized a system consisting of a low-frequency and a high-frequency hydrophone, with the crossover between the two occurring at either 2 or 25 kHz depending on the deployment (S2 Table). Crossover frequency is important to note as changes in sensitivity at the crossover frequency can affect analyses. In all cases, sensors were connected to custom-built preamplifiers and bandpass filters. Frequency-dependent sensitivity of representative systems was calibrated at the Navy's Transducer Evaluation Center (TRANSDEC). Locations of specific deployments varied slightly due to the difficulty of at-sea deployment of seafloor moorings.

Data from three recording sites were included in this study: one off the west side of Hawai‘i Island (henceforth referred to as Kona), one off the western side of Kaua‘i, and one on the northern side of Manawai (also known as Pearl and Hermes Atoll and henceforth referred to as PHR) (Fig 2.1; S2 Table). Deployment setup varied at these sites in terms of recording schedule, instrument depth, and duty cycle regime (S2 Table). Duty cycling refers to alternating periods of recording and non-recording (e.g., recording of 5 minutes out of every 25-minute period) to extend battery life and allow for longer deployments. Data from these sites were recorded at a 200 kHz or 320 kHz sampling frequency and 16-bit quantization at depths ranging from 550-1150 meters (S2 Table). All hydrophones were buoyed approximately 10-30 meters from the seafloor. The data from the three sites combined represents approximately 15 instrument years of recordings (S2 Table).

2.3.2 Data processing

2.3.2.1 Click detection

Odontocete echolocation clicks were detected using an energy detector that ran as an added package of the MATLAB-based software program *Triton* (52). This detector first determined periods for which acoustic energy in a frequency band of interest exceeded a user-defined threshold, then searched those time periods for impulsive signals that met several criteria characterizing odontocete echolocation clicks. The underlying mechanics of the detector are described in Frasier et al. (2017) and in Frasier, K.E. (2021) in more detail. Specifications for this detector included application of a high pass filter at 10 kHz to exclude low frequency noise sources. A low pass filter was set at 100 kHz, regardless of sampling frequency, to simplify clustering and neural network steps. Additionally, a peak-to-peak amplitude threshold of 115 dB_{pp} re 1 µPa was set after manual review of a subset of the data determined that this was an acceptable threshold to consistently detect a majority of odontocete clicks while excluding most low amplitude impulsive signals from ships and other noise sources. Signal duration was used to exclude non-target signals; only detections between 30-1200 µs in duration were retained, and detections with less than 100 µs of separation were merged. Features of retained clicks including time and date, peak-to-peak received level, and frequency spectra were stored for subsequent analyses. Frequency spectra were calculated using a 400-point (sampling frequency fs = 200 kHz) or 640-point (fs = 320 kHz) FFT of Hanning-windowed data centered on the click peak amplitude.

2.3.2.2 Unsupervised clustering methods and click type identification

Detected impulsive signals were separated into distinct types via a two-step clustering method. At this point, a minimum received level of 120 dB_{pp} re 1 μPa was set to perform clustering on higher-quality detections. In the first clustering step, data were split into 5-minute bins. Individual detections in each bin that passed the received level threshold were compared against one another and clustered together based on spectral shape (pairwise correlation distance, (53)) using the Chinese Whispers (CW) algorithm (54). This process was iterative, with each detection within a 5-minute bin beginning as a single-node cluster and being iteratively re-assigned to larger, closely related clusters until reassignment ceased (i.e., until all detections were assigned the same label as detections to which they were most strongly connected). Minimum cluster size was set at 50 detections, and maximum network size was set at 10,000 nodes (chosen at random from all detections in the bin) due to computational limitations. A maximum of 15 iterations of this process were completed, though clustering usually ceased before reaching this threshold. The final partition for each bin was chosen based on highest average normalized mutual information (NMI) score (55), which compares clusters across multiple partitions to determine consistency of types.

Though not used as a feature for clustering, ICI distributions were calculated for retained bins for use in later classification steps. These distributions were calculated for each cluster found in a 5-minute bin by calculating the timing between successive detections in that cluster, with distributions being truncated at 0.6 seconds. This value was inclusive of known modal inter-click interval values for target odontocete species. ICI distribution shape and modal ICI values were used in later evaluation steps instead of 'raw'

ICI values between detections to overcome issues related to recording multiple animals instead of a single individual.

Mean normalized spectra and mean normalized waveform envelope were also calculated for each cluster in every bin. To calculate mean normalized spectra, power spectral density of clicks was computed and converted to a dB scale. These spectra were normalized by setting the minimum amplitude to zero and maximum to one. Normalized spectra were then averaged to determine mean normalized spectra on a dB scale (henceforth 'mean spectra').

In the second step, mean spectra and waveform envelopes determined in the first clustering step were compared across a large subset of the data to determine the dominant detection types in each deployment, again using pairwise distances and the CW algorithm. Thresholds for this step were similar to those used in the first clustering step, though in this case the maximum allowable network size was 20,000 bins, and retained clusters were required to contain a minimum of at least 25 5-minute bins. In this step, 1% of the least-connected nodes were pruned from within each cluster to result in cleaner final clusters. This second clustering step was performed for a total of five trials, with the best partition being chosen automatically based on NMI. More detail on this process can be found in Frasier, K.E. (2021).

Once clusters were determined for each deployment, detected signals were visualized using *LabelVis*, a custom script developed by the author as an add-on package to *Triton* software (52) that allows users to visualize various depictions of the acoustic data overlaid with manually or automatically generated labels. This program is publicly

available on GitHub (56) and allowed for manual examination of timeseries and spectral information for individual clicks from retained clusters to determine which might be combined or discarded. For each deployment, several months of data were examined to be sure that signals contributing to each cluster were distinct from others and not data artifacts. Clusters from a given deployment were determined to be the same if they were spectrally similar, had similar ICI distributions and modal ICI values, and were often concurrently or sequentially present. Some clusters (approximately 7% of total clusters) were alternatively determined to be mixed based on spectral or ICI similarities and high co-occurrence with multiple, distinct types. Such clusters were not grouped into the final types and did not contain any types that weren't also found in non-mixed clusters. Clusters were then compared across deployments and sites and were grouped based on spectral similarity as well as shape of the ICI distribution to determine a final set of echolocation click types, as well as an outgroup of noise detections.

Final echolocation click types were described in terms of frequency and -3 dB bandwidth of their spectral peaks as well as peak ICI values using a subset of clicks from all three sites determined by inspection to be representative of the overall variability in spectra and ICI. Peaks and -3dB bandwidths were found using the main peak of individual click spectra for all available high-quality clicks of a given type (minimum = 2500 clicks). Click quality was determined by manual review, with a focus on removing detections for which spectra were subject to data artifacts. The distribution of these values was plotted and considered in conjunction with mean spectra for the type in order to determine whether or not multiple peaks should be described (i.e., whether the distribution of peak values was

unimodal). ICI distributions were constructed and fit with Gaussian curves to determine the peak ICI value and approximate standard deviation. Where possible based on previous literature, click types were attributed to specific odontocetes at the genus or species level as detailed below.

2.3.2.3 Classifier creation and evaluation

For the purposes of classifier training and testing, the echolocation click types distilled above were used as input classes. An additional 'junk' class containing clusters of detections from noise sources such as ships and echosounders was included to prevent misclassifications of these sources as odontocetes. These noise sources were picked up by the detector due to their commonality in the data, particularly at the Kona site (57), and the similarity of these signals to echolocation clicks. Clusters of sperm whale, *Physeter macrocephalus*, echolocation clicks were also grouped into this 'junk' class due to the difficulty of separating these clicks from high-frequency ship noise as both can occupy the same frequency range between ~5-20 kHz. Additionally, there was a high likelihood of missing many sperm whale clicks beneath the lower end of the 10 kHz bandpass filter employed in click detection.

For each class, 5000 examples (e.g., 5000 bins from each final click type) were chosen at random from the input set and used in the train/test/validation data with a 70/20/10 split. For the class representing Cuvier's beaked whale, input vectors of mean spectra, waveform envelope, and ICI values were augmented with additional example bins from similar data recorded off the coast of Southern California due to a limited number of

observations in the Hawai‘i dataset. Approximately 50% of the final train/test/validation examples for Cuvier’s beaked whale were from this additional dataset. Training, testing, and eventual labelling of novel data was completed at the 5-minute bin level based on groupings made in the first step of the clustering algorithm, i.e., all clicks clustered as one ‘type’ at the 5-minute bin level received the same label from the network. Labelling at this level allowed for the inclusion of ICI distribution as an input feature and tends to lead to higher classification accuracy (49). Where the total number of example bins was less than 5000, existing examples were chosen at random and data were augmented to create “new” examples for the classifier to learn from. For mean spectra and waveform envelope, low-amplitude Gaussian white noise was generated and added to existing examples to create these “new” examples. For ICI, data points were augmented via addition of random values selected from a distribution generated from original input ICI values.

Click features used in network training were ICI distribution, spectral shape, and waveform envelope. A single classifier was developed using data from all sites. The network itself was compiled using an add-on package of *Triton* (52) that allows the user to construct a deep feed-forward neural network with user-specified parameters such as total number of epochs, size and number of hidden layers, and dropout rate. Networks with variations in the above parameters were compiled and evaluated based on accuracy for each type as well as confusion amongst types in both the training and testing sets. The top three networks were chosen from these based on minimizing confusion and maximizing accuracy across types. These networks were evaluated based on performance on novel data compared to manual labelling of that data. Novel data were chosen as a pseudo-random

subset of all available data, and manual labelling of this dataset was completed using *DetEdit*, a graphical user interface for annotating acoustic events (58).

Performance was evaluated based on the accuracy, precision, misclassification rate, specificity (proportion of true negatives), and recall of each network to each class both at individual sites as well as the three sites combined. A final network was chosen based on highest accuracy, recall, and precision values across types and sites (Eq. 1-2). For the final chosen network, additional comparisons of network results versus manually labelled data were undertaken so that final performance metrics would cover the widest number of months and years possible at each site. Only bins containing clicks with a received level above 125 dB_{pp} re 1 µPa were considered in this final evaluation to account for differing sensitivities across hydrophones and sites. Performance on the novel data was again evaluated using accuracy, recall, and precision (Eq. 1-3). These metrics were evaluated by class and by site, as well as for all sites combined.

$$Accuracy = \frac{true\ positives + true\ negatives}{all\ detections} \quad (1)$$

$$Recall = \frac{true\ positives}{true\ positives + false\ negatives} \quad (2)$$

$$Precision = \frac{true\ positives}{true\ positives + false\ positives} \quad (3)$$

Resulting classifications on the full dataset were used to provide relative acoustic presence estimates of each class at each site, to bolster species or genus assignments via comparison with established sighting, tag, and acoustic records. All detections, including those from mixed clusters, received a label in this analysis step. Relative acoustic presence

estimates were calculated per deployment as the percentage of recording days with presence of a given type. Final relative acoustic presence was then calculated by taking the average percent of odontocete presence attributable to a class across deployments at a site.

2.3.2.4 Auxiliary data sources and type classification

For echolocation click type distilled in the clustering process without clear assignments from previous literature, additional data sources were included in analyses in an attempt to assign these types to species. Towed array data available from the NOAA Hawaiian Islands Cetacean and Ecosystem Assessment Survey (HICEAS) 2017 cruise (59) around the Hawaiian Islands was used in this process. This dataset consisted of visual sightings of animals in conjunction with concurrent acoustic recordings, allowing bioacoustic signals to be reliably matched to species. Acoustic data from this cruise was collected using two 3-channel hydrophone arrays connected by 100 meters of cable, towed 300 meters behind the ship. The same detector used on the HARP data was used again on this acoustic data to examine clicks present during encounters where relevant species (i.e., rough-toothed dolphins, *Steno brednanesis,* common bottlenose dolphins (hereafter referred to as bottlenose dolphins), *Tursiops truncatus*, melon-headed whales, *Pepnocephala electra,* striped dolphins, *Stenella coeruleoalba,* pantropical spotted dolphins, *Stenella longirostris,* and spinner dolphins *Stenella attenuata*) were sighted. False positive detections during these encounters were removed using *DetEdit*. Concatenated and mean spectra were then calculated for these encounters for comparison to the potential click type.

Additional support for click type assignment was obtained from sighting data from the region of the Kona and Kaua‘i HARPs, obtained through boat-based sighting efforts (3). When sightings occurred near HARP locations, recorded clicks may be attributable to concurrently sighted animals. Sightings were assessed for any detections of relevant species that occurred within a 10 km radius of the HARPs. Sightings within this distance and within two hours of echolocation clicks labelled as the unknown click type were assessed for viability of providing a match based on the distance from the HARP and the time offset between the sighting and the acoustic encounter.

2.4 Results

2.4.1 Type classification

The click detection and clustering process resulted in ten echolocation click types, presumably representing ten or more species: false killer whale, *Pseudorca crassidens,* low-frequency 1 (LF1, possibly rough-toothed dolphin), short-finned pilot whale, *Globicephala macrorhynchus* (two click types), bottlenose dolphin/melon-headed whale, Blainville’s beaked whale, Cuvier’s beaked whale, stenellid dolphins (two click types), and dwarf (*Kogia sima*) or pygmy (*K. breviceps*) sperm whale (pooled as *Kogia* spp). Descriptive statistics for each type are provided in Table 2.1. Information on validation data used to attribute types to species is provided in Table 2.2. Available data for validation included previous acoustic records, spatial distributions (including abundance information), temporal behavior studies, and auxiliary sighting/acoustic data.

2.4.1.1 A - False killer whale

The false killer whale echolocation click type was described by a single spectral peak at 16.5 kHz with -3 dB bandwidth of 6.5 kHz. The ICI distribution for this click type was bimodal, with a first peak at 28.4 ms and a second peak at 166 ms (Table 2.1, Fig 2.2A). The first peak in ICI was determined to be a result of multiple animals clicking at the same time, as well as single animals approaching a target. Labels of this type matched well with the encounters used for acoustic discrimination of false killer whales in Baumann-Pickering et al. (2015). For this type, acoustic presence determined from automated labelling was recalculated via manual checking of all false killer whale labels after manual review of labels revealed that many noise detections were being incorrectly labelled as this type. Final type assignment was based on previous acoustic and spatial records (Table 2.2, S2 File).

2.4.1.2 B - Low-frequency type 1 (LF1) - possible rough-toothed dolphin

The LF1 click type was described by a single spectral peak at 22.0 kHz with a -3 dB bandwidth of 5.5 kHz. The ICI distribution for this type had a single peak at 169 ms (Table 2.1, Fig 2.2B). This class did not match any well-established records of echolocation clicks, or have a match within click type 'libraries' previously produced using these clustering methods in other regions (21,60–62). However, the peak frequency and -3 dB bandwidth of this type were very similar to the limited previous descriptions of clicks of the rough-toothed dolphin (63). This species has one of the highest abundance estimates of any in the Hawaiian Islands (64). Additionally, small boat surveys over the

course of 2000-2012 found >25% of all sightings of cetaceans near Kaua‘i, where LF1 is most common (present 83% of recording days), were attributable to rough-toothed dolphin (3). This type was less common at the Kona and PHR sites (acoustically present 40% of days in both cases). This general trend (most common near Kaua‘i) is reflected in the sighting record of rough-toothed dolphins, in which this species represents only ~10% of sightings leeward of Hawai‘i Island (3). Less data is available in the vicinity of PHR, though the species has been sighted previously in the area (64). Recently updated habitat-based density models for Hawaiian odontocetes suggest that the locations of the Kaua‘i and PHR HARPs are within predicted regions of highest density for the rough-toothed dolphin (65). Preliminary exploration into diel trends in this type revealed an overwhelming decrease in acoustic activity during daylight hours, which fits with a recent study of rough-toothed dolphin diving behavior that has suggested the species is more active during dusk/night (66).

Labelled towed array data from HICEAS 2017 supported the hypothesis that LF1 was a rough-toothed dolphin click type. Four acoustic encounters with visually verified rough-toothed dolphins were compared to LF1 clicks to determine the suitability of this classification. The mean spectra from these encounters were compared to the type spectrum for LF1, and found to be a fairly consistent match across all encounters, though the mean spectra for encounter 1 had a higher-frequency peak and less content in the band from 20-30 kHz when compared to the type example and other encounters (Fig 2.3). It is notable that a spectral ‘notch’ existed in the towed array data at about 50 kHz. This notch

was determined to be an artifact of the data and not related to the clicks presented here due to its persistence across the dataset (Fig 2.4).

2.4.1.3 C - Short-finned pilot whale

Two click types in the data were likely attributable to the short-finned pilot whale. The first of these types was characterized by two spectral peaks, one at 13.0 kHz, and a more dominant peak at 28.0 kHz. For these peaks, -3 dB bandwidths were 1.5 and 5.0 kHz respectively. The peak ICI for this type was 184 ms (Fig 2.2C1, Table 2.1). The second type was characterized by three spectral peaks: two more minor peaks at 13.0 and 18.5 kHz, and one higher amplitude peak at 48.5 kHz. In this case, -3 dB bandwidths were 1.5, 3.0, and 3.0 kHz, respectively. This type had a peak ICI of 206 ms (Fig 2.2C2, Table 2.1). An attempt was made to group these types together under one 'short-finned pilot whale' class for neural network training and testing purposes; however, classifier performance was improved by leaving the two types as separate classes. Validation for this type description was provided by previous acoustic records and spatial distribution data (Table 2.2, S2 File).

2.4.1.4 D – Bottlenose dolphin and Melon-headed whale

The combined bottlenose dolphin and melon-headed whale (Tt/Pe) echolocation click type was characterized by a dominant peak at 32.5 kHz with a -3 dB bandwidth of 5.5 kHz and an often-present lower frequency peak at 12.5 kHz with a -3 dB bandwidth of 1.5 kHz. Peak ICI for this type was 109 ms (Fig 2.2D, Table 2.1). It is worth noting that

the lower frequency peak was likely the result of residual energy from whistles that often accompany echolocation clicks of this type. Validation for this mixed type was provided by previous acoustic records, spatial distribution data, and temporal behavior records (Table 2.2, S2 File).

2.4.1.5 E - Blainville's beaked whale

The Blainville's beaked whale echolocation click type was characterized by a dominant higher-frequency peak at 36.0 kHz with a -3 dB bandwidth of 9.0 kHz and a minor, not always present, lower-frequency peak at 24.0 kHz with a -3 dB bandwidth of 2.5 kHz. This click type had a peak ICI of 319 ms (Fig 2.2E, Table 2.1). The type was determined to be Blainville's beaked whale based on previous acoustic records and spatial distribution data (Table 2.2, S2 File).

2.4.1.6 F - Cuvier's beaked whale

The Cuvier's beaked whale echolocation click type was characterized by a dominant peak at 40.0 kHz and lower-amplitude spectral peaks at 17.0 and 24.0 kHz (Fig 2.2F, Table 2.1). This click type had a peak ICI of 433 ms. This type distinction was validated using previous acoustic and spatial distribution records (Table 2.2, S2 File).

2.4.1.7 G - Stenellids

The stenellid echolocation click type was defined by spectral peaks at 18.5 and 50 kHz, with a peak ICI of 48.5 ms (Fig 2.2G1, Table 2.1). The lower frequency spectral

peak in this type was likely the result of residual energy from underlying whistles. A second type of stenellid clicks was identified in this dataset (Fig 2.2G2, Table 2.1), defined by spectral peaks at 25.0 and 39.5 kHz, with a peak ICI of 53.5 ms. However, it was determined that the differences between these two subtypes that lead to their separation during clustering was most likely due to differences in recording equipment. The second type was seen almost exclusively in deployments where the crossover frequency between the low- and high-frequency hydrophones was 25 kHz, which may introduce artificial notches in click spectra, likely causing the peak at 25 kHz seen for this type (Fig 2.2G2). It would be reasonable to group these types into one stenellid group; however, as with short-finned pilot whale, the two types were left separate due to improved classifier performance. Validation of these types as stenellid was provided based on previous acoustic and spatial distribution data (Table 2.2, S2 File).

2.4.1.8 H - *Kogia* spp.

The *Kogia* spp. click type was defined by a single high-frequency peak at 93.5 kHz and a peak ICI of 90.3 ms (Fig 2.2H, Table 2.1). The full spectral shape of these clicks was not captured here as it is above the limit of the bandpass filter used in the original click detection step (100 kHz), but the partial peak captured was indicative of aliasing from higher-frequency (i.e., 125 kHz) *Kogia* spp clicks (17). Acoustic differentiation between species of *Kogia* is not possible with the available data; hence description of this type must be left at the genus level. Validation for this type was provided by previous acoustic and

spatial distribution records (Table 2.2, S2 File). Information provided in said records suggested that this type was mostly composed of dwarf sperm whale clicks (S2 File).

2.4.2 Classifier Performance

The best performing neural-network based classifier consisted of the following: an input layer, four 512-node fully-connected layers with 50% dropout between each, and a softmax output layer. Networks of this type were trained on a variety of feature combinations, with the best performance (highest accuracy and recall values across classes and sites) resulting from training on clustered 5-minute bin values of peak ICI, mean spectral shape, and mean waveform envelope. Accuracy for this classifier on novel data, which was manually labelled at the 5-minute bin level for network evaluation purposes, was high across classes and sites (> 96 % in all cases), with lowest accuracy occurring for false killer whales at the Kona and PHR sites (96.2 % and 96.6%, respectively), and rough-toothed dolphin (97.3 %) at the Kaua‘i site. The false killer whale class also had the lowest accuracy score for the combined-sites results (96.9 %) followed by rough-toothed dolphin (98 %). Accuracy was highest for the Cuvier’s beaked whale and *Kogia* spp. classes at the Kona site (99.7%), Blainville’s and Cuvier’s beaked whales at Kaua‘i (99.8%), and Cuvier’s beaked whale at PHR (99.7%); though in the full-site data accuracy was highest for Cuvier’s beaked whale and stenellid type 2 (99.7%) (Table 2.3).

While accuracy was markedly high for all types, recall and precision presented a more nuanced picture. Lower recall values (i.e., below 75%) indicating that bins of a given type were missed by the network were found for short-finned pilot whale class 2 at Kaua‘i

and PHR (Table 2.3). However, this type is also fairly uncommon at these sites as indicated by a low number of presence bins within the manually labelled dataset for that type (36 bins at Kauaʻi and only 11 bins at PHR, Table 2.3). Lower precision values, indicating a high presence of false positive bins for a type, were concerning for the false killer whale type at all sites except Kauaʻi, short-finned pilot whale type 2 in the full data, short-finned pilot whale type 1 at PHR, and the bottlenose dolphin/melon headed whale type at Kona (Table 2.3). Cases where low precision values were likely related to a small number of bins (corresponding to those with low recall as well as Cuvier's beaked whale at Kona, *Kogia* spp. at PHR, and short-finned pilot whale type 2 at Kauaʻi and PHR) were not considered of concern at this time. The lower precision value for short-finned pilot whale type 2 in the full dataset is likely driven by lower recall at Kauaʻi and PHR, and hence was also not considered concerning.

2.5 Discussion

This study demonstrated the efficacy of machine learning for processing and classifying available large acoustic datasets for odontocete species, in this case in the tropical Pacific islands. Using machine learning methods, it was possible to discriminate the echolocation clicks of five species of odontocetes (false killer whale, short-finned pilot whale, rough-toothed dolphin, Cuvier's beaked whale, and Blainville's beaked whale) as well as three additional groups (stenellid dolphins, *Kogia* spp., and bottlenose dolphin/ melon-headed whale). The classification of the LF1 click type as rough-toothed dolphin highlights a unique advantage of the clustering methodology that allows for quantitative

grouping of unknown types more easily than manual labelling. While manual identification might allow one to classify data as a known type, or a general 'unknown' type, clustering provides a more standardized, facilitated way to determine one or more unknown types in a large dataset, particularly when differences appear to be small yet consistent. As seen with rough-toothed dolphin in this case, combination of click features from an unknown type with other acoustic and sighting records from the region can lead to new classifications and provide insights for species with few previous acoustic descriptions.

It is worth noting, however, that comparisons of acoustic data from multiple recordings requires consideration of system differences. Exact spectral matches between encounters recorded on HARPs versus those recorded by towed acoustic arrays are unlikely due to the differences in both equipment and recording schemes (e.g., recording at the ocean floor versus near the surface, increased noise due to active towing, differences in animal behavior and/or orientation to the receiver). As such, in this study, the general spectral shape of mean spectra from towed array encounters versus the type spectrum from HARP data were given more weight than exact peak values. This study also demonstrates the usefulness of comparing observed relative species presence to sighting records to bolster classifications. While this process did not lead to distinction of the bottlenose dolphin/ melon-headed whale, *Kogia* spp., or stenellid types, the comparisons provide context for what the makeup of these types might be. Similar methodology has recently been applied to delphinid species in the Atlantic Ocean (22).

One potential downfall of this clustering method is the loss of rarer types. By clustering clicks or bins together and setting various pruning thresholds, some connections

and clusters were removed from the data, or grouped into larger, more dominant types. In the Hawaiian region, there are at least 18 species of odontocetes (3), but only ten distinct click types were identified using our clustering methods, though sperm whales were purposefully excluded from analysis. Other, rarer species including Risso's dolphin, *Grampus griseus,* Longman's beaked whale, *Indopacetus pacificus,* Fraser's dolphin, *Lagenodelphis hosei,* and pygmy killer whale, *Feresa attenuata*, were not identified in this dataset using these methods. While it is possible that none of these species were present in the dataset, it is more likely that some (primarily pygmy killer whales, given their spatial use off Kona (67)) were present in the record in small numbers and hence not represented by their own cluster. In the case of this study, this lack of representation in the final types resulted in no corresponding class in the neural-net classifier. Detections of these species have hence been unavoidably mislabeled as either a different odontocete class or noise; the effect of this is likely small but difficult to quantify without labelled data for these species.

Noise floor differences between earlier and later models of the HARP recording systems used in this study resulted in differences in detectability for echolocation clicks below 125 dB_{pp} re 1 µPa. Over the course of this study the received level threshold was therefore increased from 115 to 125 dB_{pp} re 1 µPa to mitigate detectability-related artifacts over the 12-year period. This reduced the dataset size by approximately 10%.

The success of the machine learning tools applied here on other datasets may be somewhat dependent on the noise floor. The HARP data used in this case had a very low broad band noise floor (i.e., high signal to noise ratio) for most deployments, facilitating the use of lower amplitude detections for classification. Higher noise recordings, such as

those collected using moving towed arrays, may further limit similar analyses to detections with higher received levels.

The development of the input data for the Cuvier's beaked whale neural network class in this study used examples from Hawaiian HARP data, augmented with additional examples from Southern California. This process seemed to have successfully complemented available Hawaiian examples without causing classifier confusion, as Cuvier's beaked whale had some of the highest accuracies across all three sites, as well as for all sites combined (> 99% in all cases) (Table 2.3). Future studies employing these methods might consider the efficacy of augmenting regionally developed classes with additional data from other locations, particularly in the case of species that are not represented in local clusters but are known to be present. When augmenting existing regional classes with additional global examples, researchers must also be wary of species whose echolocation clicks have shown significant regional variation (68), as well as species that produce multiple, distinct types of echolocation clicks (69), which should perhaps not be combined together for classification purposes.

For other classes, training and testing data were augmented using noise to reach a total of 5000 example bins. It is possible that this may introduce artifacts into the data, which can then be learned by the network (49). However, this process seemingly did not cause issues for the classifier created in this study; inspection of augmented data revealed no noticeable spectral artifacts, and classification accuracy was high amongst both augmented and non-augmented types. As an example, one can compare performance of the non-augmented stenellid type 1 class to performance of the augmented Blainville's beaked

whale class on novel data (Table 2.3). In all three cases, accuracy and recall across sites was >94 %, suggesting that augmenting input features did not have harmful effects on classifier performance. The classifier produced in this process demonstrated a high degree of classification accuracy on novel data across sites and classes, and fairly high (> 66 % in all cases) values for recall (Table 2.3). The success of these augmentation techniques imply that these methods can be useable on smaller datasets. However, network training on less than a few hundred examples of determined types, with no ability to augment these types using additional data, should proceed with caution. The clustering and neural network steps employed here were developed to expedite processing of large acoustic datasets and are best suited to this task.

In some cases, examination of confusion matrices provides useful context for performance metric values. For false killer whales, confusion matrices at all sites revealed that the low precision seen for this type was mainly due to bins of noise being mislabeled as false killer whale (Table 2.3 - 2.6). This result was most likely due to the spectral similarities between the false killer whale click type and detections attributed to boats and sperm whales that were part of the input noise class, particularly after applying a 10 kHz high-pass filter. This issue was less pronounced at Kauaʻi, where false killer whales were more common relative to noise detections (Table 2.3; Table 2.6).

Other recent classification efforts of false killer whale have found success using a variety of vocalizations instead of only echolocation clicks, however, accuracy was slightly reduced when attempting to classify multiple species instead of only false killer whales and a conglomerate outgroup of other odontocetes (41). Due to the regional significance of this

species, and their rarity in the dataset, manual data verification was required to remove false positives from false killer whale time series before discussion of relative acoustic presence in this dataset, as mentioned in the results section of this study. This adjusted methodology highlights how the classifier can still be used to efficiently select time periods of presence for this type (i.e., high recall). Though the false positive rate on these detections was high (i.e., low precision), the additional manual checking required to remove these was much faster than manual logging of the entire dataset.

Low precision in classes other than false killer whales and types with few bins evaluated (e.g., Cuvier's beaked whale at Kona; Table 2.3) occurred primarily for short-finned pilot whale and bottlenose dolphin/melon headed whale types (Table 2.3). Though the number of manually labelled bins for short-finned pilot whale class 1 at PHR exceeded the threshold for evaluation (50 bins), it was still fairly low (nBin = 72; Table 2.3). Based on precision values for this type at the other two sites, low bin number is considered the most likely reason for lower precision observed in this case. For the bottlenose dolphin/melon-headed whale type, confusion exists primarily with short-finned pilot whale, stenellid, and rough-toothed dolphin types (Tables 2.4 – 2.6). This is potentially due to several factors. Differences between the structure of the training set, which contained equal proportions of each type, and the real data, where types may be less common at certain sites than the network expects (e.g., rough-toothed dolphin at Kona) may increase confusion. Additionally, the ICI distribution and overall frequency range of rough-toothed dolphin, short-finned pilot whale, and bottlenose dolphin/ melon-headed whale clicks were fairly similar, as was the spectral content of rough-toothed dolphin, bottlenose dolphin/

melon-headed whale, and stenellid clicks, particularly in low received level encounters where the higher frequency content of stenellid clicks was not as prevalent. Confusion amongst these classes was lower at Kaua‘i than at Kona, potentially due to the lower level of vessel presence at this site. The Kona site has an overall much higher noise background than the Kaua‘i site related to the commonality of ships and echosounders. These noise sources may alter spectral content of click mean spectra as well as ICI distributions by introducing false positive detections, hence increasing network confusion. There is not much that can be done with the current classifier structure to reduce this confusion, though it is notable that even in the most drastic case (i.e., bottlenose dolphin/melon headed whale at Kona), the precision value was still fairly high (74.9%). Network confidence, which accompanies all labels from the neural network used in this study, could potentially be used in future applications of this dataset to improve upon these false positive rates by only using detections above a certain confidence threshold.

Using the machine learning methods applied in this study, we were able to develop a catalogue of click types for the Hawaiian Islands region and attribute those click types to species, including the novel description of a click type for rough-toothed dolphins. We were then able to develop and implement a neural-net based classifier, from which we were able to label encounters with 8 or more species of odontocetes in 15 instrument years of passive acoustic data. The success of this classifier in labeling passive acoustic data from multiple sites demonstrates its efficacy for analyzing existing and future acoustic datasets from this region, as well as potentially from other regions where these species are thought to be present. Future work related to improving the success of these methods in

identifying and classifying echolocation clicks might consider a tiered approach, in which original clustering and labelling take place at a more generalized level (e.g., 'unidentified dolphin', 'beaked whale', 'ship'). Then, parsing of subtypes could be completed using additional clustering as well as other methods that have proved useful here such as comparison to known click records, species patterns, and auxiliary data. Such a method would likely minimize misclassifications as well as avoid the issue of species without a specific class being unavoidably mislabeled as a different odontocete or potentially as noise. At present, however, a usable workflow has not yet been developed for the method proposed above.

In this paper, knowledge of rough-toothed dolphin diel behavior was used as additional evidence in the attribution of click type LF1 to this species. Further research using the timeseries produced in this study may find that examining diel patterns helps bolster the classifications made here. This may be particularly true for the stenellid type, as spinner dolphins are active nearly exclusively at night and spend their days in shallow resting bays (70), whereas spotted dolphins, while still more active at night, are somewhat active during the day as well (24,71). In addition to this, Blainville's beaked whales have demonstrated diel and lunar variation in activity (37,72,73), short-finned pilot whales have been noted to move inshore/offshore in relation to the lunar cycle (74), and differences in diel presence among sites may help determine the makeup of the bottlenose dolphin/melon headed whale class. For *Kogia* spp. and some others, comparisons to timeseries produced using subsets of this HARP dataset (e.g., (75)) will provide additional useful context for those derived using the methods of this paper. For false killer whales, marked presence

during night-time hours may help explain the mismatch between rare sightings and common presence in the Kauaʻi HARP dataset (31% of days with presence); this could also be investigated using existing satellite tag data (76,77) to see whether they are more likely to use the area off western Kauaʻi during night-time hours. Work on describing and exploring some of these comparisons is ongoing and will be addressed more completely in a future paper. The records developed here can also be used in species monitoring efforts as well as to answer complex questions about animal behavior, habitat requirements, and ecosystem relationships of odontocetes in the Hawaiian Islands.

2.6 Acknowledgements

Thanks to Ann Allen, Erik Norris, and others at the NOAA Pacific Islands Fisheries Center for their instrument deployment, retrieval, and work at all sites used in this study. A special thanks to Jennifer McCullough for her help procuring HICEAS data and her mentorship at sea. Thank you to all members of the Scripps Whale Acoustics Lab and the Scripps Acoustic Ecology Lab for support over the course of this project. In particular, thanks to Erin O'Neill for her work in processing HARP deployments and Bruce Thayre and John Hurwitz for their work on the HARP instruments. Thanks to Macey Rafter for providing in-lab support and facilitating remote work over the past year-plus of quarantine, and to Michaela Alksne for providing additional Cuvier's beaked whale clicks. Thanks to fellow graduate students Rebecca Cohen, Natalie Posdaljian, and Vanessa ZoBell for edits to this manuscript. This work was funded by the NOAA Pacific Islands Fisheries Science Center. Manawai (i.e., Pearl and Hermes Reef) HARP

deployments were permitted by the Papahānaumokuākea Marine National Monument under permits PMNM-2008-020 and PMNM-2010-042 and the Co-Managers permit since 2015.

Chapter 2, in full, is a reprint of the material as it appears in PLOS One, Ziegenhorn, Morgan A., Kaitlin E. Frasier, John A. Hildebrand, Erin M. Oleson, Robin W. Baird, Sean M. Wiggins, and Simone Baumann-Pickering. "Discriminating and classifying odontocete echolocation clicks in the Hawaiian Islands using machine learning methods." *PloS one* 17, no. 4 (2022): e0266424. The dissertation author was primarily responsible for the investigation and writing of this material.

2.7 Figures and Tables

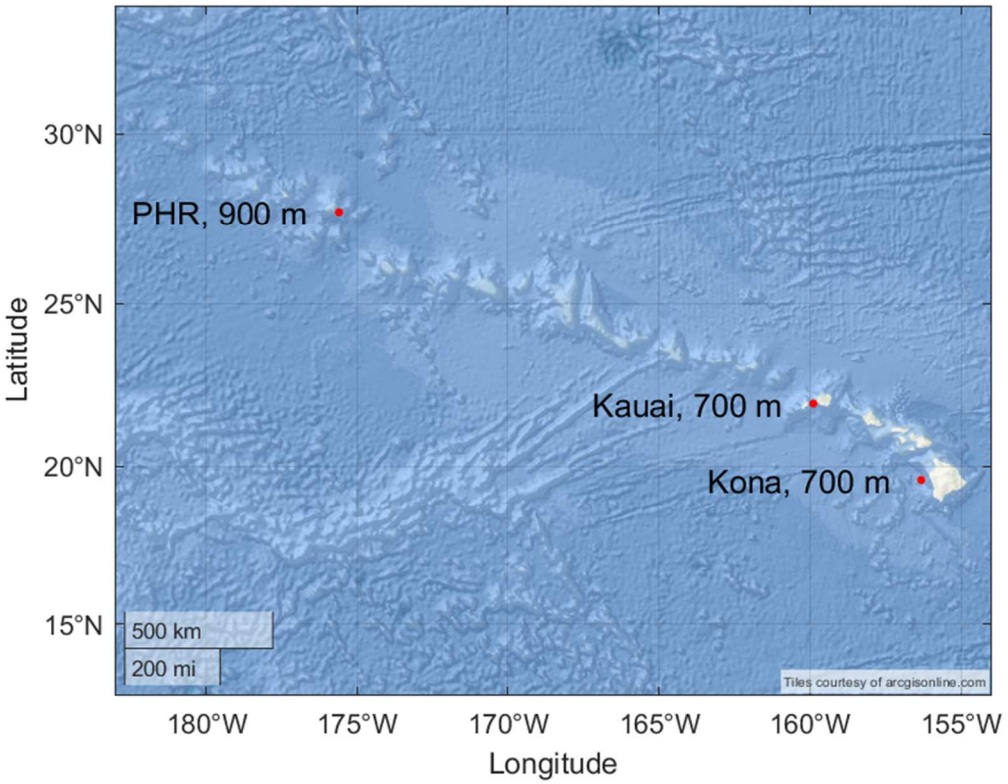

Figure 2.1. Map of Recording Locations. Map showing the latitude-longitude locations of the Kona, Kaua‘i, and PHR sites. Location and depth of each site was averaged among deployments from that site. Basemap image is the intellectual property of Esri and is used herein with permission. Copyright © 2022 Esri and its licensors. All rights reserved.

Figure 2.2. Echolocation click types. Plots A-H depicting data from representative clicks from each of 10 final click types: (A) False killer whale, (B) Low-frequency type 1 (LF1), (C1) Short-finned pilot whale 1, (C2) Short-finned pilot whale 2, (D) Bottlenose dolphin/ melon-headed whale, (E) Blainville's beaked whale, (F) Cuvier's beaked whale, (G1) Stenellid 1, (G2) Stenellid 2, and (H) *Kogia* spp. Panels 1-4 (left to right) depict the following: (1) mean spectra, shown along with 10^{th} and 90^{th} percentile values, (2) modal inter-click interval distribution, (3) concatenated click spectra of all clicks included, and (4) click waveform envelope for all clicks. Click waveform envelope has been sorted by peak amplitude (highest to the left), and concatenated clicks have been sorted correspondingly. Types are ordered by peak frequency.

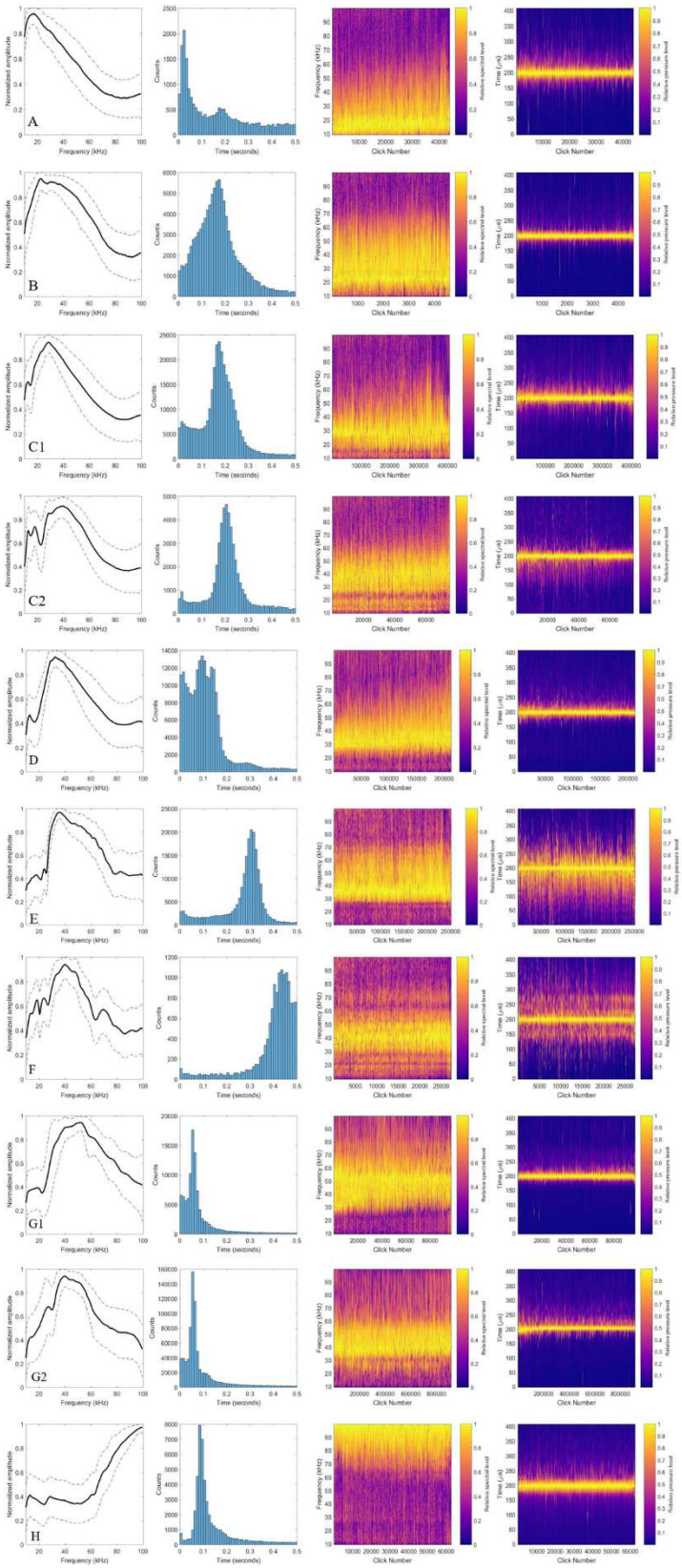
A
B
C1
C2
D
E
F
G1
G2
H
Normalized amplitude
Frequency (kHz)
Counts
Time (seconds)
Frequency (kHz)
Click Number
Relative spectral level
Time (mS)
Relative pressure level

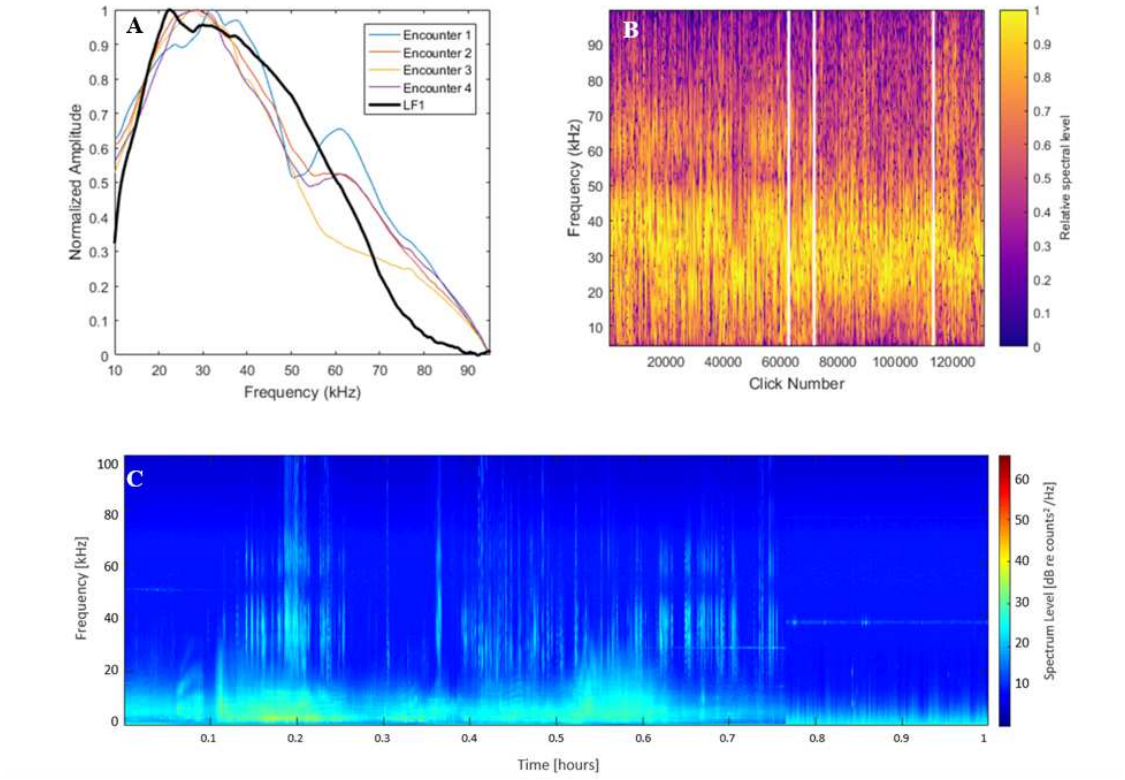

Figure 2.3. Towed-array *S. bredanensis* encounters. Figure depicting (a) mean spectra, (b) concatenated click spectra, and (c) an example long-term spectral average of a towed-array acoustic encounter of verified rough-toothed dolphins. Panel (a) includes the mean type spectra of the LF1 click type for comparison. Delineations in panel (b) (white lines) separate clicks coming from encounters 1-4. Panel c shows a long-term spectral average of raw data from an example encounter coming from the towed array dataset.

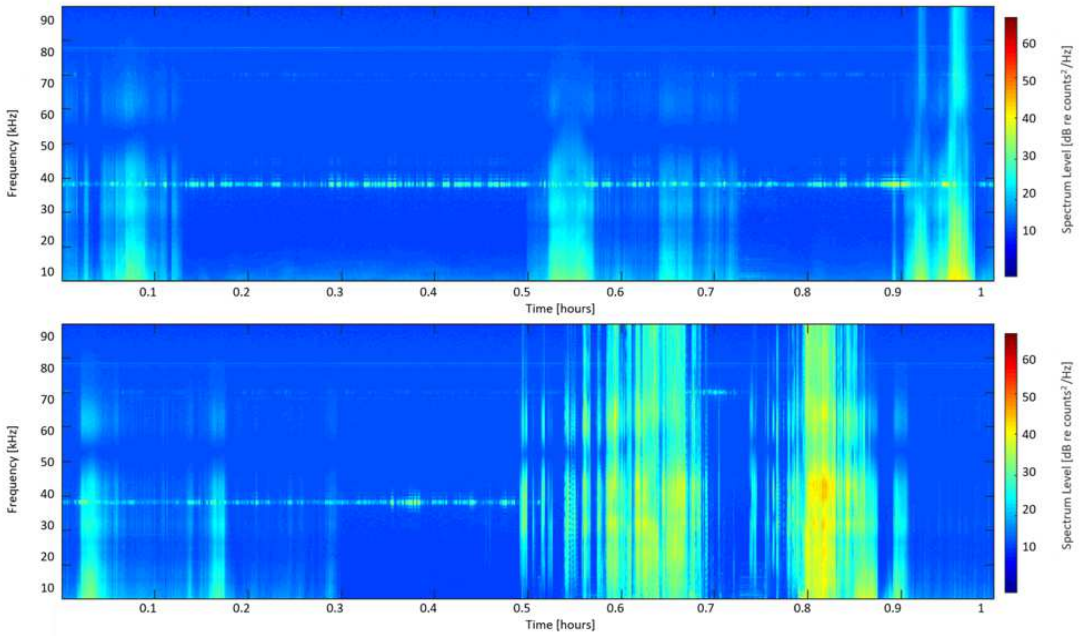

Figure 2.4. Additional towed-array examples. Long-term spectral average of two different hours of towed-array data, displaying the persistence of a notch in sensitivity at ~ 50 kHz regardless of species present. Panel (a) displays sound data from anthropogenic sources, while (b) displays both anthropogenic noise and a delphinid encounter (starting at ~ 0.5 hours).

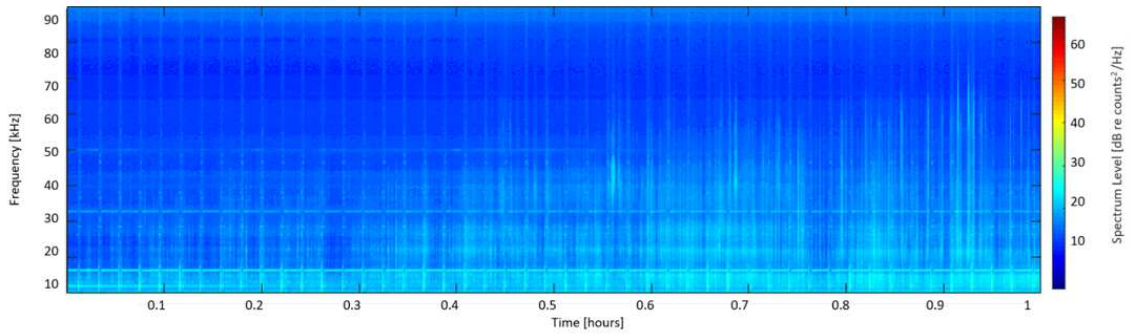

Figure 2.5. Long-term spectral average of an LF1 encounter. Long-term spectral average of data from 11/13/2015 including clicks labelled as type LF1. A sighting of rough-toothed dolphins occurred about 1 hour after this encounter, approximately 5 km from the location of the HARP.

Table 2.1. Quantitative Click Type Descriptions. Parameters of click types (i.e. neural network classes) including median location of spectral peaks for all evaluated clicks as well as peak value for ICI distributions of evaluated acoustic encounters of each class. Species are organized based on overall frequency content of clicks (lowest to highest) and then by number of spectral peaks. Number of clicks evaluated is given along with class name. For spectral peaks, values in parentheses give the 10th and 90th percentiles of the data. For ICI, standard deviation from the peak (i.e. modal) value is given instead. For the false killer whale class, the ICI distribution was bimodal; in this case, two ICI values are given instead of one. The bottlenose dolphin/melon-headed whale type is abbreviated as Tt/Pe.

Neural Network Class, Number of Clicks	Spectral Peak 1 (kHz)		Spectral Peak 2 (kHz)		Spectral Peak 3 (kHz)		Modal ICI (milliseconds)
	Peak frequency	-3 dB bandwidth	Peak frequency	-3 dB bandwidth	Peak frequency	-3 dB bandwidth	
False killer whale, n = 4000	16.5 (13.0–20)	6.5 (1.0–12.0)	--	--	--	--	28.4 (+/- 28.0) 166 (+/- 109)
Low-frequency 1, n = 4000	22.0 (20–25)	5.5 (1.5–19.5)	--	--	--	--	169 (+/- 132)
Short-finned pilot whale 1, n = 7000	13.0 (12.0–13.5)	1.5 (1.0–6.5)	28.0 (26.0–31.0)	5 (2.0–10.0)	--	--	184 (+/- 66.9)
Short-finned pilot whale 2, n = 40000	13.0 (12.5–14.0)	1.5 (1.0–2.0)	18.5 (16.5–20.5)	3 (1.5–9.5)	48.5 (36.0–40.5)	3.0 (2.0–8.5)	206 (+/- 56.0)
Tt/Pe, n = 20000	12.5 (11.5–13.5)	1.5 (1.0–3.0)	32.5 (30.0–35.5)	5.5 (2.5–12.0)	--	--	109 (+/- 109)
Blainville's beaked whale, n = 25000	24.0 (23.0–25.5)	2.5 (1.5–4.5)	36.0 (32.0–41.5)	9.0 (4.5–15.0)	--	--	319 (+/- 109)
Cuvier's beaked whale, n = 2500	17.0 (16.0–18.5)	2.5 (2.0–3.5)	24.0 (22.0–25.5)	4.0 (2.0–9.0)	40.0 (37.0–44.0)	6.5 (3.0–12.5)	433 (+/- 59.0)
Stenellid 1, n = 100000	18.5 (16.5–20.5)	4.25 (3.0–9.75)	50.0 (45.0–54.0)	9.0 (3.5–18.5)	--	--	48.5 (+/- 43.5)
Stenellid 2, n = 90000	25.0 (22.5–27.0)	4.5 (3.0–6.5)	39.5 (35.0–44.5)	8.5 (4.0–18.0)	--	--	53.5 (+/- 0.0401)
Kogia spp., n = 6000	93.5 (87.5–99.5)	10.0 (5.0–17.5)	--	--	--	--	90.3 (+/- 41.8)

Table 2.2. Validation Types. Validation sources (with references) for each echolocation click type. Validation types are previous acoustic, spatial distribution (including abundance information), temporal behavior, and auxiliary sighting/acoustic data. The Tt/Pe abbreviation corresponds to the bottlenose dolphin/melon-headed whale type.
* Validation of this type as likely rough-toothed dolphin is included in the main manuscript as this represented a novel type description. Further detail regarding all other types is available in S1 File.

Echolocation Click Type	Validation Type [References]
False killer whale	previous acoustic [26], spatial distribution [4, 27–29]
Low-frequency 1*	previous acoustic (limited) [33], spatial distribution [4, 34–35], temporal behavior [36], auxiliary sighting/acoustic data
Short-finned pilot whale 1	previous acoustic [16, 26], spatial distribution [4, 37, 38, 39]
Short-finned pilot whale 2	previous acoustic [16, 26], spatial distribution [4, 37, 38, 39]
Tt/Pe	previous acoustic [40], spatial distribution [4, 37, 43], temporal behavior [41–42]
Blainville's beaked whale	previous acoustic [17], spatial distribution [4, 35, 44–46]
Cuvier's beaked whale	previous acoustic [17], spatial distribution [3–4, 45]
Stenellid 1	previous acoustic [40, 47], spatial distribution [4, 28, 35, 37, 48, 49]
Stenellid 2	previous acoustic [40, 47], spatial distribution [4, 28, 35, 37, 48, 49]
Kogia spp.	previous acoustic [9, 50], spatial distribution [4, 51]

Table 2.3. Neural Network Results. Results describing the accuracy, recall, and precision on novel, manually-labelled data for each class at each site, as well as for all sites combined. Values less than 75% with >50 bins have been bolded. NBins gives the number of manually labelled positive bins for each type. For full-site results, NClicks gives the average number of clicks in each NBin.
*Manual evaluation of all Kaua‘i data found no clicks of Cuvier’s beaked whale, so recall and precision could not be evaluated.

Neural Network Class	Kona				Kaua‘i				PHR				All Sites			
	Accuracy (%)	Recall (%)	Precision (%)	nBins	Accuracy (%)	Recall (%)	Precision (%)	nBins	Accuracy (%)	Recall (%)	Precision (%)	nBins	Accuracy (%)	Recall (%)	Precision (%)	nBins, nClicks
False killer whale	96.2	88.0	**48.5**	324	98.1	93.4	75.9	259	96.6	96.5	**34.9**	86	96.9	91.2	**53.3**	669, 7938
Rough-toothed dolphin	98.4	83.1	83.8	468	97.3	96.7	98.9	4602	98.1	94.1	94.7	801	98	95.3	97.1	5871, 7293
Short-finned pilot whale 1	98.1	89.6	89.0	988	97.8	92.2	79.1	230	98.4	80.6	**58.6**	72	98.1	89.5	84.9	1290, 13271
Short-finned pilot whale 2	98.2	96.3	81.1	463	98.7	66.7	37.5	36	99.2	72.7	25.8	11	98.5	93.7	**74.1**	510, 95262
Tt/Pe	98.5	75.6	**74.9**	213	98.4	94.8	80.5	192	98.2	82.7	91.0	307	98.4	83.8	82.9	712, 3291
Blainville’s beaked whale	99.4	96.0	90.8	227	99.8	98.9	98.9	91	99.5	98.9	99.8	2008	99.5	98.6	98.9	2326, 11713
Cuvier’s beaked whale	99.7	83.3	45.5	6	99.8	N/A	0	0*	99.7	97.3	100	546	99.7	97.1	98.5	552, 271561
Stenellid sp. 1	98.4	97.8	97.9	5840	98.5	98.4	95.6	1219	98.4	94.5	90.3	364	98.4	97.8	97.1	7423, 9802
Stenellid sp. 2	99.5	99.7	93.9	729	99.6	97.8	94.7	183	100	100	96.0	24	99.7	99.4	94.1	936, 824
Kogia spp.	99.7	99.6	93.6	250	99.6	100	91.2	52	99.4	100	52.0	13	99.6	99.7	90.2	315, 81444

Table 2.4. Classifier Confusion Matrix- Kona. Confusion matrix showing the number of 5 minute bins (from novel data not used in training/testing/validation) labelled as each class. Diagonal cells across classes show the number of correctly labelled positive bins for that class. Cell(i,j) is the number of bins of i that were labelled j by the network.

	False killer whale	Rough-toothed dolphin	Short-finned pilot whale 1	Short-finned pilot whale 2	Tt/Pe	Blainville's beaked whale	Cuvier's beaked whale	Stenellid 1	Stenellid 2	*Kogia* spp.	Noise
False killer whale	285	0	25	8	1	0	0	0	0	0	5
Rough-toothed dolphin	1	389	19	14	2	1	0	33	3	0	6
Short-finned pilot whale 1	45	23	885	5	6	2	0	14	2	0	6
Short-finned pilot whale 2	6	3	5	446	0	0	0	2	0	0	1
Tt/Pe	0	14	16	11	161	1	0	3	7	0	0
Blainville's beaked whale	0	0	0	1	1	218	1	3	0	1	2
Cuvier's beaked whale	0	0	0	0	0	0	5	0	0	0	1
Stenellid 1	1	24	19	17	35	3	5	5713	16	1	6
Stenellid 2	0	1	0	1	0	0	0	0	727	0	0
Kogia spp.	0	0	0	0	1	0	0	0	0	249	0
Noise	250	10	25	47	8	15	0	67	19	15	3662

Table 2.5. Classifier Confusion Matrix- Pearl and Hermes Reef. Confusion matrix showing the number of 5 minute bins (from novel PHR data not used in training/testing/validation) labelled as each class. Diagonal cells across classes show the number of correctly labelled positive bins for that class. Cell(i,j) is the number of bins of i that were labelled j by the network.

	False killer whale	Rough-toothed dolphin	Short-finned pilot whale 1	Short-finned pilot whale 2	Tt/Pe	Blainville's beaked whale	Cuvier's beaked whale	Stenellid 1	Stenellid 2	*Kogia* spp.	Noise
False killer whale	83	1	2	0	0	0	0	0	0	0	0
Rough-toothed dolphin	11	754	21	1	4	0	0	7	0	2	1
Short-finned pilot whale 1	11	0	58	0	2	0	0	1	0	0	0
Short-finned pilot whale 2	1	1	0	8	1	0	0	0	0	0	0
Tt/Pe	0	33	0	0	254	0	0	20	0	0	0
Blainville's beaked whale	0	0	8	7	2	1986	0	1	0	2	2
Cuvier's beaked whale	0	0	4	7	1	1	531	0	1	0	1
Stenellid 1	0	4	2	0	14	0	0	344	0	0	0
Stenellid 2	0	0	0	0	0	0	0	0	24	0	0
Kogia spp.	0	0	0	0	0	0	0	0	0	13	0
Noise	132	3	4	8	1	3	0	8	0	8	1187

Table 2.6. Classifier Confusion Matrix- Kaua‘i. Confusion matrix showing the number of 5 minute bins (from novel Kaua‘i data not used in training/testing/validation) labelled as each class. Diagonal cells across classes show the number of correctly labelled positive bins for that class. Cell(i,j) is the number of bins of i that were labelled j by the network.

	False killer whale	Rough-toothed dolphin	Short-finned pilot whale 1	Short-finned pilot whale 2	Tt/Pe	Blainville's beaked whale	Cuvier's beaked whale	Stenellid 1	Stenellid 2	*Kogia* spp.	Noise
False killer whale	242	14	1	0	0	0	0	0	0	0	2
Rough-toothed dolphin	20	4450	38	7	29	0	1	44	9	0	4
Short-finned pilot whale 1	5	9	212	0	4	0	0	0	0	0	0
Short-finned pilot whale 2	2	7	1	24	0	0	0	0	1	0	1
Tt/Pe	0	3	5	0	182	0	0	2	0	0	0
Blainville's beaked whale	0	0	0	1	0	90	0	0	0	0	0
Cuvier's beaked whale	0	0	0	0	0	0	0	0	0	0	0
Stenellid 1	0	4	1	3	8	0	0	1199	0	0	4
Stenellid 2	0	1	0	1	1	0	1	0	179	0	0
Kogia spp.	0	0	0	0	0	0	0	0	0	52	0
Noise	50	12	10	28	2	1	0	9	0	5	1088

Chapter 3: Odontocete spatial patterns and temporal drivers of detection at sites in the Hawaiian Islands

Morgan A. Ziegenhorn[1*], John A. Hildebrand[1], Erin M. Oleson[2], Robin W. Baird[3], Sean M. Wiggins[1], Simone Baumann-Pickering[1]

[1] Scripps Institution of Oceanography, University of California San Diego, La Jolla, CA, USA

[2] NOAA Fisheries Pacific Islands Fisheries Science Center, Honolulu, HI, USA

[3]Cascadia Research Collective, Olympia, WA, USA

3.1 Abstract

Successful conservation and management of marine top predators relies on detailed documentation of spatiotemporal behavior. For cetacean species, this information is key to defining stocks, habitat use, and mitigating harmful interactions. Research focused on this goal is employing methodologies such as visual observations, tag data, and passive acoustic monitoring (PAM) data. However, many studies are temporally limited or focus on only one or few species. In this study, we make use of an existing long-term, labelled PAM dataset to examine spatiotemporal patterning of at least 10 odontocete (toothed whale) species in the Hawaiian Islands using compositional analyses and modelling techniques. Species composition differs amongst considered sites, and that this difference is robust to seasonal movement patterns. Temporally, hour of day was the most significant predictor of detection across species and sites, followed by season. We describe long-term trends in species detection at one site and note that they are markedly similar for many species. These trends may be related to long-term, underlying oceanographic cycles. We demonstrate the variability of temporal patterns even at relatively close sites, which may imply that wide-ranging models of species presence are missing key fine-scale movement patterns. Documented seasonal differences in detection also highlights the importance of considering season in survey design both regionally and elsewhere. We emphasize the utility of long-term, continuous monitoring in highlighting temporal patterns that may relate to underlying climatic states and help us predict responses to climate change. We conclude that long-term PAM records are a valuable resource for documenting

spatiotemporal patterns and can contribute many insights into the lives of top predators, even in highly studied regions such as the Hawaiian Islands.

3.2 Introduction

Documenting spatiotemporal patterns of species presence is a crucial part of the conservation and management of marine top predators. Detailed spatial information about species presence often aids in the definition of new or distinct stocks as well as the understanding of habitat use and movement patterns (e.g., 78,79). Continuous temporal data facilitates description of key diel patterns in animal activity, which is crucial for understanding foraging preferences and mitigating harmful anthropogenic interactions (80,81). Characterization of spatiotemporal patterns in odontocete (toothed whale) species presence may also facilitate the creation and comparison of habitat models (e.g., 82,83). Studies focused on these goals provide valuable baselines to which additional work can be compared, allowing scientists to monitor populations and detect changes over time that may be related to underlying changes in oceanographic and climate patterns or anthropogenic activity.

In the Hawaiian Islands, odontocetes are one of the most speciose groups of marine top predators, with at least 18 species frequenting or residing in this region (3). Factors such as quality of environment (84), foraging opportunities related to island-associated prey (85), and movement to or from important geographical features (86) may influence fine-scale movements of these animals. Much of what is known about these species' general distribution has been documented in National Oceanic and Atmospheric

Administration (NOAA) stock assessments. These assessments are largely derived from multi-month line-transect visual surveys (e.g., 64), tag data (e.g., 13), and regional studies involving small boat surveys (e.g., 3). Passive acoustic monitoring (PAM) has also been used to study these animals but has often been limited by the difficulty of classifying multiple species using the detected sounds, focusing instead on only one or few species of odontocetes whose calls are well-described (81,87–89). These methods of study have resulted in an overall base of knowledge that contains extensive information for some species but is compiled from disparate records, often with limited spatial or temporal coverage.

A passive acoustic monitoring (PAM) dataset from the Hawaiian archipelago presents a unique opportunity to examine odontocete fine-scale temporal patterns at several sites over a longer time frame (2009-2019) than most other studies. These recordings include data from two subsites at a remote island in the Northwestern Hawaiian Islands (Manawai, otherwise known as Pearl and Hermes Reef), where records of odontocete spatiotemporal trends are limited compared to the Main Hawaiian Islands. A recent study which applied a machine learning toolkit to this dataset resulted in labelled data for 8 groupings of odontocetes (20). These groupings included 5 species-specific labels: false killer whale (*Pseudorca crassidens)*, rough-toothed dolphin (*Steno bredanensis),* short-finned pilot whale (*Globicephala macrorhyncus),* Blainville's beaked whale (*Mesoplodon densirostris),* and Cuvier's beaked whale (*Ziphius cavirostris).* Additional genus or group level labels were stenellid dolphins (including some mixture of pantropical spotted dolphin (*Stenella attenuata),* striped dolphin (*S. coeruleoalba),* and spinner dolphin (*S.*

longirostris)), *Kogia* spp. (primarily dwarf sperm whale (*K. sima),* but potentially containing detections of pygmy sperm whale (*K. breviceps)* based on sighting record (90), and a type representing an unknown mixture of common bottlenose dolphin (*Tursiops truncatus)*, and melon-headed whale (*Pepnocephala electra).* However, descriptions of patterns within these labelled data, and comparisons to literature, have not been completed.

Analysis of long-term acoustic data from these sites can provide new perspectives on temporal presence, particularly for more cryptic species or those averse to human activities. In some cases (e.g., *Kogia* spp.), temporal analyses and documentation of patterns are relatively novel, as few previous studies have had sufficient detections of these species to describe patterns. In the case of rough-toothed dolphin, description of spatiotemporal trends based on a novel click type described by Ziegenhorn et al. (20) will represent one of very few descriptions of temporal patterns in this species' behavior. Even in cases where strong patterns in presence have been documented, additional data, particularly data arising from differing methodologies, can prove useful by filling in knowledge gaps. In addition to this, concurrently analyzing timeseries for all species of odontocetes commonly found in this dataset presents an opportunity to compare composition and temporal patterning across species and sites without concern for differences in sampling and processing regimes.

In this study, timeseries of species' echolocation click detection (henceforth 'detections') were derived from the existing, labelled PAM dataset to examine spatiotemporal patterning in the Hawaiian Islands for the eight groupings of odontocetes mentioned above. Composition amongst sites was evaluated, and significance of temporal

patterns was determined using Generalized Additive Models (GAMs) with Generalized Estimating Equations (GEEs). Significant temporal patterns were described and compared to available previous literature for included species. The patterns described improve upon previous research for many species where records at various scales (e.g., lunar, seasonal, yearly) are lacking, providing a baseline for studies of behavior of included species. The breadth of results presented here highlights the utility of long-term, fine-scale detection data in species monitoring efforts.

3.3 Methods

3.3.1 Data collection

Passive acoustic data was collected in the Hawaiian Islands using High Frequency Acoustic Recording Packages (HARPs) (19). Deployments used for this study spanned the years 2009-2019 (see Table S3.1.1 in Supplementary Information). Sites for data collection were off the west coast of Hawai‘i Island (henceforth, ‘Hawai‘i’), west of Kaua‘i, and in the vicinity of Manawai (Fig. 3.1). In the case of Manawai, the exact recording site shifted over the recording period (2009-present), primarily to combat low-frequency hydrophone cable strumming from strong currents at depth. As such, two subsites have been designated (henceforth, ‘Manawai 1’, ‘Manawai 2’). Deployment setup varied at these sites in terms of recording schedule, instrument depth, and duty cycle regime (i.e., alternating periods of recording and non-recording; see Table S3.1.1). Duty cycling was employed to extend battery life and allow for longer deployments. Data from these sites were recorded at a 200 kHz or 320 kHz sampling frequency (16-bit quantization) at depths ranging from 550-

1150 meters (see Table S3.1.1). All hydrophones were buoyed approximately 10-30 meters from the seafloor.

3.3.2 Data processing

An energy-based detector was run on all data to identify echolocation clicks, which were then evaluated to determine relevant click features (i.e., timing between clicks in a click train, or 'inter-click interval', spectral shape, peak frequency)(e.g., 42,91). These clicks were then clustered using unsupervised clustering methods, resulting in several echolocation click types (e.g., 21,23). These types were identified to species level where possible based on known records and auxiliary data from the region. Then, types were used as classes to train a neural network-based classifier, which was run on all data to label the entirety of the dataset as either one of the echolocation click types or noise (e.g., 20,49).

Detections of all types were originally binned in 5-minute increments for network training and labelling. Numbers of clicks in 5-minute bins were multiplied by type-specific precision values (a measurement of the percentage of all network labels of a given type that were true positives) to approximate the number of 'true' clicks in that bin. Bins were retained for timeseries only if they had more than a certain number of 'true' clicks (>50 for delphinids, >20 for beaked whales and *Kogia* spp.). For false killer whales, neural-network classifications included many false detections from noise sources, which were removed manually in lieu of this process. Final timeseries were binned in counts of minutes with detections per hour. It was assumed that all minutes within a given 5-minute bin contained clicks of a type if that type was present in the bin. Short-finned pilot whale and stenellids

each had two associated click types, which were left separate during classification to improve network performance but were determined to not represent different species or populations. Timeseries for these types were consolidated to one stenellid type and one short-finned pilot whale type for this analysis.

As the full dataset for all sites included both continuous and duty cycled deployments, it was necessary to further account for the effects of duty cycles (see Table S3.1.1). This was done on both a site and type-specific basis, as duty cycling does not necessarily affect all species equally (92). For each type at each site, timeseries of detections were subsampled to replicate duty cycle used at that site. These subsamples were evaluated in comparison to the continuous timeseries to determine what percentage of minutes per hour of detections would have been lost if the given duty cycle had been in effect. This was repeated for all duty cycles at each site. The resulting percentages of missed minutes per hour were used to linearly boost the counts of minutes per hour in duty cycled deployments for each type. Manawai subsites were combined into one 'Manawai' site due to their close proximity.

3.3.3 Data analysis

Full timeseries data for each type were plotted along with lunar and solar information extracted using the *suncalc* package in R (93). In addition, seasonal variation in detection were calculated as average hours per week of detections across available years of data (Fig. 3.1). Seasons were defined as winter (January through March), spring (April through June), summer (July through September), and fall (October through December).

Percentage of days with detections of each type was evaluated by-site to examine compositional differences between sites. A Bray-Curtis dissimilarity test was used to look at compositional relationships amongst sites (94). This test compares species diversity and abundance at each site to that of a determined 'focal site', resulting in a value of one if the same species are present in the same numbers, and zero if the sites have none of the same species. For this study, percentage of recording days with a given species detected was used as a proxy for abundance at that site. Hawai'i was used as the 'focal site' for analysis, and data were split up by-season to evaluate how composition changed.

Basic temporal models were built using R (95) to test the significance of predictors (hour of day, lunar fraction, Julian day) for each type at each site. Lunar illumination and phase were extracted using the *suncalc* package in R (93,95) but were ultimately removed from final models due to a lack of compelling relationships with detections. Year was included only at Hawai'i where more than five years of consecutive data were available. To simplify modeling, minutes per hour were transformed into binomial presence-absence (i.e., an hour was given a value of one if clicks were present, and zero otherwise) for use as the response variable. For a given type, models were evaluated only if the number of total detection hours exceeded 100. Temporal autocorrelation was assessed using the residuals of a basic Generalized Linear Model (GLM) including all variables. The time step for temporal blocking was determined as the point where the autocorrelation of residuals dropped below 0.1. These time steps were used to define clusters of self-similar data in subsequent modeling steps.

Generalized Additive Models (GAMs) with Generalized Estimating Equations (GEEs) were used as a model framework to additionally combat the autocorrelation expected in continuous passive acoustic datasets (7,96,97). Lunar illumination was included as a smoothed or linear term depending on Quasilikelihood under the Independence model Criterion (QIC) values (98) for a basic model including only lunar illumination as a predictor. Julian day and hour of day were included as cyclic smooths, and year was included as a smooth at Hawai‘i given the long time-series at this site. All smoothed terms used multivariate splines (*mSpline()*, from the *splines2* package in R (99) with four knots to avoid overfitting. Variable significance was determined based on p-values calculated via an ANOVA of the final model, with $p<0.05$ as the cutoff for significance. Non-significant ($p \geq 0.05$) terms were removed before creation of the final model. Term order in the final model was determined through backwards selection, based on comparing QICs from models with each term removed sequentially to evaluate their relative contribution to the model's predictive power. P-value, degrees of freedom and chi-squared values from an ANOVA of final models were noted.

For final models, partial-fit plots were developed to visualize the probability of species detection in response to each temporal variable considered. To create these plots, model coefficients were bootstrapped using the covariance matrix included in the model output. Bootstrapped values were then used to determine the spread of possible spline fits; confidence intervals were taken from the 2.5% and 97.5% percentiles of this distribution. Best fit splines were calculated using the model coefficients from final models and plotted along with confidence intervals (code adapted from (97)). Effort was plotted across the

bottom of these plots and observed patterns in significant predictors were compared to previous literature as well as amongst sites for included species. Models were evaluated using binned residuals via the *performance* package in R (100). This process split data into bins based on fitted values, and plotted average fitted values against average residual values for each bin. The results of this were evaluated based on how many values fell outside of the theoretical 95% error bounds; a good model was expected to have at least 95% of values fall within these error bounds (101). Coefficients of Discrimination (also known as Tjur's R^2) were also evaluated for this final model using *r2_tjur()* in the *performance* package in R, as typically used for generalized linear models with binary outcomes (102).

3.4 Results

3.4.1 Species detection

Species detections varied amongst types and sites (Fig. 3.2-3.4). All types were found at all sites except for Cuvier's beaked whales, which were not found at Kaua'i (Fig. 3.3). There was variable effort across weeks over all years. For Kaua'i, a maximum of three years of data were available for a given week, resulting in large standard errors in many cases.

3.4.2 Species composition

Species composition varied by site. At Hawai‘i, the most common species were stenellid dolphins, short-finned pilot whales, and Blainville’s beaked whale (present 90%, 62%, and 38% of days, respectively; Fig. 3.5a). At Kaua‘i, stenellids were also common, along with rough-toothed dolphins and then short-finned pilot whales (79%, 82%, 40%; Fig. 3.5b). At Manawai, Blainville’s beaked whales were by far the most common species (present 91% of days; Fig. 3.5c), though stenellids and Cuvier’s beaked whales were also common at this site (58% and 57% of days). Bray-Curtis dissimilarity tests further illuminated site-specific compositional differences. With Hawai‘i as the focal site (i.e., the site to which composition at all other sites was compared), Kaua‘i was most similar, with composition at Manawai being less similar (Fig. 3.6).

Comparing compositional results by-season provided additional context for these relationships. At Hawai‘i, changes were small (<16% in all cases, only 10% of between-season changes were larger than 10%) and the relative commonality of types (i.e., which type was most common, least common, etc.) changed very little across seasons (see Fig. S3.2.1 in Supporting Information). For Kaua‘i, variability was higher (seasonal differences up to 23%, 16% of differences >10%). As with Hawai‘i, these changes had little effect on the relative commonalities of types at this site, though the relationship between false killer whale and Blainville’s beaked whale shifted from summer to fall (i.e., false killer whales were more common than Blainville’s beaked whales in summer, but not fall; see Fig. S3.2.2).These smaller changes at Hawai‘i and Kaua‘i were reflected in the Bray-Curtis relationship between the two across all seasons (Fig. 3.6). Of the three sites, Manawai had the most seasonal variability in presence, with 22% of differences >10%, and a highest

difference of 29% (Table 3.1, see Fig. S3.2.3). This site saw the most notable change from winter to spring, with detections of nearly half the species considered increasing by at least 10% between these seasons (see Fig. S3.2.3). Seasonal shifts in detections were most dramatic for rough-toothed dolphins, with >10% difference in three of four seasons (exception being spring to summer, largest change (23%) from winter to spring; Table 3.1). Composition amongst all sites was most similar in the spring, and most different in the winter, though composition between Hawai‘i and Kaua‘i was most similar in the fall (Fig. 3.6).

3.4.3 Temporal Patterns

Temporal patterns were modeled with GAM-GEEs using hourly presence or absence of all types as response variable and hour of day, Julian day (as a proxy for seasonal changes), and year (Hawai‘i only) as explanatory variables. This provided information on the significance of these temporal scales to detection of species or types (Table 3.2). Types with fewer than 100 hours of detection at a site were not considered in modelling and pattern description efforts. Across all species and sites, hour of day (local time) was the most common significant variable, with only three cases in which it was not significant ($p>0.05$), and only four additional cases where it was not highly significant ($p>0.001$) (Table 3.2). Julian day was significant for all but five models. At Hawai‘i, where year was considered as a smoothed variable, year was a highly significant predictor for all species ($p< 0.001$ in all cases).

Performance of final models was generally poor, with no models having > 95% of values within the error bounds of the binned residuals plot, though several models (5 of 22) reached >90% (Table 3.3). These values did not necessarily correspond to higher R^2 values, nor was there a relationship between more detection hours and better model performance. Model results are discussed in further detail below. Full timeseries of detections for each species and site can be found in Supporting Information (Fig. S3.3.1 – Fig. S3.3.23).

3.4.3.1 Diel patterns

Clear diel patterns were found for most species and sites (Fig. 3.7). For false killer whales, Cuvier's beaked whales, and *Kogia* spp., detections increased during daylight hours. Probability of false killer whale detection was higher during mid-morning at Kaua'i (peak at 10:00- 11:00 HST; Fig. 3.7). For Cuvier's beaked whales, hour of day was a significant driver at Manawai with a peak in detections at 8:00-9:00. For this species at the Hawai'i site, timeseries examination revealed that diel detection changed over the years considered. Little to no diel pattern was present during the 2010 peak in detections, but a distinct increase in detection during daylight hours was seen in later years. Peak detection for *Kogia* spp. was slightly later in the day (around 13:00), with a strong diel trend only at Hawai'i. For rough-toothed dolphins, the bottlenose dolphin and melon-headed whale class, short-finned pilot whales, and stenellids, models showed a distinct diel trend, with echolocation detections being much lower in daylight hours (Fig. 3.7). For stenellids, this was particularly strong at Hawai'i (Fig. 3.7). For rough-toothed dolphins, there were fewer

detections during midday hours at Hawai‘i and Manawai, but this dip occurred slightly later (14:00-15:00 HST) for Kaua‘i. For short-finned pilot whales, diel patterning varied over considered years at Hawai‘i (see Fig. S3.3.16). Diel patterning was also more variable for Blainville’s beaked whales. For this species, there was an overall decline in detection throughout daylight hours at Kaua‘i. However, at Hawai‘i there was a slight increase in detections during midday. Examination of timeseries at this site showed that this diel patterning was much less evident during time periods with higher detections (e.g., 2011, 2017, see Fig.S3.3.22-S3.3.23).

3.4.3.2 Seasonal patterns

Seasonal patterning varied amongst species and sites. For false killer whales, detections were more common in the fall at Hawai‘i, versus an earlier peak in summer at Kaua‘i (Fig. 3.8). For rough-toothed dolphins, detections were more frequent in the spring at Kaua‘i and summer at Manawai, but in the winter for Hawai‘i (Fig. 3.8). Short-finned pilot whales had a seasonal pattern only at Kaua‘i, with higher detections during winter. For stenellids, detections were more common in spring at Kaua‘i and Manawai. At Hawai‘i, stenellids were detected in the highest numbers during winter (Fig. 3.8). Seasonal patterning for Blainville’s beaked whales was only apparent at Manawai, where there was a slight increase in detections in July-August. Patterning for Cuvier’s beaked whales indicated a fall-winter peak in detections at both Manawai as well as Hawai‘i. For the bottlenose dolphins and melon-headed whale class, seasonal trends were significant at

Kaua‘i and Manawai, with a slight peak in detections during the late winter and early spring at both sites.

3.4.3.3 Multi-year patterns

Long-term trends of species presence at Hawai‘i were significant for all types considered (Fig. 3.9). Short-finned pilot whales, rough-toothed dolphins, Blainville’s beaked whales, and Cuvier’s beaked whales all had markedly similar patterns in the years considered. For these species, predicted presence was highest in 2010-2011 and 2016, and lowest in 2014 and 2018 (Fig. 3.9). These species (with the exception of short-finned pilot whales) then saw an increase in presence in 2019 (Fig. 3.9). For rough-toothed dolphins and Cuvier’s beaked whales, years with lower probability of presence corresponded partially to years in which key seasons for those species were times of no-effort (Fig. 3.9). However, this did not hold true for the other species with this pattern. Variations on this pattern were observed for stenellids as well as the bottlenose dolphin and melon-headed whale class. For stenellids, a decrease was observed until 2014 and a 2016 peak was present before a decline again until the end of the dataset. The bottlenose dolphin and melon-headed whale class had a 2016 peak and 2018 decrease similar to many other species, but fairly consistent predicted presence prior to 2016. False killer whales had a peak in 2010-2011 similar to what was seen for other species, but then consistently low presence after this (large error bars make it difficult to conclude much about the trend post-2017). *Kogia* spp. had a slight dip in 2014, but a shifted peak with highest predicted presence in 2017-2018 before a steep 2019 drop off (Fig. 3.9).

3.5 Discussion

This study analyzed timeseries of species echolocation click detection for 8+ species of odontocetes in the Hawaiian Islands region at multiple sites and over a wide range of years and seasons. This allowed for novel comparisons of species composition and commonality amongst sites. It is worth noting that the species considered produce a variety of other vocalizations that were not considered in this study. Incorporation of these vocalizations (e.g., whistles, buzzes, burst pulses) would further contribute to fully describing acoustic presence patterns of the species considered. There are likely some vocalizations from pygmy killer whales, *Feresa attenuata*, in our dataset due to a resident population off the coast of Hawai‘i (103). These vocalizations would bolster detections of some species at this site, particularly during night-time hours when this population is thought to forage (104). It is not possible to quantify this effect, though based on knowledge of this species' echolocation (105), it is most likely being misclassified as a fellow delphinid species rather than a beaked whale. The effect of these misclassifications is probably mitigated by the small size of this population (103), although individuals from this population do use slope waters spanning the depth range of the HARP (67). Risso's dolphins, *Grampus griseus,* Fraser's dolphin, *Lagenodelphis hosei*, Longman's beaked whales, *Indopacetus pacificus,* and killer whales, *Orcinus orca,* are also known to be present around the islands but likely represent a very small proportion of misclassifications due to low sighting rates near the HARP sites (3). Some detections of beaked whales may also be misclassifications of an unidentified beaked whale species first detected at Cross

Seamount, Hawai‘i; this would be most likely at Kaua‘i where this species has been acoustically recorded on the U.S. Pacific Missile Range Facility (PMRF) (106).

Composition amongst sites generally followed expected trends, with observed Bray-Curtis values being presumably mostly related to spatial proximity. Examining changes in these relationships by-season demonstrated the robustness of the overall compositional results. Despite shifts in species detections amongst season that were demonstrated both in by-season compositional results as well as through temporal modelling, seasonal Bray-Curtis relationships remained markedly stable and similar to the full-data result (Fig. 3.6). While relationships between sites did not differ much, the spread of Bray-Curtis values compared to Hawai‘i did change, with sites being most similar in the spring and least similar in the winter. This is an interesting result that is mostly driven by changes in composition at Manawai. In the spring, higher similarity amongst sites is driven primarily by the increase in stenellids making composition at Manawai more like Hawai‘i than in other seasons. In the fall, lower similarity compared to Hawai‘i is driven by fewer stenellids and more Cuvier’s beaked whales at Manawai. The degree of seasonal changes in species detections (e.g., most consistent at Hawai‘i, less consistent at Manawai) may be driven by patterns in underlying oceanographic features, particularly those that affect prey availability (e.g., fronts, chlorophyll-a concentration). In particular, the higher degree of seasonal composition shifts at Manawai is likely related to movements of the Transition Zone Chlorophyll Front, which is closer to the islands in the winter and enhances local productivity (107). Differences in productivity between the Main Hawaiian Islands and Northwestern Hawaiian Islands are complex, and this likely leads to variations in species

behavior. Such differences are the subject of ongoing research efforts and will be the focus of a future paper.

Some distributional differences observed were also well-supported by existing sighting and tag records. The lack of Cuvier's beaked whales at Kauaʻi and higher presence at both Hawaiʻi and Manawai is corroborated by existing sighting records (24). Rough-toothed dolphin sighting rates are much higher off Kauaʻi than off Hawaiʻi (108), similar to our results. Documented trends in *Kogia* spp. (specifically *K. sima*) sightings also match our findings, in which detections were more common off Hawaiʻi than off Kauaʻi (90).

Using a neural network classifier, rather than manual labelling, to derive timeseries of detections necessarily resulted in some classification error. In this study, we used type and site-specific precision values to help mitigate these errors and avoid the obfuscation of actual patterns. The false killer whale class presents an opportunity to explore this in some detail. Due to low precision values (many misclassifications with noise), manual review was completed for all false killer whale detections, and this manually modified dataset was used moving forward (20). When comparing this timeseries to the precision-modified timeseries we might have used otherwise, it is clear that noise detections would have created artificial patterns. As an example, confusion with boat noise results in a diel pattern (higher detections during daylight) in the precision-based dataset at Hawaiʻi (see Fig. S3.3.24). Such effects are less pronounced at Kauaʻi and Manawai. This level of misclassification is more egregious than was seen for other sites and species, where the precision-based reductions were likely enough to mitigate errors. However, it bears

acknowledging that there may be residual errors in the patterns observed. Residual classification errors would likely affect short-finned pilot whales at Manawai and the bottlenose dolphin and melon-headed whale class at Hawai‘i more than other types, based on established precision values. Further study using this dataset might consider evaluating whether patterning existed in misclassifications, and how that might be used to better account for error in resulting timeseries.

For short-finned pilot whales as well as stenellids, multiple neural network classes existed for each type; these were combined for this analysis. Differences in stenellid click types were due to artificial spectral peaks introduced by a 25 kHz crossover frequency between low and high frequency hydrophones in some HARP setups (see Table S3.1.1). However, for short-finned pilot whales, it is possible that the types we combined could have different patterns in the data. In this case, reasoning for combining types was partially due to their scarcity, particularly at Manawai. If short-finned pilot whale classes had been left separate, one or both types might have had insufficient data for modelling at this site.

One aim of this study was to further examine temporal patterning to determine the species makeup of the stenellid and combined bottlenose dolphin and melon-headed whale class. For stenellids, the diel trends observed point to potentially different makeups of the types amongst sites. In addition to this, the preference of striped dolphins for deeper water (3) and apparent lack of resident population of spotted dolphins near Kaua‘i (109) may suggest that, at least at this site, the stenellid type is primarily composed of spinner dolphins. Site-specific differences in type makeup may also hold true for the bottlenose dolphin and melon-headed whale class. Some of the results presented (i.e., strong diel

cycle) may suggest that melon-headed whales make up a significant portion of this type. However, detailed sighting records from the Main Hawaiian Islands indicate a much higher presence of bottlenose dolphins near Hawai‘i and Kaua‘i (3). Based on this information, it is likely that the type makeup in the Main Hawaiian Islands is mostly bottlenose dolphins, though this may be different at Manawai. Discrimination of these species within this type might be possible with the addition of examining characteristics of underlying whistles that often accompany clicks of these types.

3.5.1 Temporal modeling

Overall, modelled patterns of detections corroborated patterns that were seen in the timeseries. Examining the importance of temporal variables in final models and across species and sites also provided a useful framework for considering temporal patterns of odontocete echolocation click detections in a given region. Hour of day was found to be the most significant temporal driver of species detections in this region, across all species and sites (except Hawai‘i, where year was significant for all species) (Table 3.1). Evaluation of models using binned residuals and Tjur's R^2 suggested that many of the models produced are not particularly good predictors of animal detections (Table 3.2). This is not an unexpected result, as only temporal patterning was considered here. Models would likely be improved by the inclusion of a variety of environmental variables that have been shown to be correlated with presence of odontocetes (e.g., chlorophyll-a, salinity, temperature). As the purpose of this study was to highlight spatiotemporal

patterning rather than provide predictive models, the poor fit of model residuals found here was not of particular concern.

3.5.1.1 Diel patterns

Hour of day was a significant driver of species detections in nearly all cases. Diel trends for false killer whales corroborated previous acoustic study of the species, which has suggested that the main Hawaiian Islands stock forages primarily during the day (110). This pattern could also be the result of inshore-offshore diel movement patterns resulting in animals being nearer to HARP locations (i.e., inshore) during the day, and further away at night. For rough-toothed dolphins and short-finned pilot whales, diel patterns across all sites (i.e., less acoustic activity during daylight) match with previous studies of these species in Hawai‘i (66,110). Increased acoustic activity during the night was also observed for the bottlenose dolphin and melon-headed whale class, which matches with existing knowledge of melon-headed whale behavior (111,112). Bottlenose dolphins, in contrast, have been known to forage during both day and night-time periods (24). However, it is possible that the diel pattern seen could be related to spatial movements of a species that is foraging during both time periods.

For Blainville’s beaked whales, detections were more frequent during the day at Hawai‘i. The daytime peak in detections for this species is congruent with previous studies in Hawai‘i which used a subset of this dataset (15). However, other regional work on beaked whales has not noted diel differences in foraging-related behavior (73,113). Fewer detections during the night at Hawai‘i may be related to horizontal movements—whales

may be moving further offshore, leading to a dip in detections at the HARP site during those hours. Temporal patterning of species off Kaua‘i, particularly beaked whales, may also be impacted by frequent sonar events. The Kaua‘i HARP is close to the southernmost extent of the PMRF. Previous study on this range has noted that diel behavior of Blainville’s beaked whales is impacted by multi-day Navy training events, with no diel pattern before training events, but peaks in acoustic detections in both morning and afternoon during and after training events (37). More recent research has found that both multi-day training events and the presence of mid-frequency active sonar can greatly reduce the presence of vocalizing whales (114).

For stenellid dolphins, detections were far fewer during daylight hours, though the degree of this pattern varied amongst sites. This trend may elucidate species makeup of this type. Spinner dolphins echolocate nearly exclusively at night and spend days resting in shallow bays (70), whereas spotted dolphins echolocate during the day, although still much more actively at night (24,71). For *Kogia* species, no regional comparable studies existed. However, a study of *Kogia* spp. temporal behavior from the Gulf of Mexico found higher acoustic presence during the day at some sites, which is consistent with the pattern seen here for Hawai‘i (17).

3.5.1.2 Seasonal patterns

For false killer whales and rough-toothed dolphins, the seasonality of use seen at various sites (Hawai‘i and Kaua‘i for false killer whales, all modeling sites for rough-toothed dolphins) have been noted in very few previous studies. Research on the Main

Hawaiian Islands insular stock of false killer whales found some spatial variability in use of the Main Hawaiian Islands region for one social cluster of animals, with highest presence west of Hawai‘i during spring and early summer (May through July) and west of Kaua‘i in summer and early fall (August through October) (115). This is somewhat in agreement with our results (i.e., spring-summer peak in Kaua‘i, SFig 3.2.2), though peak season in our data from Hawai‘i is fall rather than spring (SFig 3.2.1, Fig. 3.8). As there are few detections of this species in our record at Hawai‘i, and previous seasonal variation was noted for only one social cluster so far, more data would be needed to examine the reasons for this discrepancy. The area near the Hawai‘i HARP is not a high-use area for this stock, so this record may not represent their overall use of the Hawai‘i Island lee particularly well. It is also worth noting that the Main Hawaiian Islands insular stock is one of three stocks of false killer whales present in the Hawaiian Islands (116), all three of which use the waters around Kaua‘i. For two of these three stocks (i.e., Northwestern Hawaiian Islands and Hawai‘i pelagic stocks), seasonality of presence has not been documented. Shifting presence of these stocks may also have effects on overall false killer whale detections at Kaua‘i (76).

Rough-toothed dolphin detections were higher in the spring-summer in our data from Kaua‘i, which matches with previously modelled high-use areas during these seasons (117). For short-finned pilot whales, previous work near Kaua‘i found seasonality in detections southwest of the island, in a similar location to the HARP (118). This study also found an increase in detections in the April-June period. Additional study of this species has suggested that animals may spend more time diving further from shore during fall and

winter (74). In this case, we might expect to see a decrease in detections during these seasons, which matches the general seasonal trend seen at Kauaʻi. The lack of seasonality observed at Hawaiʻi is in accordance with previous studies which have modelled the region west of Hawaiʻi as high-use area for this species year-round (117).

For Blainville's beaked whales increased detections in the fall at Kauaʻi and summer at Hawaiʻi have been noted in a previous study which used a subset of this HARP dataset (5). The patterns shown here matches this prior report, though with this larger sample size, the trend was no longer statistically significant. Seasonal patterning here may suggest movement around the island or offshore, potentially related to shifts in a nearby foraging hotspot (85). Records of Blainville's beaked whale acoustic detections in the PMRF range have noted decreased detections after multi-day naval training events (i.e., prolonged sonar activity periods), which occur in February and August (37). This behavior does not seem to have been captured in our data, despite the Kauaʻi site location's proximity to the southern edge of the PMRF. Previous research on Cuvier's beaked whales near Hawaiʻi Island did note a seasonal peak in the fall similar to what was noted here (5). However, other studies of Cuvier's beaked whales in the region have noted that the species uses the waters near Hawaiʻi Island year-round and saw no seasonal changes (119). For stenellid dolphins, observed seasonal patterns in presence have not previously been noted. Seasonal trends in *Kogia* spp. detections have no comparable previous records, though recent study of *K.* sima has indicated the detections of a resident population off Hawaiʻi, with much lower encounter rates off Kauaʻi, particularly on the western side of the island (90). No previous studies have considered seasonality at Manawai.

3.5.1.3 Multi-year patterns

Multi-year analysis at Hawai‘i yielded interesting results in several cases, though in most cases these patterns had no comparable records in the literature. A distinct peak in presence in 2010 was observed for rough-toothed dolphins, short-finned pilot whales, and Blainville's and Cuvier's beaked whales. In 2014, a dip in presence was observed for many types. Presence then peaked again in 2016 for all types except false killer whale and *Kogia* spp., before a dip in presence in 2018. This decline was particularly sharp for rough-toothed dolphins, the bottlenose dolphin and melon headed whale class, and Cuvier's beaked whale. Some of these dips may be exacerbated by low effort during key seasons (i.e., lower presence for false killer whales in 2014-2016 may be related to lack of recordings during fall in those years). One downside of including year as a smoothed term in this model is that the representative figures necessarily indicate relationships during years where there is little to no data (i.e., 2012, 2013). It is not possible to say whether the true relationship during those years would be similar to what the model suggests, so we refrained from drawing conclusions related to those time periods. Changes in presence may also be linked to oceanographic variables, particularly those that affect the presence of various prey species. The dip in presence in 2018 is particularly interesting as there was continuous effort throughout that year. Future work on this dataset using environmental correlates may illuminate the reasons for this decrease in detections.

3.6 Conclusions

Discussion of various temporal predictors in relation to previous studies highlights the importance of continued monitoring efforts, in this region and others, to inform understanding of odontocete spatiotemporal patterns. This is especially true for species where this study presents the first regional description of a given pattern, or previous records are not comparable to the effort of the PAM dataset used (e.g., seasonal trends for false killer whale, rough-toothed dolphin, and *Kogia* spp.). The work presented here highlights the utility of using multiple methodologies for studying species in this region and others.

In terms of multi-year trends, results of this study at Hawai‘i are novel for most species, though it is worth noting that, as the detection range covered by the HARPs is relatively small, shifts in acoustic presence may represent small shifts in high-use areas by island-associated populations. In Hawai‘i, few long-term trends have been described, though portions of this dataset have been used for long-term assessments of sperm whales (7) and humpback whales (120). Additionally, there are multiple species (e.g., rough-toothed dolphin, *Kogia* spp.) where the records provided here have little to no comparison in previous literature. In that way, this study may provide a useful starting point for other species-specific studies of these animals. Future work employing these results in models considering environmental and anthropogenic parameters will help provide explanations for the patterns observed. These will be useful in the further understanding of these species habitats and behaviors and may help to explain any existing behavioral discrepancies between this and previous studies. These behaviors and movements are important to understand in the context of the Hawaiian ecosystem to which these odontocetes belong.

The work completed emphasizes the merits of establishing baselines and comparing patterns of detections on fine temporal and spatial scales in marine top predator monitoring efforts. The patterns established in this study provide useful records to which additional studies of included species can be compared, allowing for documentation of regional differences in temporal behaviors which may be relevant for conservation purposes. These processes are necessary for management and conservation efforts of these species regionally as well as worldwide.

3.7 Acknowledgements

This work was funded by the NOAA Pacific Islands Fisheries Science Center. Manawai HARP deployments were permitted by the Papahānaumokuākea Marine National Monument under permits PMNM-2008-020 and PMNM-2010-042 and the Co-Managers permit since 2015. Thanks to Ann Allen, Erik Norris, and others at the NOAA Pacific Islands Fisheries Center for their instrument deployment, retrieval, and work at all sites used in this study. Thank you to all members of the Scripps Whale Acoustics Lab, the Scripps Acoustic Ecology Lab, and the Scripps Machine Listening Lab for support over the course of this project. Thanks to Erin O'Neill for her work in processing HARP deployments and Bruce Thayre and John Hurwitz for their work on the HARP instruments. A special thanks to fellow graduate students Rebecca Cohen and Natalie Posdaljian for numerous discussions on the methods employed here which greatly improved the work.

Chapter 3, in full, is in preparation for publication of the material (Global Ecology and Biogeography). Ziegenhorn, Morgan A., John A. Hildebrand, Erin M. Oleson, Robin

W. Baird, Sean M. Wiggins, and Simone Baumann-Pickering. "Odontocete spatial patterns and temporal drivers of detection at sites in the Hawaiian Islands." The dissertation author was primarily responsible for the investigation and writing of this material.

3.8 Figures and Tables

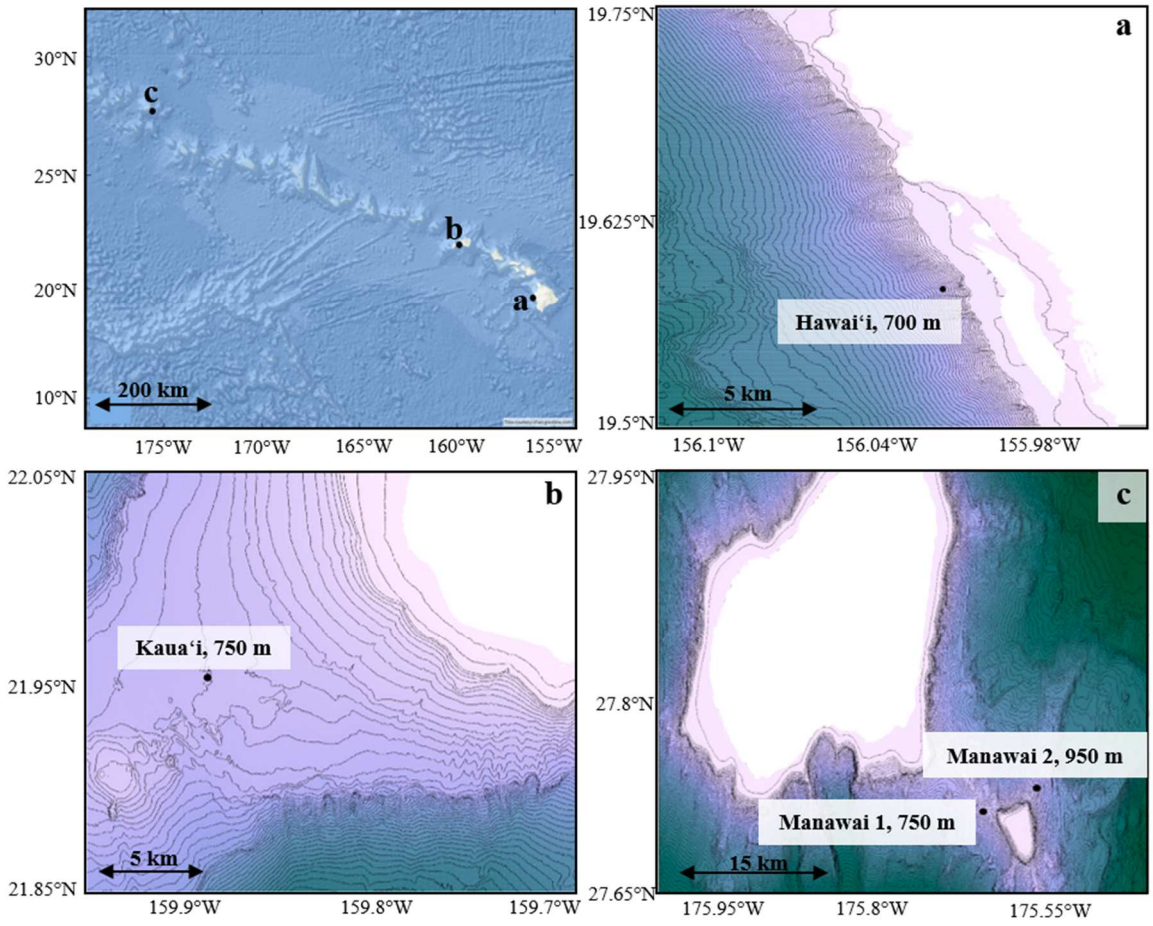

Figure 3.1. Deployment locations. Recording sites for this study, showing the location and average depth of each site, with 50m contour lines. Top left panel shows site locations in context of the Hawaiian Islands chain. Panels a-c show locations of Hawaii, Kaua'i , and Manawai sites (respectively). Basemap in top left image is the intellectual property of Esri and is used herein with permission. Copyright © 2022 Esri and its licensors. All rights reserved. Bathymetry data used for panels a-c accessed from the Hawai'i Mapping Research Group at the University of Hawai'i at Manoa. (a-b, accessible here: http://www.soest.hawaii.edu/hmrg/multibeam/bathymetry.php) and Pacific Islands Ocean Observing System (c, accessible here: https://pae-paha.pacioos.hawaii.edu/thredds/bathymetry.html?dataset=hurl_bathy_60m_nwhi).

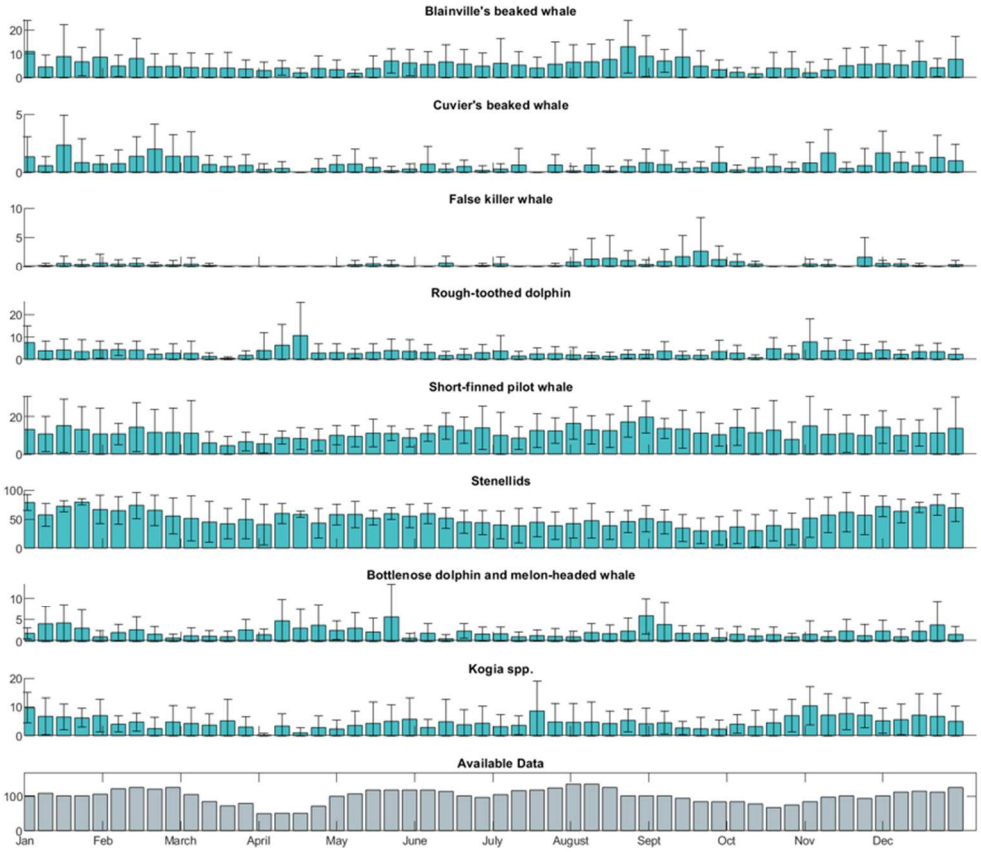

Figure 3.2. Seasonal detections at Hawai‘i. Seasonal detections (hours per week) of all types at Hawai‘i. Note that Y-axis scales vary for each species. Average detections with standard error across available years of data is shown. Detections are not corrected for total hours of available data during a given week.

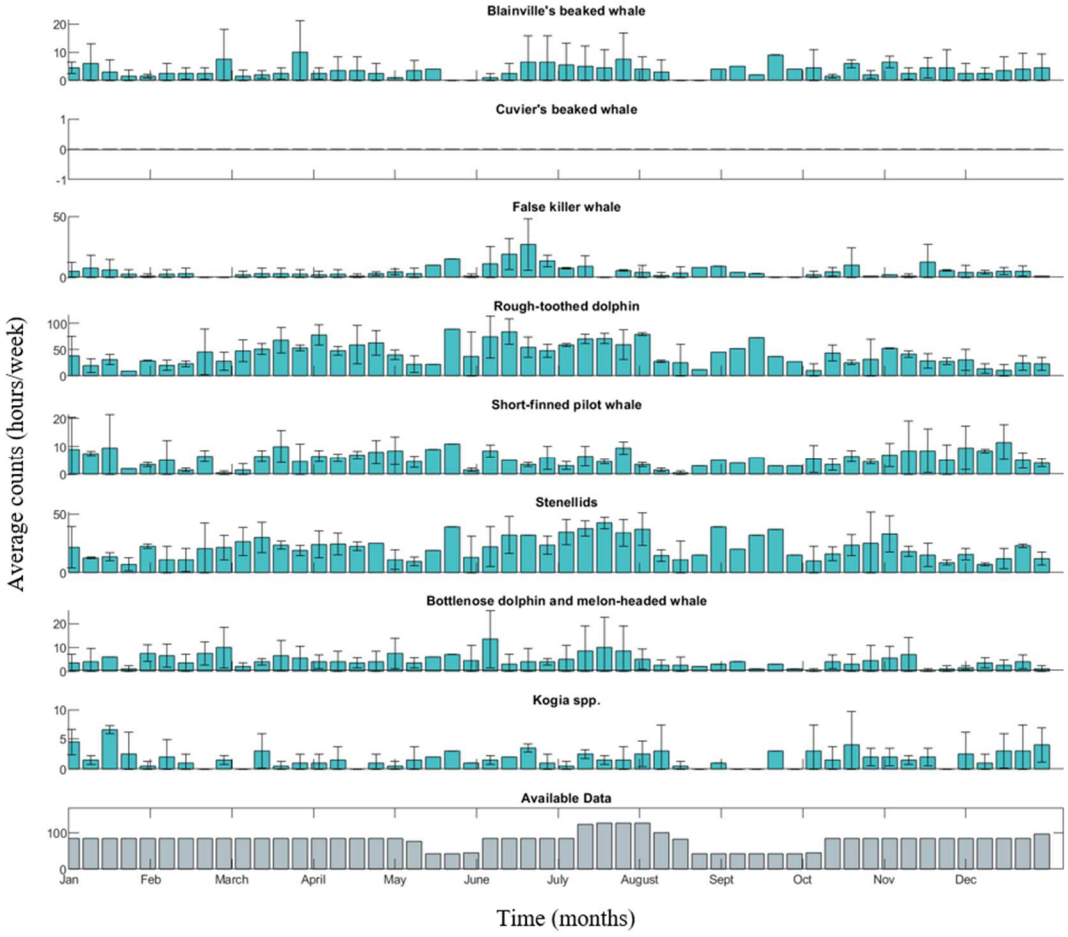

Figure 3.3. Seasonal detections at Kaua‘i. Seasonal detections (hours per week) of all types at Kaua‘i. Note that Y-axis scales vary for each species. Average detections with standard error across available years of data is shown. Detections are not corrected for total hours of available data during a given week.

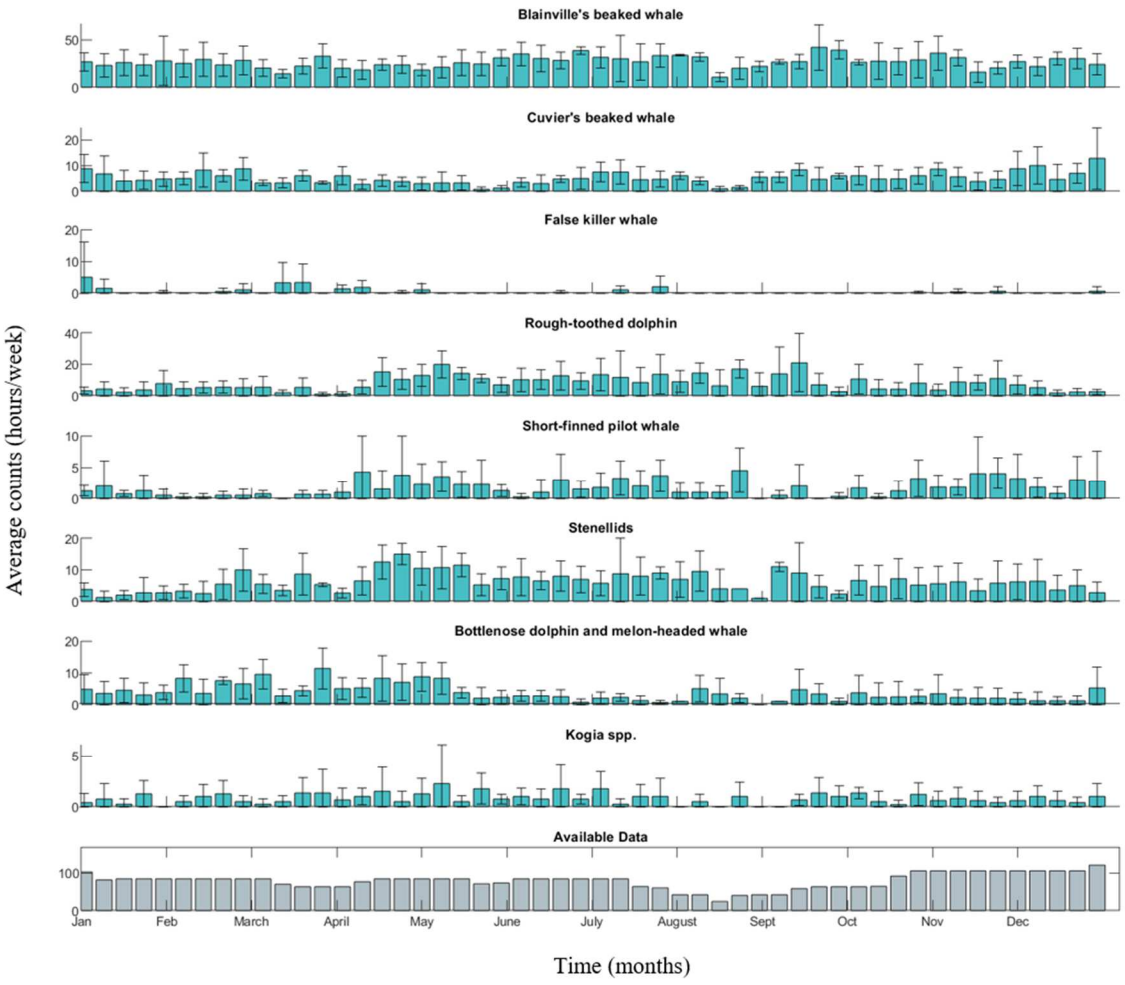

Figure 3.4. Seasonal detections at Manawai. Seasonal detections (hours per week) of all types at Manawai. Average detections with standard error across available years of data is shown. Detections are not corrected for total hours of available data during a given week.

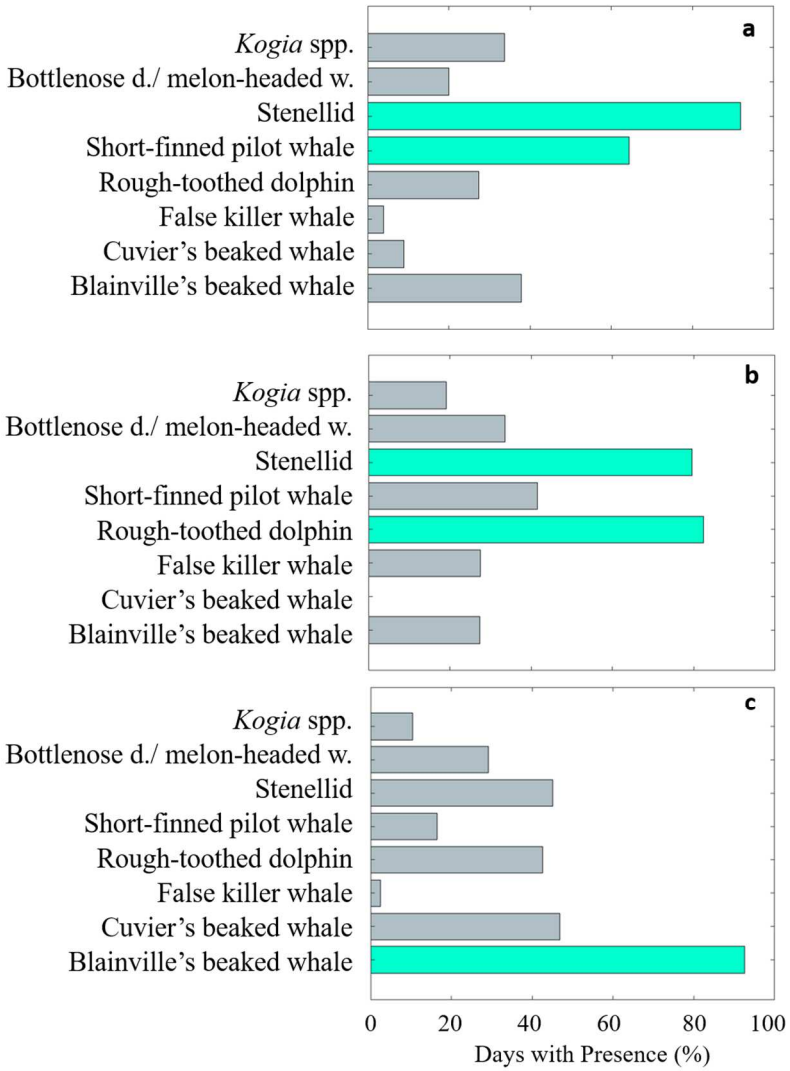

Figure 3.5. Percentage days with detections. Percent days out of total recording days at each site with detections of each type. Sites are (a) Hawai‘i, (b) Kaua‘i, and (c) Manawai. Values greater than 50% are shown in green.

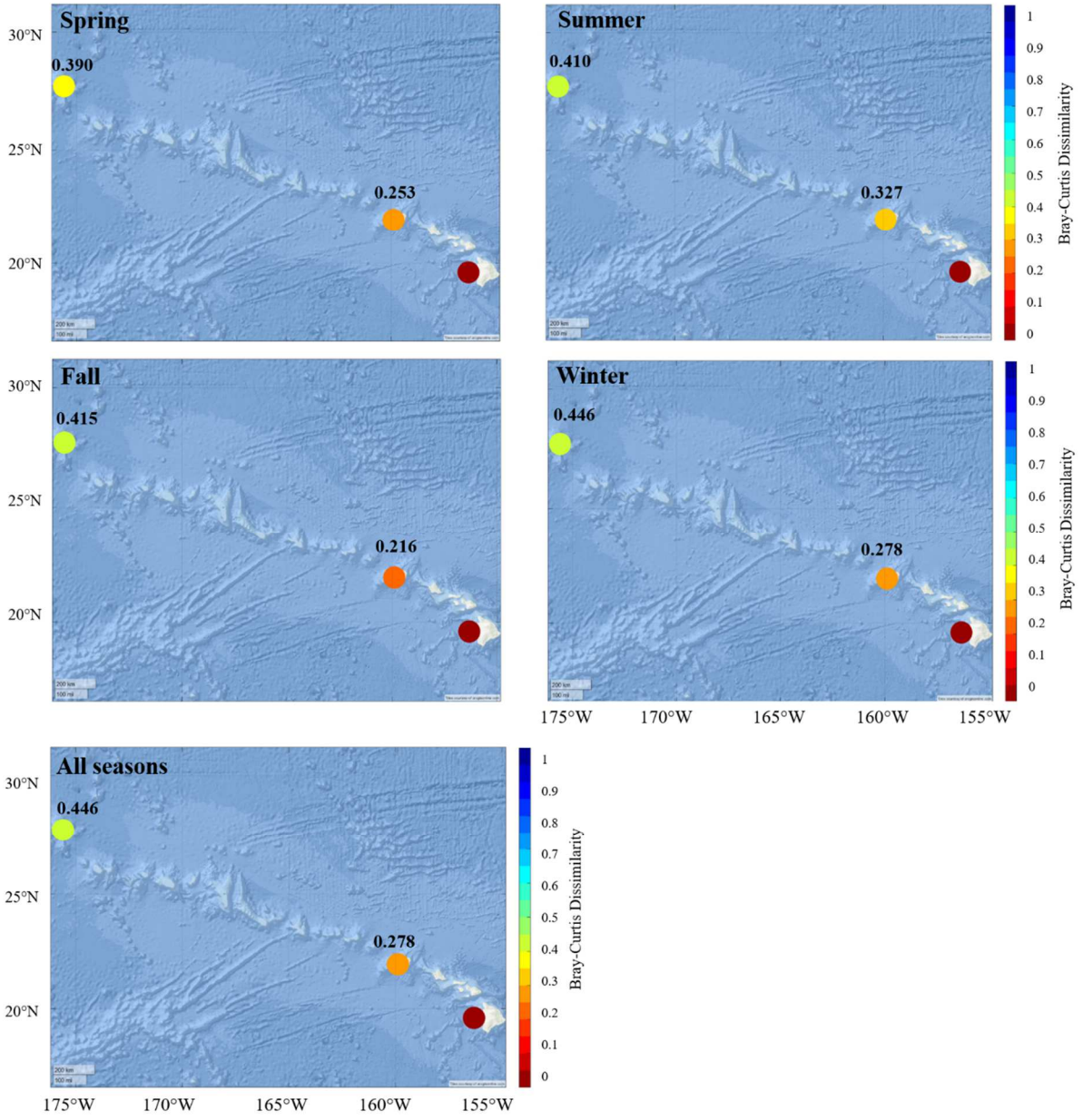

Figure 3.6. Bray-Curtis dissimilarity map. Depiction of Bray-Curtis dissimilarity amongst sites with Hawai‘i as the focal site in each season, as well as overall. Color is used to depict Bray-Curtis value between the focal site and each other site, with red representing sites where composition is the same, and blue representing sites with no overlap in species. Exact Bray-Curtis values are shown above corresponding sites. Basemap image is the intellectual property of Esri and is used herein with permission. Copyright © 2022 Esri and its licensors. All rights reserved.

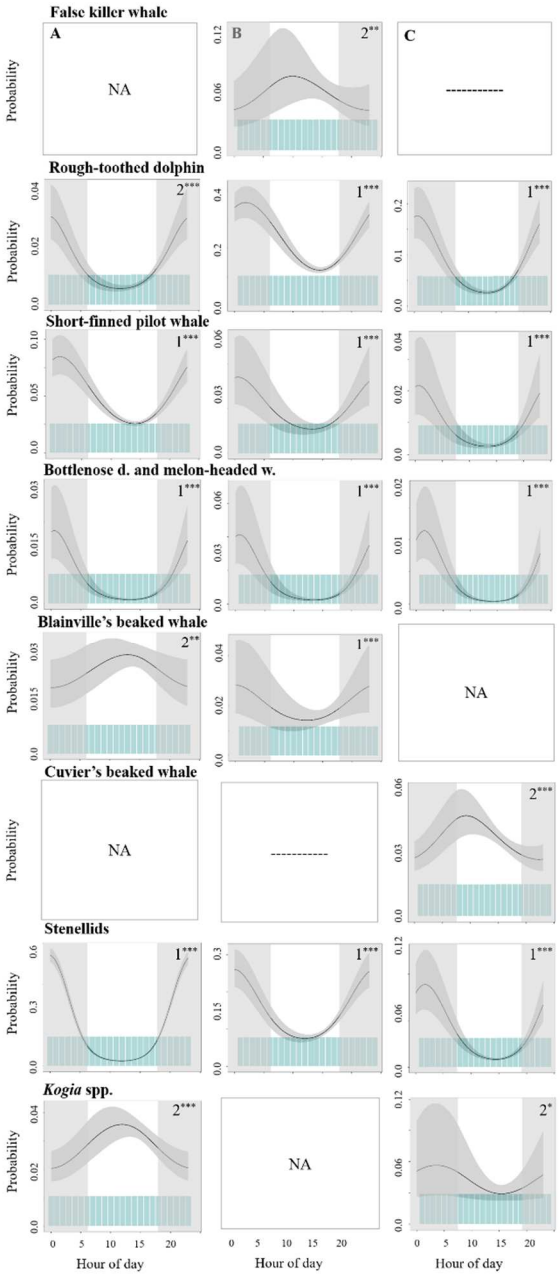

Figure 3.7. Diel patterns. Partial-fit plots for hour of day (in HST) for all types at (A) Hawai‘i, (B) Kaua‘i, (C) Manawai. Plots show the probability of species detections with 2.5 and 97.5 percentile value confidence intervals. Blue polygons at the bottom of each plot give the distribution of the underlying data. Model order is given for significant variables (1st- 4th). Asterisks show significance level (*** = p< 0.005, ** = p<0.01, * = p<0.05). Non-significance is denoted by ‘NA’; sites without a model are represented by ‘—‘.

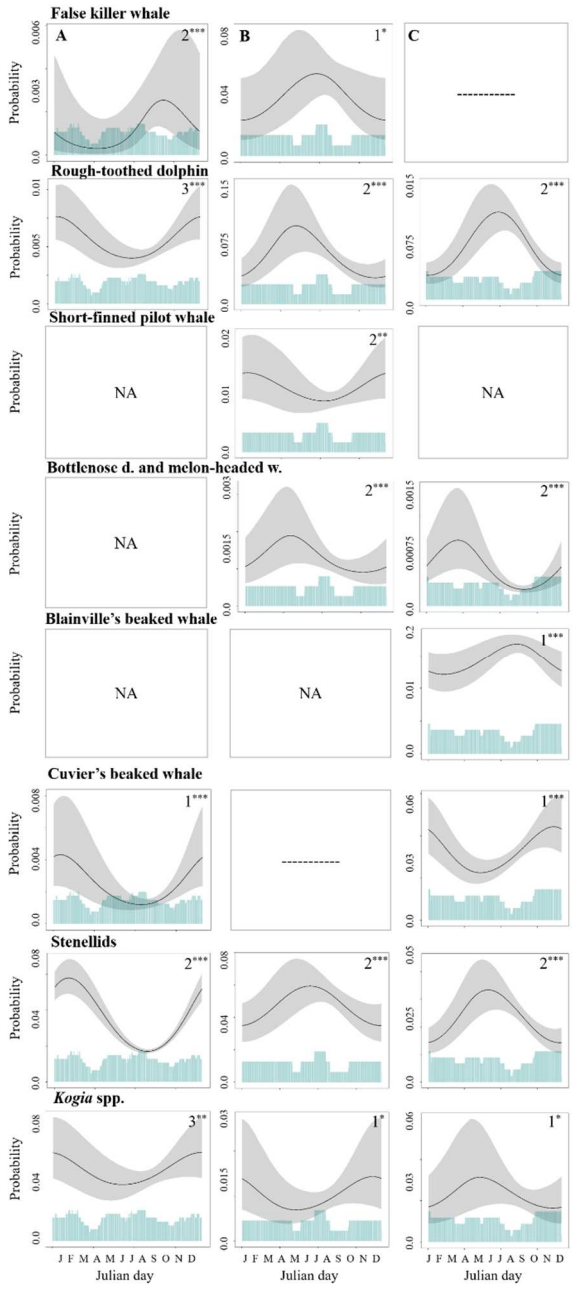

Figure 3.8. Seasonal patterns. Partial-fit plots for Julian day for all types at (A) Hawai‘i, (B) Kaua‘i, (C) Manawai. Plots show the probability of species detections with 2.5 and 97.5 percentile value confidence intervals. Blue polygons at the bottom of each plot give the distribution of the underlying data. Model order is given for significant variables (1st-4th). Asterisks show significance level (*** = p< 0.005, ** = p<0.01, * = p<0.05). The first letter of each month is shown instead of day of year, for ease of readability. Non-significance is denoted by ‘NA’; sites without a model are represented by ‘—‘.

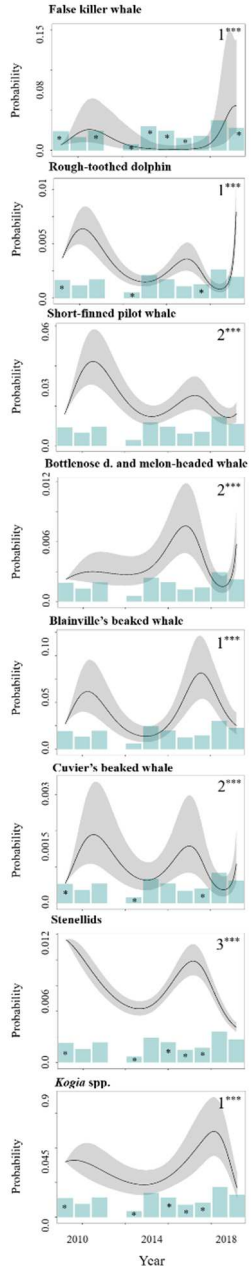

Figure 3.9. Multi-year patterns. Partial-fit plots for year for all types at Hawai‘i. Plots show the probability of species detections with 2.5 and 97.5 percentile value confidence intervals. Blue polygons at the bottom of each plot give the distribution of the underlying data. Model order is given for significant variables (1^{st}- 4^{th}). Asterisks show significance level (*** = p< 0.005, ** = p<0.01, * = p<0.05). The first letter of each month is shown instead of day of year, for ease of readability. Asterisks on histogram data indicate years in which data from a key season for this type was missing.

Table 3.1. Seasonal differences in percent presence. Seasonal changes in percentage of recording days with presence at all sites. Season codes are SpSu = spring to summer change, SuFa = summer to fall, FaWi = fall to winter, WiSp = winter to spring. Changes greater than +/- 10 are given in bold.

Percentage Detections Difference (%)		Type							
		Blainville's beaked whale	Cuvier's beaked whale	False killer whale	Rough-toothed dolphin	Short-finned pilot whale	Stenellids	Bottlenose d./ Melon-headed w.	*Kogia* spp.
Hawai'i	SpSu	7.98	-2.19	1.52	-5.76	8.82	-5.73	-5.06	2.47
	SuFa	-9.58	3.95	2.82	7.81	**-10.9**	-8.16	-0.12	7.28
	FaWi	**10.3**	4.57	-2.94	3.33	7.25	**16.8**	3.36	1.36
	WiSp	-8.74	-6.32	-1.40	-5.38	-5.19	-2.90	1.82	**-11.1**
Kaua'i	SpSu	-7.97	NA	7.99	**-10.4**	-9.32	-6.20	1.37	3.66
	SuFa	**18.4**	NA	**-12.7**	-4.02	8.38	-2.92	-9.37	1.05
	FaWi	-9.34	NA	3.08	-9.03	-2.85	-8.77	5.38	2.36
	WiSp	-1.06	NA	1.67	**23.4**	3.79	**17.9**	2.98	-7.07
Manawai	SpSu	3.30	3.98	-2.13	3.43	2.30	-6.62	**-23.9**	-2.01
	SuFa	-0.511	9.09	-0.63	**-14.5**	-0.16	-7.13	1.89	-1.24
	FaWi	-1.29	0.82	1.63	**-12.3**	-7.90	**-15.2**	6.58	-0.03
	WiSp	-1.49	-13.9	1.13	**23.4**	5.76	**29.0**	**15.4**	3.28

Table 3.2. Model results. Table showing model results for all types at all sites. Included variables are hour of day (Hour), percentage of lunar illumination (Lunar), Julian day, and year. Number of hours with presence of a type is given by nPres. Significant variables are marked with their order (o) in the model (i.e., 1st – 4th) and with *** = p <0.001, ** = p<0.01, and * = p<0.05. Degrees of freedom (d) and Chi-squared values (χ^2) are given for all variables. Blank spaces indicate lack of significant variables. Gray boxes indicate insufficient presence hours for modelling.

Model Results (order and significance, df, χ^2)		Type							
		False killer whale	Rough-toothed dolphin	Short-finned pilot whale	Bottlenose d./ Melon-headed w.	Blainville's beaked whale	Cuvier's beaked whale	Stenellids	*Kogia* spp.
Hawai'i	Hour		2***, 5, 232	1***, 2, 294	1***, 2, 373	2**, 2, 9.93		1***, 2, 6478	2***, 2, 33.2
	Julian day	2**, 2, 12.3	3***, 2, 34.3				1***, 2, 38.4	2***, 2, 469	3**, 2, 10.3
	Year	1***, 5, 34.8	1***, 2, 197	2***, 5, 67.1	2***, 5, 74.5	1***, 5, 48.2	2***, 5, 43.0	3***, 5, 386	1***, 5, 58.5
	nPres	141	1036	3843	678	1836	234	17509	1612
Kaua'i	Hour	2**, 2, 10.8	1***, 2, 311	1***, 2, 64.4	1***, 2, 309	1***, 2, 17.2	--	1***, 2, 233	
	Julian day	1*, 2, 6.89	2***, 2, 34.1	2**, 2, 10.1	2***, 2, 16.1		--	2***, 2, 21.8	1*, 2, 8.68
	nPres	480	4038	546	436	346	<100	2049	170
Manawai	Hour	--	1***, 2, 337	1***, 2, 126	1***, 2, 357	2**, 2, 10.2	2***, 2, 46.3	1***, 2, 481	2*, 2, 7.70
	Julian day	--	2***, 2, 86.6		2***, 2, 62.9	1***, 2, 17.9	1***, 2, 48.8	2***, 2, 53.8	1*, 2, 8.63
	nPres	<100	1558	358	1233	5343	1059	745	162

Table 3.3. Model evaluation. Table showing model evaluation for all types at all sites with number of hours with presence (nPres), percentage of values that were within 95% error bounds in binned residual plots (% Res), and Tjur's R^2 values for each model (Res R^2). Gray boxes indicate insufficient presence hours for modelling. Models with greater than 90% percent res values are bolded.

Type	Hawai'i			Kaua'i			Manawai		
	nPres	Percent Res	Res R^2	nPres	Percent Res	Res R^2	nPres	Percent Res	Res R^2
False killer whale	141	22	0.005	480	84	0.005	<100	--	--
Rough-toothed dolphin	1036	75	0.020	4038	**91**	0.067	1558	87	0.034
Short-finned pilot whale	3843	82	0.028	546	**86**	0.006	358	78	0.005
Bottlenose d./ Melon-headed w.	678	59	0.015	436	60	0.021	745	64	0.026
Blainville's beaked whale	1836	73	0.009	346	**91**	0.001	5343	**96**	0.003
Cuvier's beaked whale	234	48	0.002	<100	--	--	1095	**92**	0.004
Stenellids	17509	47	0.322	2049	85	0.033	1233	87	0.026
Kogia spp.	1612	86	0.006	170	68	0.001	162	59	0.006

Chapter 4: Oceanographic conditions as indicators of odontocete detection in the Hawaiian Archipelago

Morgan A. Ziegenhorn[1*], John A. Hildebrand[1], Erin M. Oleson[2], Robin W. Baird[3], Simone Baumann-Pickering[1]

[1] Scripps Institution of Oceanography, University of California San Diego, La Jolla, CA, USA

[2] NOAA Fisheries Pacific Islands Fisheries Science Center, Honolulu, HI, USA

[3] Cascadia Research Collective, Olympia, WA, USA

4.1 Abstract

For many taxa, understanding environmental drivers of species' behavior can be key for successful management and conservation, and can also aid in predicting response to future conditions and climate change scenarios. Within cetacean research, studies focused on these goals often consider local conditions (e.g., currents, bathymetry), but usually records are not long nor complete enough to consider larger climate indices. We make use of a long-term passive acoustic monitoring (PAM) dataset to examine relationships between toothed whale detections and climate indices (El Niño Southern Oscillation (ENSO), Pacific Decadal Oscillation (PDO), and North Pacific Gyre Oscillation (NPGO)) as well as surface conditions (temperature, salinity, sea surface height) at several sites in the Hawaiian Islands. We find that, of the surface variables considered, temperature was the best predictor of detections. Sea surface height was the only variable where correlations with detections were consistent for a given species across sites, with the exception of the bottlenose dolphin and melon-headed whale class. Of the climate indices considered, ENSO may have the most effect on species detections at monitored sites. In many cases, detection patterns match well with combinations of one or more climate indices. In some cases, combinations of fluctuations in surface conditions and climate indices matched well with the detection patterns observed. We highlight the importance of considering climate indices in habitat modelling. We conclude that habitat modelling using long-term records can provide valuable insights into top predator behavior in relation to both surface conditions and long-term climate cycles.

4.2 Introduction

As a productive oasis in the generally oligotrophic North Pacific Subtropical Gyre (121), the Hawaiian archipelago provides a unique study site for toothed whales (odontocetes), with at least 18 species of odontocetes residing in the region. The archipelago consists of volcanic islands, separated into the Northwestern Hawaiian Islands (older, lower islands) and the Main Hawaiian Islands (newer, higher islands). Oceanographic conditions in these regions differ significantly, with the Main Hawaiian Islands experiencing high nearshore upwelling (8), regional fronts and leeward eddies (1,9–12), and increased mixing and turbulence in channels between islands that encourage high primary productivity (8). This subsequently provides rich foraging grounds for many odontocete prey species. Nutrient input along coastal areas from frequent rainfall and steep island slopes also promotes the flourishing of odontocete prey; this effect is concentrated nearshore on the windward side of the islands but more dispersed and diluted in the islands' lees due to westerly winds (122). In the Northwestern Hawaiian Islands, the contrast between inshore and offshore production is less marked because of a lack of high islands and eddies, as well as a proximity to the Subtropical Convergence Zone (123). However, proximity to the transition zone chlorophyll front near this convergence zone also results in higher productivity and increased abundance of odontocete prey species compared to the surrounding gyre (84). The heightened production supported by these processes provides prime habitat for odontocete species and causes many species to stick close to the islands.

Both parts of the island chain are also influenced by large-scale climate events, including the El Niño Southern Oscillation (ENSO), the Pacific Decadal Oscillation (PDO), and the North Pacific Gyre Oscillation (NPGO). The ENSO cycle describes the anomalous coupling of tropical Pacific ocean-atmosphere conditions, which is naturally occurring and varies on a 4-7 year scale, with global effects (e.g., 124–126). The PDO cycle is a longer-lived climate variability pattern, with warm and cool phases classified by anomalous surface temperatures in the northeast and tropical Pacific Ocean, varying on a scale from 15-25 years (127). The NPGO is also longer-lived. This index is related to the second dominant mode of sea surface height variability in the Pacific and reflects changes in the circulation of the North Pacific Subtropical Gyre (128).

In the Main Hawaiian Islands, positive ENSO and PDO conditions are linked to higher sea surface temperature as well as lower sea surface salinity, mixed-layer depth, chlorophyll-a concentrations, and net primary productivity (129). Negative ENSO and PDO conditions are linked to opposite trends, resulting in higher productivity during negative ENSO and PDO phases. In contrast, in the Northwestern Hawaiian Islands, relationships to ENSO and PDO are more likely to be related to movements of the transition zone chlorophyll front that fluctuates seasonally and is closest to the islands during the winter (30-35 N), furthest away in the late summer (40-45 N) (130). In this case, positive ENSO and PDO conditions lead to southward movement of the front, resulting in higher productivity in the region; this is especially pronounced in the winter (131,132). This is primarily driven by the PDO but is enhanced by positive ENSO conditions (133). These patterns are driven by the tradeoff between the predominant northeasterly trade

winds (which are stronger during negative ENSO and PDO phases), as opposed to stronger westerly winds during positive phases (133). Across the entirety of the islands, it has been noted that positive PDO causes more frequent positive ENSO events, and vice versa (134), further emphasizing the combined effects of these two climate indices.

Fluctuations in the NPGO seem to have the same affect across the entirety of the Hawaiian archipelago. In this case, the positive phase is related to faster currents in the North Pacific Subtropical Gyre, which results in lower sea surface temperature in Hawai‘i (135). In addition, positive NPGO conditions have been related to higher sea surface salinity and mixed-layer depth as well as higher net primary productivity (129), with the opposite being true for negative NPGO conditions. These fluctuations in productivity may influence influence the distributions and patterns of odontocetes in the area over long timescales as they follow shifting prey.

Habitat modeling of cetaceans has become a high-priority goal for scientists and managers in the past several decades. Using habitat models, scientists can become better informed about patterns of cetacean movement and their drivers. These drivers can include both intrinsic and extrinsic factors such as behavior, life-history strategies, foraging considerations, and anthropogenic influences. Studies of this nature often include surface-related variables (i.e., sea surface height, temperature, salinity (82,136–138)), bathymetric data (139–141), prey-associated variables (82,136,142), distances to oceanographic features (e.g., eddies (12,143,144), seamounts (144,145), shore (146,147)), and anthropogenic influences (37,148).

Previous studies in the Hawaiian region have generally obtained the odontocete detections data necessary for modeling from tag data, sighting data, and limited passive acoustic data (108,149–151). However, temporal resolution these studies has often been limited, resulting in little consideration of long-term climate states. An existing passive acoustic monitoring (PAM) dataset from the region covering the years 2009-2019 at sites in both the main and northwestern Hawaiian Islands provides unique opportunities to understand the relationships between both surface conditions and long-term climate indicators (ENSO, PDO, NPGO) in the Hawaiian Islands in relation to odontocete species. This dataset has been used in a previous study to extract and classify echolocation clicks, which are produced by odontocetes in a variety of behavioral states, though primarily while foraging. This study resulted in timeseries of echolocation click detections for 8 groupings of odontocetes, including five species-specific groups: false killer whale (*Pseudorca crassidens)*, rough-toothed dolphin (*Steno bredanensis),* short-finned pilot whale (*Globicephala macrorhyncus),* Blainville's beaked whale (*Mesoplodon densirostris),* and Cuvier's beaked whale (*Ziphius cavirostris).* Additional genus or group level categories were included for stenellid dolphins (including some mixture of pantropical spotted dolphin (*Stenella attenuata),* striped dolphin (*S. coeruleoalba),* and spinner dolphin (*S. longirostris)*), *Kogia* spp. (primarily dwarf sperm whale (*K. sima),* but potentially containing detections of pygmy sperm whale (*K. breviceps)* based on sighting record (90)), and a type representing an unknown mixture of common bottlenose dolphin (*Tursiops truncatus)*, and melon-headed whale (*Pepnocephala electra)* (20).

Resulting timeseries from this effort were then used to document spatial and temporal patterns in detections, noticing that composition amongst sites considered was robust to season, and that temporal changes in detections varied primarily on a diel scale but also often on a seasonal scale (Ziegenhorn et al. (in prep)). Long-term trends were assessed at one site, and several distinct changes in detections were noted. However, relationships between detections and oceanographic indicators that may provide explanations for the patterns seen have not yet been assessed. Understanding the oceanographic and climatological base for odontocete detections in the islands aids in the understanding of their movement patterns over a variety of timescales. As marine top predators, odontocetes are an important part of the regional marine ecosystem and localized shifts in presence, reflected in acoustic detections, may have significant effects on lower trophic levels due to top-down trophic effects (152). In addition to this, understanding changes in animals' distributions related to oceanographic features is important for predicting future range shifts, responses to climate change, and in mitigating potentially harmful anthropogenic interactions such as ship strikes and fisheries bycatch.

In this study, existing timeseries of species detections from a PAM dataset were used in conjunction with environmental indicators to explore potential relationships with odontocete movements for the eight groupings mentioned above. Relationships between oceanographic variables and detections were determined using Generalized Additive Models (GAMs) and compared to previous literature where possible. The patterns described improve upon previous records by including climate indices along with more traditionally considered variables. In many cases, detection patterns match well with

combinations of one or more climate indices. Analysis of patterns in this dataset in relation to oceanographic variables provides novel information about odontocete responses to climate states that can provide a baseline for future studies.

4.3 Methods

4.3.1 Acoustic data collection and processing

Sites for data collection were off the west coast of Hawai‘i Island (henceforth, ‘Hawai‘i’), west of Kaua‘i, and in the vicinity of Manawai (Fig. 4.1). In the case of Manawai, recording site shifted over time to combat low-frequency hydrophone cable strumming from strong currents at depth. As such, two subsites have been designated (henceforth, ‘Manawai 1’, ‘Manawai 2’) (Fig. 4.1c). Collection time periods varied amongst sites, with the longest timeseries being from Hawai‘i (2009-2019). Data collection at Kaua‘i occurred from 2009-2011 and 2016-2017, at Manawai 1 from 2009-2011, and at Manawai 2 from 2014-2017 (Table S4.1). Sites included in this study differ in terms of overall geographic location, depth, and bathymetry (Fig. 4.1). High Frequency Acoustic Recording Packages (HARPs) were used to record passive acoustic data at these sites (Wiggins and Hildebrand 2007). Duty cycling (i.e., alternating periods of recording and non-recording) was employed to extend battery life and allow for longer deployments. Setup varied in terms of recording schedule, instrument depth, and duty cycle regime (Table S4.1). All data were recorded at a 200 kHz or 320 kHz sampling frequency (16-bit quantization) at depths ranging from 550-970 meters (see Table S4.1). All hydrophones were buoyed approximately 10-30 meters from the seafloor.

Echolocation clicks were identified using an energy-based detector, which was run on all data to identify clicks and determine relevant click features (i.e., timing between clicks in a click train, or 'inter-click interval', spectral shape, peak frequency). Unsupervised clustering methods were used to group clicks into several echolocation click types (e.g., 21,23) which were identified to species level. Types were then used to train a neural network-based classifier, which was run on all data to label all detections as one of the identified echolocation click types or noise (e.g., 20,153).

Detections of all types were binned in 5-minute increments for network training and labelling. Type-specific precision values (a measurement of the percentage of true positive detections for a given type) were multiplied by numbers of clicks in 5-minute bins to approximate the number of 'true' clicks in that bin. Bins were retained for timeseries only if they had more than a certain number of 'true' clicks (>50 for delphinids, >20 for beaked whales and *Kogia* spp.). As the full dataset for all sites included both continuous and duty cycled deployments, it was additionally necessary to account for the effects of duty cycles. This was done on both a site and type-specific basis, as duty cycling does not necessarily affect all species equally (92). Timeseries of detections during continuous deployments were subsampled for each type at each site to replicate the effect of duty cycles used at that site. These subsamples were evaluated in comparison to the continuous timeseries to determine what percentage of detections would have been lost if the deployment had been duty-cycled. The resulting percentages of missed minutes per hour were used to linearly boost counts in duty cycled deployments for each type. Final timeseries presented here were re-binned into counts of 5-minute bins per day for habitat

modelling purposes. Due to similarities in composition, relatively small inter-site distance (3-5 km), and to improve timeseries length, Manawai subsites were combined into a single Manawai site for analysis.

4.3.2. Environmental data collection and processing

Environmental variables considered in this study were related to either surface conditions (sea surface height, salinity, and temperature) or climate indices (ENSO, PDO, and NPGO). All surface condition variables were acquired from the Hybrid Coordinate Ocean Model (HYCOM) (https://www.hycom.org/). These variables were extracted at a daily scale on a 9 km grid from the four closest latitude-longitude points to each HARP site. Values at these points were then averaged to give one value per variable at each site. All climate indices were available at a monthly scale. ENSO cycles were represented using Multivariate ENSO Index (MEI) values. MEI is constructed by the empirical orthogonal function of sea level pressure, sea surface temperature, zonal and meridional components of surface wind, and outgoing long-wave radiation over the tropical Pacific basin and was accessed from the NOAA Physical Sciences Laboratory (https://psl.noaa.gov/enso/mei/). The National Centers for Environmental Information (NCEI) PDO index is created via extended reconstruction of sea surface temperature (ERSST) which is then compared to the Mantua PDO index to develop the NCEI PDO index and was accessed from the NOAA NCEI (https://www.ncei.noaa.gov/access/monitoring/pdo/). The NPGO index is calculated from sea surface height anomalies and measures changes in the North Pacific Subtropical

Gyre circulation. This index was accessed via a collaboration between NSF and NASA (http://www.o3d.org/npgo/).

4.3.3. Data analysis

Timeseries of species' acoustic detections (as defined by echolocation clicks and henceforth referred to solely as 'detections') along with environmental variables were plotted to examine patterns in the data at each site. To further quantify observed patterns, habitat modelling was performed using Generalized Additive Models (GAMs) via the mgcv package in R (154). Models were run for each species at each site, and full models contained all six variables. A negative binomial distribution was used for all models to account for zero-inflation, and all variables were included as smooths with four evenly spaced knots. Autocorrelation of residuals from the full model was used to determine what level of averaging was required to avoid significant autocorrelation. In most cases, data were re-binned to a 2–4-day average for this reason (Table 4.2). Concurvity analysis was used to check for highly correlated variables, with variables with a concurvity estimate greater than 0.6 being removed from the model sequentially until all values were less than 0.6. All possible models with remaining variables were compared using *dredge()* from the R package *MuMIn* (155) in order to determine the best final model. Models were compared at this step based on a combination of Akaike's Information Criteria (156) for small sample sizes (AICc) value and degrees of freedom. Specifically, all models with an AICc difference of less than two from the lowest AICc value were considered, and the model amongst them with the lowest degrees of freedom was chosen.

Final models were evaluated and compared based on deviance explained and R^2 value. Metrics of included variables were reported, including p-value, Chi-squared value, and degrees of freedom for each predictor (Table 4.1). Partial-fit plots were created using *ggpredict()* from the *ggeffects* package in R (157). Model results were then compared with timeseries of underlying data to get the fullest possible picture of the relationship between the considered environmental covariates and species detections.

4.4 Results

Modelling of relationships to climate indices was completed for nearly all species at each of the three sites, excluding cases where the number of detections was less than 100. Of the surface predictors considered, sea surface height was retained in the highest number of models (62%), followed by sea surface temperature (48%), and then sea surface salinity (33%). For climate indices, MEI was retained in the highest number of models (81%), followed by PDO (57%), and NPGO (33%) (Table 4.1). Retention of a given variable was determined more by site than by species. Sea surface height and MEI were common predictors (i.e., present in >50% of models) at all sites, whereas sea surface salinity and PDO were common only at Hawai‘i and Manawai, respectively (Table 4.1).

Autocorrelation in models was on short to moderate timescales in all but three cases (all three at Hawaii; Table 4.2). Explained deviance in models varied from 5% (bottlenose dolphin and melon-headed whale class at Hawaii, $R^2 = 0.03$) to 47.8% (false killer whales at Kaua‘i, $R^2 = 0.31$). Deviance explained was higher at Manawai and Kaua‘i (5 of 7 models above 15%), and lower at Hawai‘i (2 of 7 models above 15%). Explained

deviance across models was highest at Manawai, followed by Kaua‘i and then Hawai‘i (Table 4.2). Of the species considered, Blainville’s beaked whales had the highest explained deviance across sites, followed by rough-toothed dolphins (Table 4.2). The bottlenose dolphin and melon-headed whale class had the widest range of explained deviance, from 5% at Hawai‘i to 26% at Manawai. Relationships to predictors are discussed in greater detail below.

4.4.1. Hawai‘i

At Hawai‘i, MEI was the most common predictor in final models, followed by salinity and sea surface height, and then sea surface temperature, PDO and NPGO (Figure 4.2-4.3). Modelling was possible at this site for all considered species except false killer whale due to limited detections (only 85 days with presence, Table 4.1).

Rough-toothed dolphins had higher detections during negative MEI and PDO indices with an additional relationship with lower surface salinity, though this variable had a lower significance level ($p<0.05$ vs $p<0.001$ for the former two variables) (Fig. 4.2-4.3). Stenellids showed a clear relationship with lower temperatures, with no strong relationships to any other variable considered ($p<0.001$, Fig. 4.2-4.3).

Bottlenose dolphins and melon headed whale detections were higher with increased sea surface height, lower salinities, and more positive NPGO values. These trends were statistically significant ($p<0.05$), but this model explained very little deviance (5.12%), the least of any at this site. The relationship with lower salinity was the clearest in the timeseries data as well as the range of y-values for this variable’s partial smooth plot (Fig.

4.2-4.3). For short-finned pilot whales, the best model included sea surface height (positive relationship, $p<0.1$) and MEI (negative relationship, $p<0.001$).

For Blainville's beaked whales, detections were higher with lower salinities and again with negative MEI values, with a greater importance of MEI value. This model explained more deviance than any other at the site (17.4%). Cuvier's beaked whales had a similar relationship to MEI value, though in this case there is a minimum at approximately -0.5 MEI (Fig. 4.3). In addition, detections increased with colder water and higher sea surface height, though the latter was not a particularly strong relationship ($p<0.05$) compared to the two former relationships ($p<0.001$ in both cases). The relationship with colder water was clearest both in the model (as represented by higher y-axis values in smoothed plots) as well as in the underlying data (Fig. 4.2-4.3). This model again explained little deviance (9.11%), potentially due to the lower detections of this species at this site (193 days, the lowest of any species considered). The model for *Kogia* spp. included more variables than any other at this site, though it explained only 15% of the deviance observed. Acoustic presence of this species had a positive relationship with sea surface height and MEI, and negatively with salinity, temperature, and PDO. The strongest relationship observed was with PDO and sea surface temperature, based on significance level ($p<0.001$) and examining the underlying data, though ranges of predicted counts were similar for all variables (Fig. 4.3).

4.4.2. Kaua‘i

MEI was the most common predictor in habitat models at Kaua‘i, included in 6 of 7 models. Sea surface height was the next most common, followed by sea surface temperature, PDO and NPGO, and then sea surface salinity. Modelling was possible for all species except Cuvier’s beaked whales at this site, as there were no detections of this species.

Kaua‘i was the only site at which false killer whale detections could be modelled, with a model that explained nearly 50% of the deviance in this dataset. This model included all six predictors, with the strongest relationships being a relationship with negative MEI value, positive PDO value, and middling sea surface height and temperature (based on p value, all four <0.001). Based on timeseries examination and predicted counts, the strongest relationship observed was likely with negative MEI, particularly the sudden onset of a strongly negative MEI event (i.e., La Niña event) in mid-2010 (Fig. 4.4-4.5). Preferences for middling sea surface height values were also apparent in the dataset, particularly the latter half of the timeseries, though these spikes in detections may also be due to seasonal relationship with higher temperatures.

The model for rough-toothed dolphins explained 23.9% of deviance seen in the data for this species but corroborated a clear observed relationship with negative MEI values and lower sea surface heights (Fig. 4.4-4.5). During the positive MEI phase seen at the beginning of the data, detection was low regardless of sea surface height trend. However, during La Niña conditions, there was variation in detections that corresponded with fluctuations in sea surface height (Fig. 4.4-4.5). As for rough-toothed dolphins,

models for stenellids also both included MEI (negative relationship) and sea surface height (positive relationship), with similar explained deviance (22.6%)

For bottlenose dolphins and melon-headed whales, the best model retained MEI (negative relationship) and PDO (positive relationship), and accounted for 16.2% of the model deviance. These relationships were particularly strong when negative MEI and positive PDO aligned (Fig. 4.4). The model for short-finned pilot whales explained far less deviance (10.7%) and included sea surface temperature, PDO, and NPGO. The strongest relationship in this case was with positive PDO, which was particularly clear in the latter part of the timeseries (Fig. 4.4-4.5).

The final model for Blainville's beaked whales included MEI (negative relationship, with a peak at approximately -0.5 MEI) and sea surface height (positive relationship) with 27.7% explained deviance. The best model for *Kogia* spp. contained MEI and sea surface temperature but explained only 8.34% of the variation observed. In this case, a combined relationship with lower surface temperatures and La Niña conditions may explain the lack of detections during the 2010 La Niña, as sea surface temperature was higher during this period (Fig. 4.4-4.5).

4.4.3. Manawai

At Manawai, modelling was possible for all types except for false killer whale due to insufficient number of detections (n = 97). At this site, PDO was the most influential variable considered, and was retained in all final models. MEI was the next most common predictor, followed by sea surface height, temperature, NPGO, and then salinity (Fig. 4.7).

For rough-toothed dolphins, the best model explained 31% of observed deviance, the highest at this site. The strongest relationship was with MEI, with a spike in presence for this species during the 2010 La Niña event. This likely drove the modelled relationship of higher presence with lower MEI value. Detections were also higher with lower sea surface heights and PDO values. Similar relationships were seen for stenellids, though in addition there was a relationship to temperature (higher detections with lower temperature) and NPGO (higher detections with higher NPGO values). Based on the model and timeseries, the strongest of these relationships was with the climate indices, particularly MEI and PDO, and then sea surface height (Fig. 4.6-4.7). The overall temperature relationship modelled here indicates that detections were higher with lower temperatures, though the significance level is lower than other included variables ($p<0.05$). This relationship is not as clear in the underlying timeseries data. The overall explained deviance of this model was 27%.

The bottlenose dolphin and melon-headed whale class had very similar explained deviance (26%). In this case, detections were higher with lower temperature, and additionally with negative MEI and PDO values, as well as somewhat with negative sea surface heights. In this case, the stronger relationship with cold-temperature seasons may explain the lack of 2010 peak in presence during the strong La Niña event. The short-finned pilot whale model explained the second-most deviance at this site (29%), with the strongest relationship again being with negative PDO values, followed by positive salinity and middling temperature preferences, which are less evident in the data (Fig. 4.6).

Blainville's beaked whale detections were also higher with negative ENSO values, again with a distinct peak observed during 2010, though detections notably do not increase during the weaker la Niña observed in 2016 (Fig. 4.6). This species also had a relationship with positive temperature and positive PDO. Cuvier's beaked whale and *Kogia* spp. models explained the leaves deviance of at this site, (10 and 12%, respectively; Fig. 4.7). For Cuvier's beaked whales, there was a distinct preference for higher sea surface height and positive PDO values, as well as weaker relationships to negative MEI and NPGO. For *Kogia* spp., the strongest observed relationship is with negative NPGO, and with MEI, with additional relationships to salinity, sea surface height, and PDO. Detections are higher during the El Niño event of 2014, particularly when MEI is weakly positive, but not during the 2009 El Niño. Additional data would likely help elucidate these results.

4.5 Discussion

In this study, we were able to describe and quantify relationships between six environmental variables and detections of more than eight species of odontocetes at three sites near the Hawaiian Islands. Across species and sites, MEI values were the most valuable predictor of echolocation click detection, followed by sea surface height and sea surface temperature, both of which may be related to local changes in wind-driven currents and associated upwelling (158) and movement of cyclonic and anti-cyclonic eddies (159). Relationships across sites were somewhat consistent, particularly for Hawai‘i, where all variables included in final models had similar relationships to the species considered (Fig. 4.2-4.3). Relationships to variables were not as consistent across species as they were

across sites. As an example, sea surface salinity was important in half of all models at Hawai‘i, but very few at Kaua‘i, and Manawai. MEI shows the most across-species consistency because of its inclusion in many final models across both sites and species (Table 4.1).

Incorporation of other vocalizations produced by odontocetes (e.g., whistles, buzzes, burst pulses) would further contribute to fully describing acoustic presence patterns of the species considered in relation to environmental variables. There are likely some vocalizations from pygmy killer whales, *Feresa attenuata*, in our dataset due to a resident population off the coast of Hawai‘i (103). It is not possible to quantify this effect, though based on knowledge of this species' echolocation (105), pygmy killer whale is most likely being misclassified as a fellow delphinid species. The small size of this population (103), probably mitigates the effect of these misclassifications, although individuals from this population do use slope waters spanning the depth range of the HARP (67). Fraser's dolphin, *Lagenodelphis hosei*, Risso's dolphins, *Grampus griseus,* killer whales, *Orcinus orca*, and Longman's beaked whales, *Indopacetus pacificus,* are also known to be present around the islands but are rarely sighted near the HARP locations (3) and likely represent a very small proportion of misclassifications. Some detections of beaked whales may also be misclassifications of an unidentified beaked whale species first detected at Cross Seamount, Hawai‘i; this would be most likely at Kaua‘i where this species has been acoustically recorded on the U.S. Pacific Missile Range Facility (PMRF) (106).

Lack of consistency in important variables across species may speak to differing behavior even within a relatively small region, and perhaps population differences as well. Many odontocetes in Hawai‘i have both recognized pelagic stocks, which are more likely to move amongst islands, as well as island-associated stocks (25), whose movements are more localized. For species with island-associated populations (e.g., spinner dolphins, pantropical spotted dolphins, Blainville's beaked whales, false killer whales (3,76,160,161)), shifts in detections may be more likely related to localized movements (i.e., inshore-offshore) rather than broad-scale movements of pelagic individuals, though some animals from pelagic populations may also use the areas near the HARP sites.

In the case of stenellids and the bottlenose dolphin and melon-headed whale class, differences may additionally be related to differing species makeup at the sites considered. The bottlenose dolphin and melon-headed whale class is likely mostly bottlenose dolphins at Main Hawaiian Island sites, but this may not hold true in the Northwestern Hawaiian Islands. The stenellid type is composed of primarily spinner and spotted dolphins, but likely fewer spotted dolphins off Kaua‘i where there is no resident population (109). The sites considered in this study differ in terms of over-arching patterns (as described in the introduction, differences between the main and northwestern Hawaiian Islands in particular), bathymetry, depth, and slope, all of which may also drive differing, site-specific behaviors (Fig. 4.1). These results may emphasize caution in creating larger, over-arching species models for a region. For sea surface temperature, for example, a model created from all sites combined might have found no relationship with stenellids, while in

truth there is a strong relationship between this variable and stenellid detections off Hawai‘i.

For several species, combinations of high-frequency fluctuations (i.e., the surface conditions considered) and low-frequency fluctuation (i.e., climate indices) revealed interesting patterns. This was observed for rough-toothed dolphins at Kaua‘i and the bottlenose dolphin and melon-headed whale class at Manawai, where combinations of temperature preferences and presumed responses to ENSO explained the complexity of patterns seen in the data. Such patterns highlight the utility of considering both types of fluctuations when performing species modelling, when possible.

4.5.1. Surface conditions

Of the surface predictors considered, sea surface height may be the most interesting due to its consistency of trends across species when included in final models. For stenellids and rough-toothed dolphins, this variable was important at Kaua‘i and Manawai, and these relationships were always negative (Table 4.1, Fig. 4.5, 4.7). However, for Cuvier’s beaked whales, there was a positive relationship with sea surface height (Hawai‘i, Manawai) (Fig. 4.3, 4.7), and this trend holds as well for Blainville’s beaked whales at Kaua‘i (Fig. 4.5). The trend did not hold for the bottlenose dolphin and melon-headed whale class, which was associated with positive sea surface height at Hawai‘i, but negative sea surface height at Manawai (Fig. 4.3, 4.7). At Hawai‘i, positive relationships with sea surface height might suggest a relationship to the warm and cold-core eddies that are known to be prevalent in the lee of Hawai‘i Island (Calil and Richards 2008). The

relationship could be alternatively be related to times of increased downwelling, which has been known to aggregate prey species near this site (Abecassis 2015).

For species with negative relationships (i.e., stenellids and rough-toothed dolphins), relationships with cold-core (e.g., productive) eddies or times of increased upwelling may better explain the patterns seen. It is interesting that the sea surface height preferences documented mostly differ for deep and shallow divers; deep divers (i.e., beaked whales (73,162)) have a relationship with higher sea surface height, whereas shallower divers (i.e., stenellids and rough-toothed dolphins (66,71)) have a relationship with negative sea surface height. Differences in relationship to the bottlenose dolphin and melon-headed whale class might suggest differential makeup of this type based on site. As established in previous study using this dataset, the type is likely mostly bottlenose dolphins at Main Hawaiian Island sites due to much higher sighting rates of this species in that region. However, this may not hold true at Manawai. Previous modelling studies of these species have noted sea surface height relationships for short-finned pilot whales, as well as pantropical spotted dolphins and spinner dolphins. However, the relevant study does not detail whether the relationship observed was positive or negative (163). The same is true for pantropical spotted and spinner dolphins (137).

At Hawai‘i, relationships with sea surface temperature were negative in all models where this variable was retained (stenellids, Cuvier’s beaked whale, *Kogia* spp.; Fig. 4.3). This was mostly true for Kaua‘i as well (short-finned pilot whale, *Kogia* spp., though these relationships are relatively weak), except for false killer whales which had a positive relationship with temperature (Fig. 4.5). At Manawai, temperature preferences were split,

with Blainville's beaked whales having some relationship with warmer conditions and short-finned pilot whales having a relationship with middling temperatures.

In contrast, detections of stenellids and the bottlenose dolphin and melon-headed whale class were higher in colder temperatures. These relationships were somewhat weak for stenellids and short-finned pilot whales, but stronger for Blainville's beaked whales and the bottlenose dolphin and melon-headed whale class. Stenellids at this site have an interesting relationship with higher temperatures in 2010 that seems to fall apart in 2011, the reason for this is unknown. The same can be said for Blainville's beaked whales, the observed higher detections with positive temperatures is stronger in the early part of the timeseries. A combined relationship between surface and climate variables may be responsible for these changes. Sea surface salinity was related to detections (negative) in half of all models at Hawai'i (rough-toothed dolphin, bottlenose dolphin and melon headed whale, Blainville's beaked whale, *Kogia* spp.), but nearly nowhere else (only false killer whale at Kaua'i and short-finned pilot whales and *Kogia* spp. at Manawai, Fig. 4.3, 4.7). At Hawai'i, all relationships were negative. Elsewhere, relationships were positive, though these relationships were weaker ($p<0.01$, Fig. 4.5, 4.7) and did not describe patterns as well as other considered variables in those models.

As mentioned, relationships with lower temperatures and salinities may be related to times of increased upwelling. It is unclear what might drive species to have relationships with higher temperatures at one site and lower temperatures at another, but it may be related to localized prey patterns. The distinct pattern for Blainville's beaked whales at Manawai during the earlier part of the timeseries (i.e., higher detections with warmer

conditions) may relate to associations with the edges of cold-core eddies (161). It is particularly interesting that stenellid distribution is explained only by sea surface temperature at Hawai‘i, and this matches the timeseries well, and yet this variable is not significant at Kaua‘i and only weakly significant at Manawai (Fig. 4.3, 4.5, 4.7).

Studies modelling habitat for many species in the Hawaiian region and North Pacific have noted relationships to surface temperature for short-finned pilot whale, false killer whales, bottlenose dolphins, spinner dolphins, and pantropical spotted dolphins, and temperature at 200 meters for rough-toothed dolphins and melon-headed whales (137,163,164). These studies focused on abundance estimates and predictive modelling and did not describe the directionality of relationships to these variables. For Cuvier's beaked whales, relationship with negative sea surface temperature has been noted previously in the Northern Line Islands (165), which matches the trend seen at Hawai‘i here. For *Kogia* spp., no regional records of relationships to these variables were available, though a strong relationship between sea surface temperature (minimum and maximum) and *K. sima* presence has been documented in the Gulf of Mexico (166). Relationships to salinity were not common in the literature, though *Kogia* spp. presence has been linked (albeit weakly) to surface salinity in the North Atlantic (167).

4.5.2. Climatic indices

Of the climate indices considered, MEI was included in more models than other indices, closely followed by PDO, which was particularly influential at Manawai. For Hawai‘i, all MEI preferences considered were for negative states, except for *Kogia* spp.,

though this trend may have been driven by a stronger relationship with negative PDO values (Fig. 4.2-4.3). All species with a relationship to MEI had a distinct peak in detections in January 2011, during which negative PDO and MEI states lined up with a positive NPGO state— likely the most productive combination of climate indices in the Main Hawaiian Islands. Likewise, at Kauaʻi and Manawai distinct 2010 peaks in detections corresponding with the onset of a particularly strong La Niña are seen for several species (Fig. 4.5, 4.7).

At Kauaʻi, no such peak is observed for bottlenose dolphins and melon-headed whales despite an overall relationship with negative MEI (Fig. 4.4-4.5). This could potentially be the result of a lagged reaction to MEI, which has been noted in previous studies of ecological responses to ENSO fluctuations (e.g., 145,168). At Manawai, the 2010 peak in detections might suggest that the site is experiencing productivity changes in the same direction as those experienced in the Main Hawaiian Islands during negative ENSO and PDO phases. Based on the proximity of the Transition Zone Chlorophyll Front (TZCF), it was expected that there would instead be a preference for positive ENSO conditions which is not observed here, except in the case of *Kogia* spp (though this was not well-captured in the model). A longer timeseries might elucidate such a pattern, particularly if it captured more variability in the PDO which is the primary driver of the TZCF climate-associated shift.

For Hawaiʻi site, there is a sudden shift in early 2019 in detections of rough-toothed dolphins, Blainville's beaked whales, and *Kogia* spp. (decrease for Blainville's and *Kogia* spp., increase for rough-toothed dolphins; Fig. 4.2). This shift lines up with the shift from

negative to positive PDO state. This is particularly interesting for rough-toothed dolphins, which, apart from this positive relationship, are negatively related to PDO values across the rest of the dataset. The distinctness of this shift may warrant further study to see whether it truly is related to PDO-related changes, or if this is coincidental. At Kaua‘i, relationships with PDO were positive, which is noteworthy considering the expected compounded effects of negative MEI and PDO in the Main Hawaiian Islands. This may suggest that preferences for more productive conditions during La Niña conditions hold more sway than changes in PDO conditions. However, previous studies of the PDO have also noted that positive phases may increase shallow, nearshore upwelling (169), which could be the reason for increased detections during positive PDO at this site.

At Manawai, relationships to PDO index were somewhat in agreement, with a general relationship with lower positive or even negative PDO values, though the error bars were wide for negative PDO conditions in many cases (Fig. 4.7). At this site, relationships with positive PDO conditions are likely related to associated shifts in the transition zone chlorophyll front. For the bottlenose dolphin and melon-headed whale class, detections were not particularly high when MEI and PDO were both positive, which is relevant as detections are seasonally highest during the winter, when the front is closest to the islands (132) and this shift is exacerbated by positive PDO and MEI states. In contrast, detections of beaked whales at this site were higher during positive PDO states, which better matched with a relationship to the movements of the TZCF. These species also showed a seasonality, with higher detections in winter months (Ziegenhorn et al. (in prep)). For short-finned pilot whales and stenellids, detections before the 2012-2014 gap

are much higher. This may point to some influence of subsite. As mentioned in the methods section, exact location of the Manawai site shifted during this data gap. Additional data from the newer subsite (i.e., Manawai 2) may illuminate whether a shift to positive PDO is truly driving the pattern observed, or if this might instead be due to granular site preferences for this species.

Across all sites, NPGO was not a very common predictor; a longer timeseries might be needed to really assess relationships to this climate index. At Hawai‘i, the only relationship with NPGO was for the bottlenose dolphin and melon-headed whale class (positive relationship). At Kaua‘i, NPGO was retained in two models (negative relationship for short-finned pilot whales, potentially slight positive relationship for false killer whales). For both sites, lack of relationship to NPGO may be related to the lower variability in NPGO states during on-effort times. Alternatively, it may be true that NPGO-related changes around the islands are not as important as those caused by ENSO and PDO cycles. At Manawai, NPGO was included in final models for stenellids (positive relationship), Cuvier's beaked whales, and *Kogia* spp. (negative relationships in both cases; Fig. 4.7). For *Kogia* spp., and potentially stenellids, these trends may be more of an artifact of responses to other variables than to NPGO index itself.

It is interesting that relationships to NPGO differ amongst shallow and deep foragers. Positive relationships were seen for species foraging in the epipelagic zone (false killer whales, stenellids, bottlenose dolphins (24,170)), while negative relationships were seen for mesopelagic and benthopelagic foragers (short-finned pilot whales, *Kogia* spp., Cuvier's beaked whales (72,85,171)). Insights into how climate indices affect prey in these

ocean layers may help explain these differences. This information is most readily available for epipelagic species with active fisheries, including skipjack tuna, *Katsuwonus pelamis,* yellowfin tuna, *Thunnus albacares,* and bigeye tuna, *Thunnus obesus*. Both skipjack and bigeye tuna may be more common near the Hawaiian Islands during the El Niño phase of ENSO (125,172). For yellowfin tuna, catch per unit effort in the Pacific has been previously positively correlated with PDO and negatively correlated with NPGO, on a 1-5 year lag (173). These trends might suggest that positive ENSO and PDO, and negative NPGO, might provide the best foraging conditions for epipelagic foragers in the islands. However, this is the opposite of patterns observed in our data in most cases. Further study of prey species' responses to climate variations might provide more insight into why this is the case.

As mentioned in the introduction to this study, few records of odontocete changes in relation to climate indices exist. In the Hawaiian Islands, a recent study of false killer whales noted that predation from long-line fisheries is higher during El Niño conditions (11 month lag), suggesting that the normal food web may be disrupted during such times (145). For this species it has also been noted that nearshore movements of satellite-tagged individuals were higher during positive PDO phases, although the relationship with PDO only explained a small amount of variance (174). This is similar to our results of detections from Kaua'i. In other regions, relationships to ENSO (e.g., 175–177) and PDO (e.g., 83) have been documented for several species of odontocetes, but records of such nature are still infrequent. A literature search revealed no studies that had examined odontocete presence in relation to the NPGO cycle.

4.6 Conclusion

Observed relationships with the climate variables considered were significant in many cases and warrant more study, where possible, in this region. The phenomena considered (i.e., ENSO, PDO, NPGO) can have long-lasting effects on environmental conditions, and subsequent effects on species behavior and movements might inform management decisions, stock assessments, and other research efforts during differing climate phases. The most striking example of this in our data comes from the strong La Niña event of 2010, which related to spikes in detections of many species at all sites. While we present preliminary examinations of climate indices in relation to detections of odontocetes, longer timeseries from all sites would be highly useful in further examining relationships to these long-lasting fluctuations in climate state. Ideally, future studies might include several cycles of these indices.

Overall, this study provides an additional look at surface variables which have been previously studied in the region while also providing new information for climate indices, which have not. The relationships documented are the first step towards understanding relationships of odontocetes in this region to climate indices and highlight that the combination of highly variable surface conditions and large-scale climate indices can provide unique insights into species detection patterns. Understanding these details provides another puzzle piece in the complex lives of odontocetes that will hopefully illuminate future studies in the years to come. Modelling habitat and understanding patterns in both space and time is crucial to preserving key spaces for these animals,

mapping changes in their movements, and predicting their current and future relationships to the waters of the Hawaiian Archipelago.

4.7 Acknowledgements

A special thanks to fellow graduate students Rebecca Cohen and Natalie Posdaljian for their input and discussions on the methods employed in this study, which had a large impact on the final product. Thank you to all members of the Scripps Whale Acoustics Lab, the Scripps Acoustic Ecology Lab, and the Scripps Machine Listening Lab for support over the course of this project. Thanks to Erin O'Neill for her work in processing HARP deployments and Bruce Thayre and John Hurwitz for their work on the HARP instruments. Thanks to Ann Allen, Erik Norris, and others at the NOAA Pacific Islands Fisheries Center for their instrument deployment, retrieval, and work at all sites used in this study. This work was funded by the NOAA Pacific Islands Fisheries Science Center. Manawai HARP deployments were permitted by the Papahānaumokuākea Marine National Monument under permits PMNM-2008-020 and PMNM-2010-042 and the Co-Managers permit since 2015.

Chapter 4, in full, is in preparation for publication of the material. Ziegenhorn, Morgan A., John A. Hildebrand, Erin M. Oleson, Robin W. Baird, and Simone Baumann-Pickering. "Oceanographic conditions as indicators of odontocete detection in the Hawaiian Archipelago." The dissertation author was primarily responsible for the investigation and writing of this material.

4.8 Figures and Tables

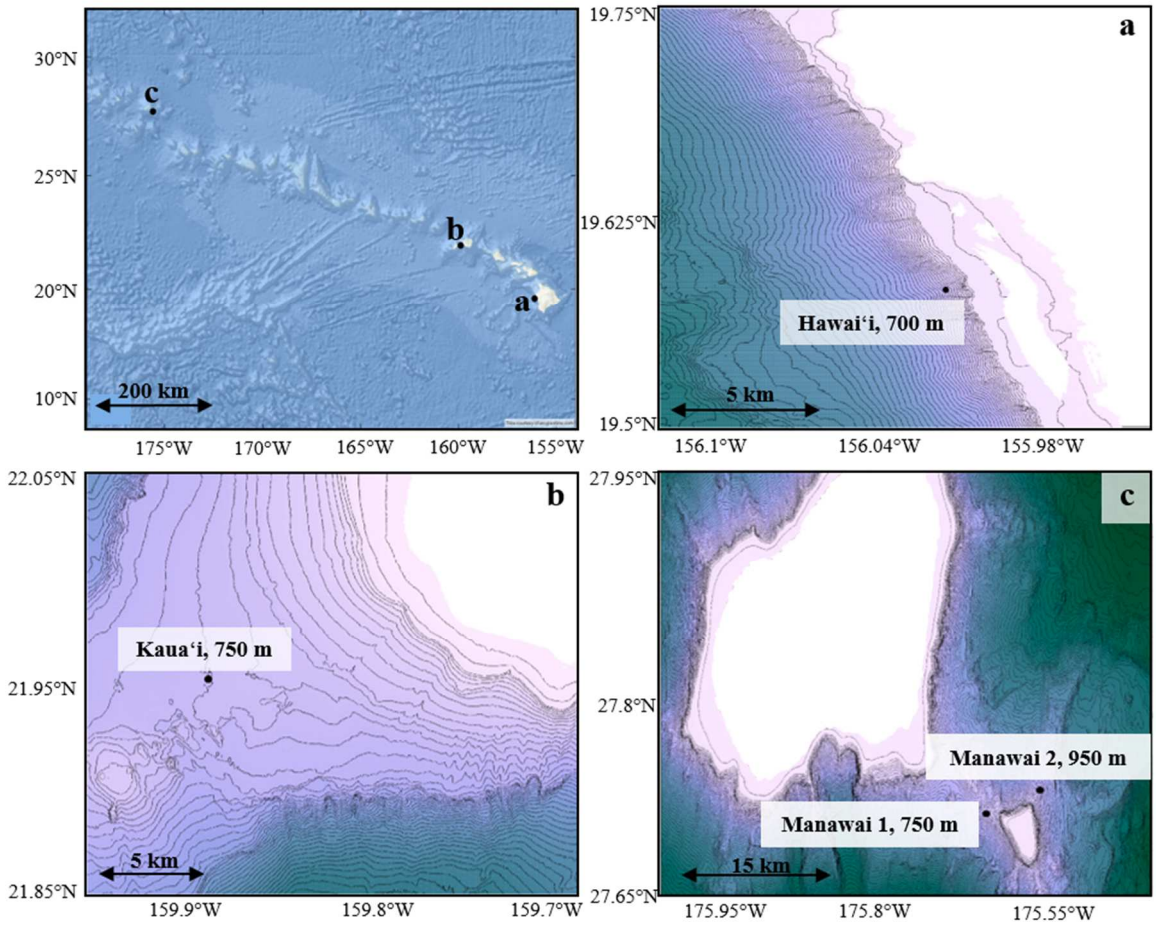

Figure 4.1. Site map. Sites for this study, showing location and average depth (50 meter contours). Top left panel shows site locations in context of the Hawaiian Islands chain. Panels a-c show locations of Hawaii, Kaua'i , and Manawai sites (respectively). Basemap in top left image is the intellectual property of Esri and is used herein with permission. Copyright © 2022 Esri and its licensors. All rights reserved. Bathymetry data used for panels a-c accessed from the Hawai'i Mapping Research Group at the University of Hawai'i at Manoa. (a-b, accessible here: http://www.soest.hawaii.edu/hmrg/multibeam/bathymetry.php) and Pacific Islands Ocean Observing System (c, accessible here: https://pae-paha.pacioos.hawaii.edu/thredds/bathymetry.html?dataset=hurl_bathy_60m_nwhi).

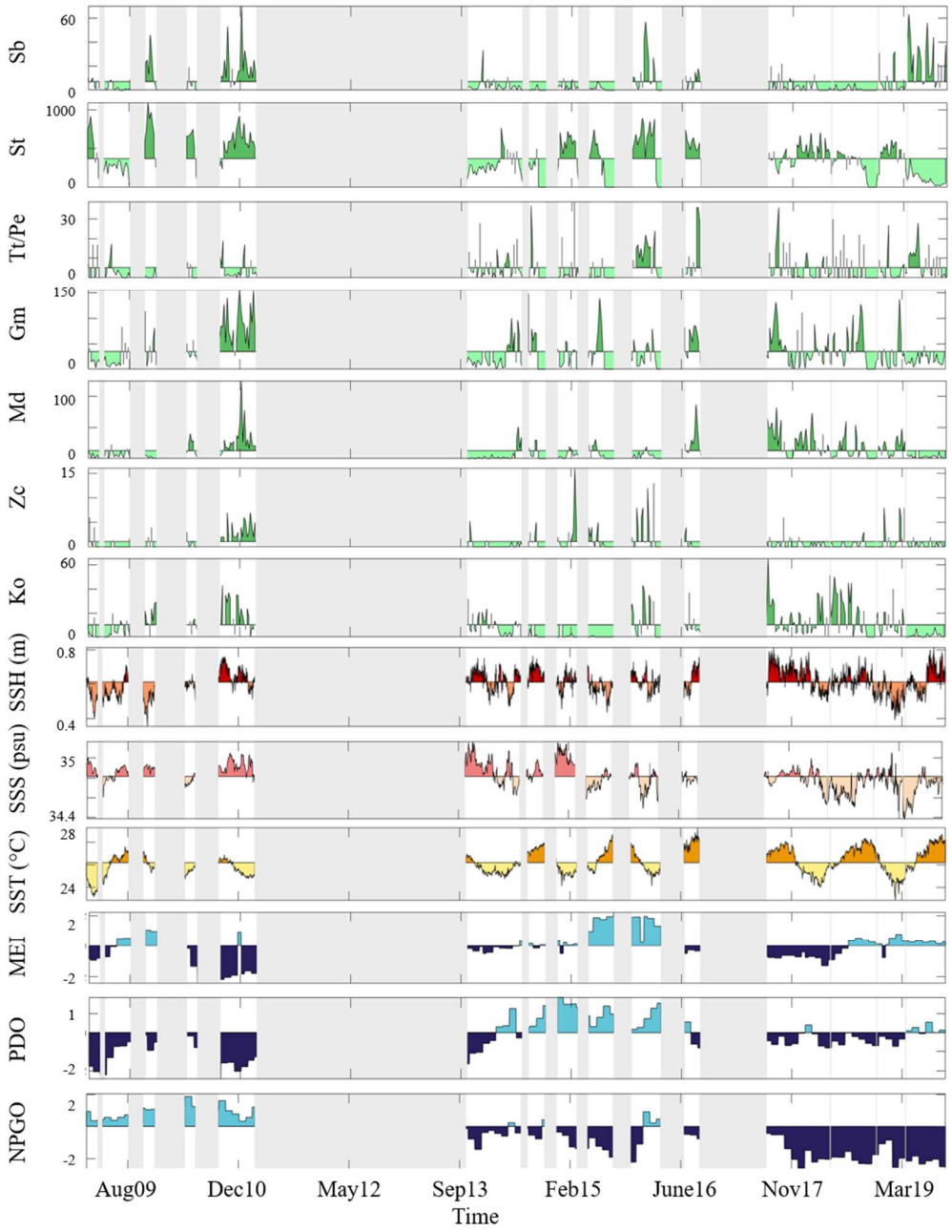

Figure 4.2. Hawai‘i site timeseries. Timeseries of all considered variables (including species detections in counts/week) across the full dataset at Hawai‘i. Times of no effort are shown in gray. Color on each plot refers to values above or below the average value of that variable (for all species and for SSH, SSS, and SST), or to positive or negative values (MEI, PDO, NPGO). Species codes are Sb = rough-toothed dolphin, St = stenellids, Tt/Pe = bottlenose dolphin and melon-headed whale, Gm = short-finned pilot whale, Md = Blainville’s beaked whale, Zc = Cuvier’s beaked whale, and Ko = *Kogia* spp.

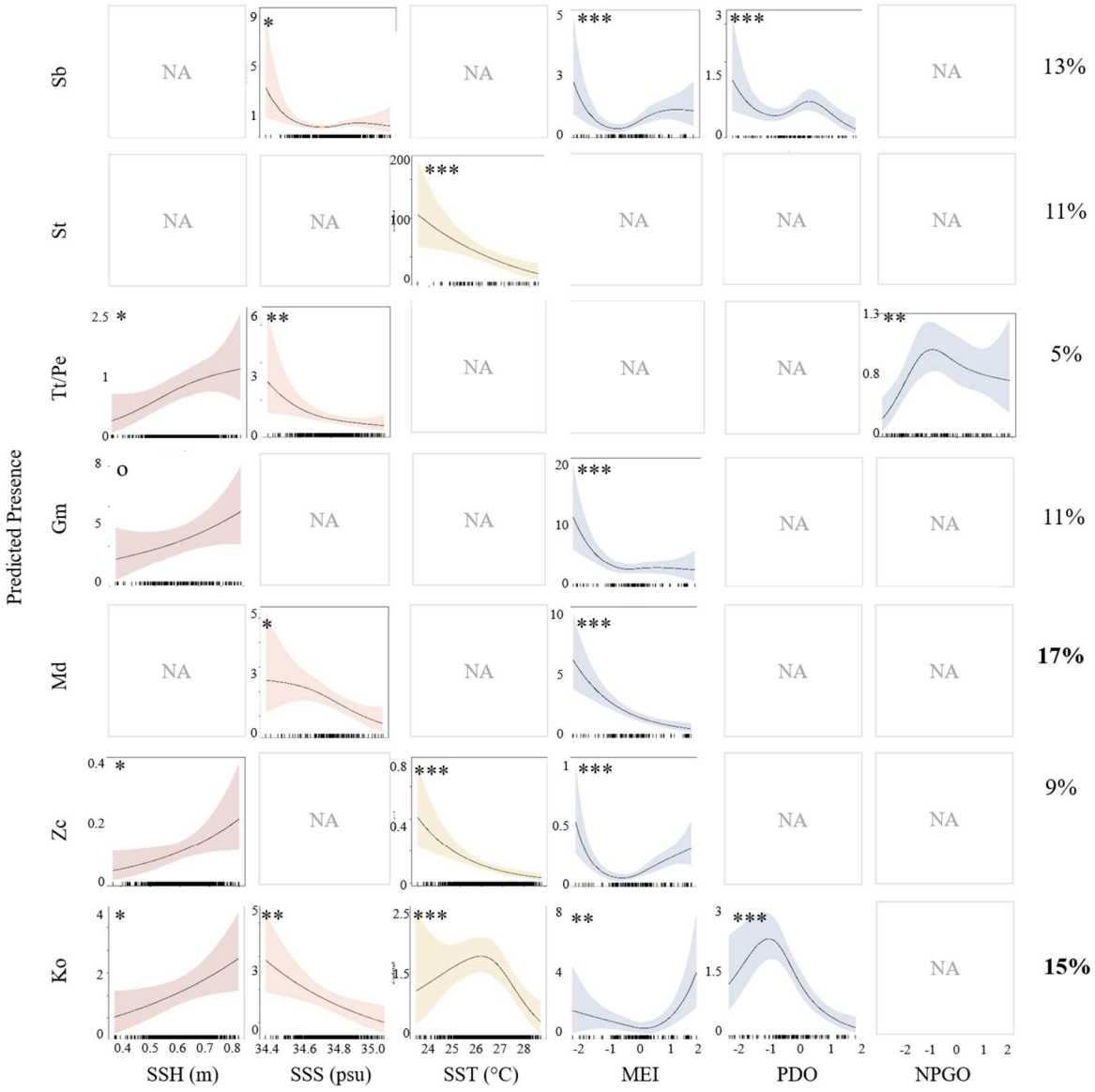

Figure 4.3. Model results for Hawai‘i. Partial fit smooths for all variables considered at Hawai‘i (columns) for each species considered (rows). Predicted detections is shown on y-axes in counts of 5-minute bins per day. Significance level is given by o = $p<0.01$, * = $p<0.05$, ** = $p<0.01$, *** = $p<0.001$. Column on the right shows explained deviance for each model, with values greater than 15% in bold. Species codes are Sb = rough-toothed dolphin, St = stenellids, Tt/Pe = bottlenose dolphin and melon-headed whale, Gm = short-finned pilot whale, Md = Blainville's beaked whale, Zc = Cuvier's beaked whale, and Ko = *Kogia* spp.

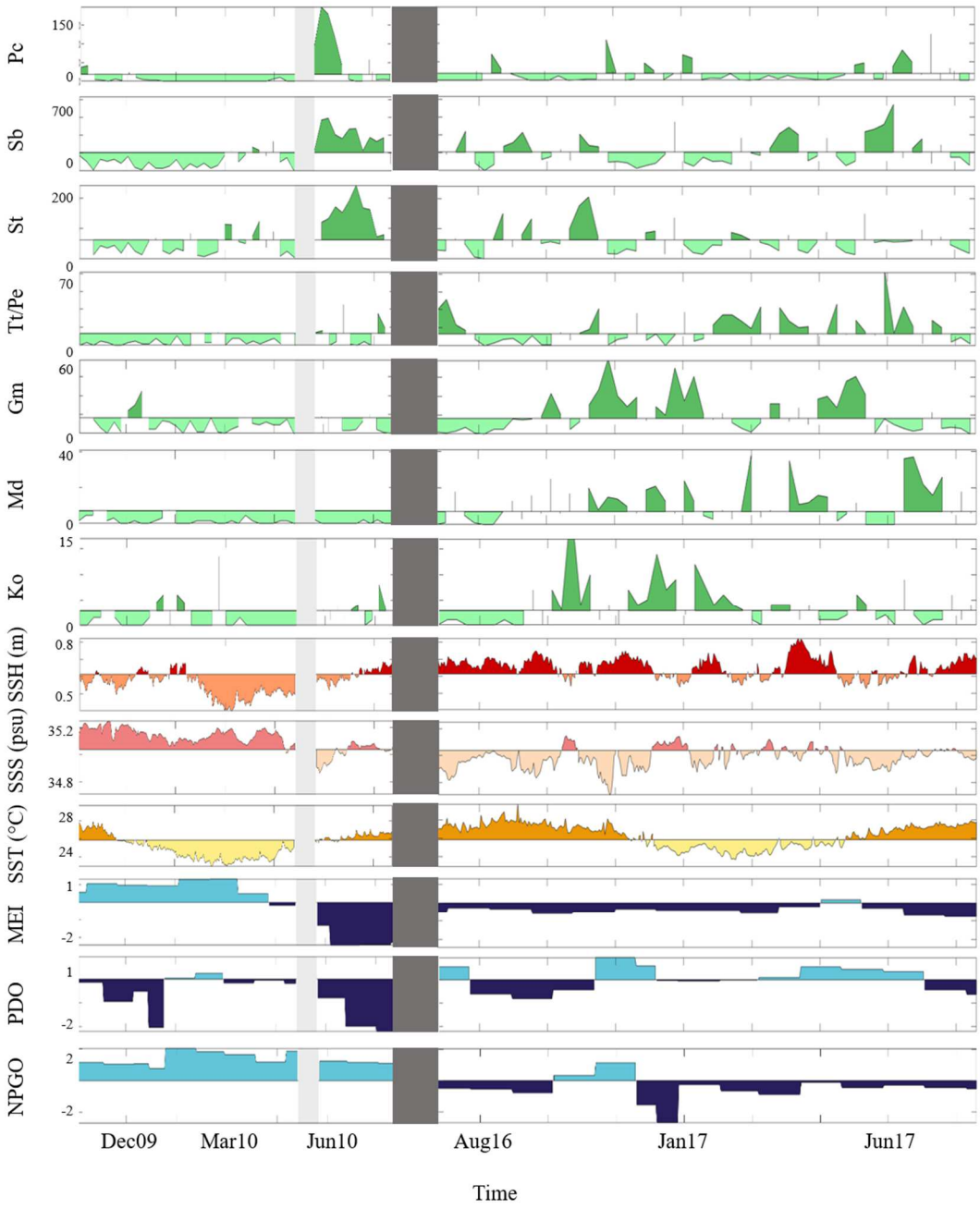

Figure 4.4. Kaua‘i site timeseries. Timeseries of all considered variables (including species detections in counts/week) across the full dataset at Kaua‘i. Times of no effort are shown in gray. Large gap in detections from 2010-2016 is denoted by dark gray boxes. Color on each plot refers to values above or below the average value of that variable (for all species and for SSH, SSS, and SST), or to positive or negative values (MEI, PDO, NPGO). Species codes are Pc = false killer whale, Sb = rough-toothed dolphin, St = stenellids, Tt/Pe = bottlenose dolphin and melon-headed whale, Gm = short-finned pilot whale, Md = Blainville’s beaked whale, and Ko = *Kogia* spp.

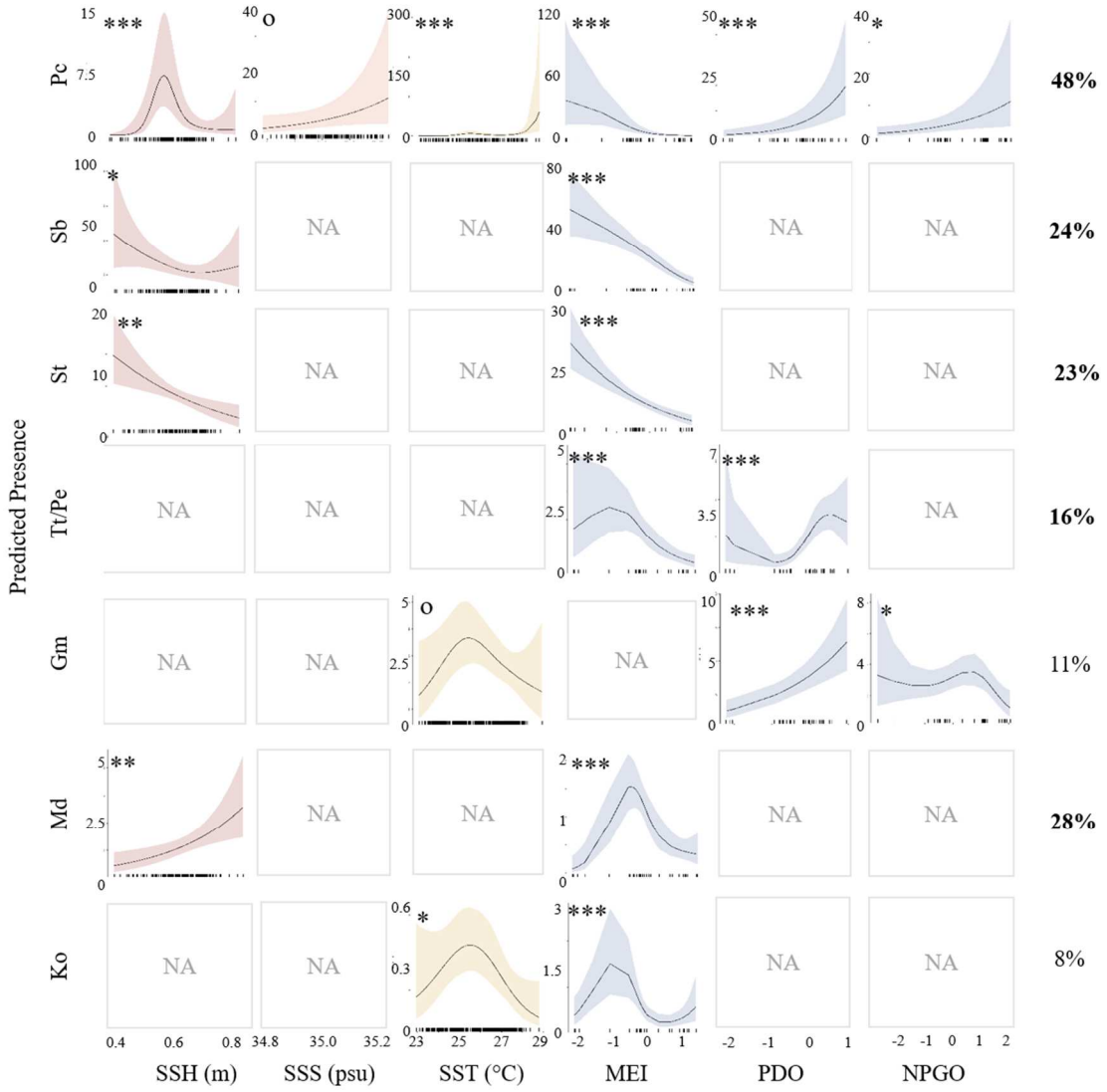

Figure 4.5. Model results for Kaua‘i. Partial fit smooths for all variables considered at Kaua‘i (columns) for each species considered (rows). Predicted detections is shown on y-axes in counts of 5-minute bins per day. Significance level is given by o = $p<0.01$, * = $p<0.05$, ** = $p<0.01$, *** = $p<0.001$. Column on the right shows explained deviance for each model, with values greater than 15% in bold. Species codes are Pc = false killer whale, Sb = rough-toothed dolphin, St = stenellids, Tt/Pe = bottlenose dolphin and melon-headed whale, Gm = short-finned pilot whale, Md = Blainville’s beaked whale, and Ko = *Kogia* spp.

Figure 4.6. Manawai timeseries. Timeseries of all considered variables (including species detections in counts/week) across the full dataset at Manawai. Times of no effort are shown in gray. Large gap in effort from 2011-2014 is denoted by dark gray boxes. Color on each plot refers to values above or below the average value of that variable (for all species and for SSH, SSS, and SST), or to positive or negative values (MEI, PDO, NPGO). Species codes are Sb = rough-toothed dolphin, St = stenellids, Tt/Pe = bottlenose dolphin and melon-headed whale, Gm = short-finned pilot whale, Md = Blainville's beaked whale, Zc = Cuvier's beaked whale, and Ko = *Kogia* spp.

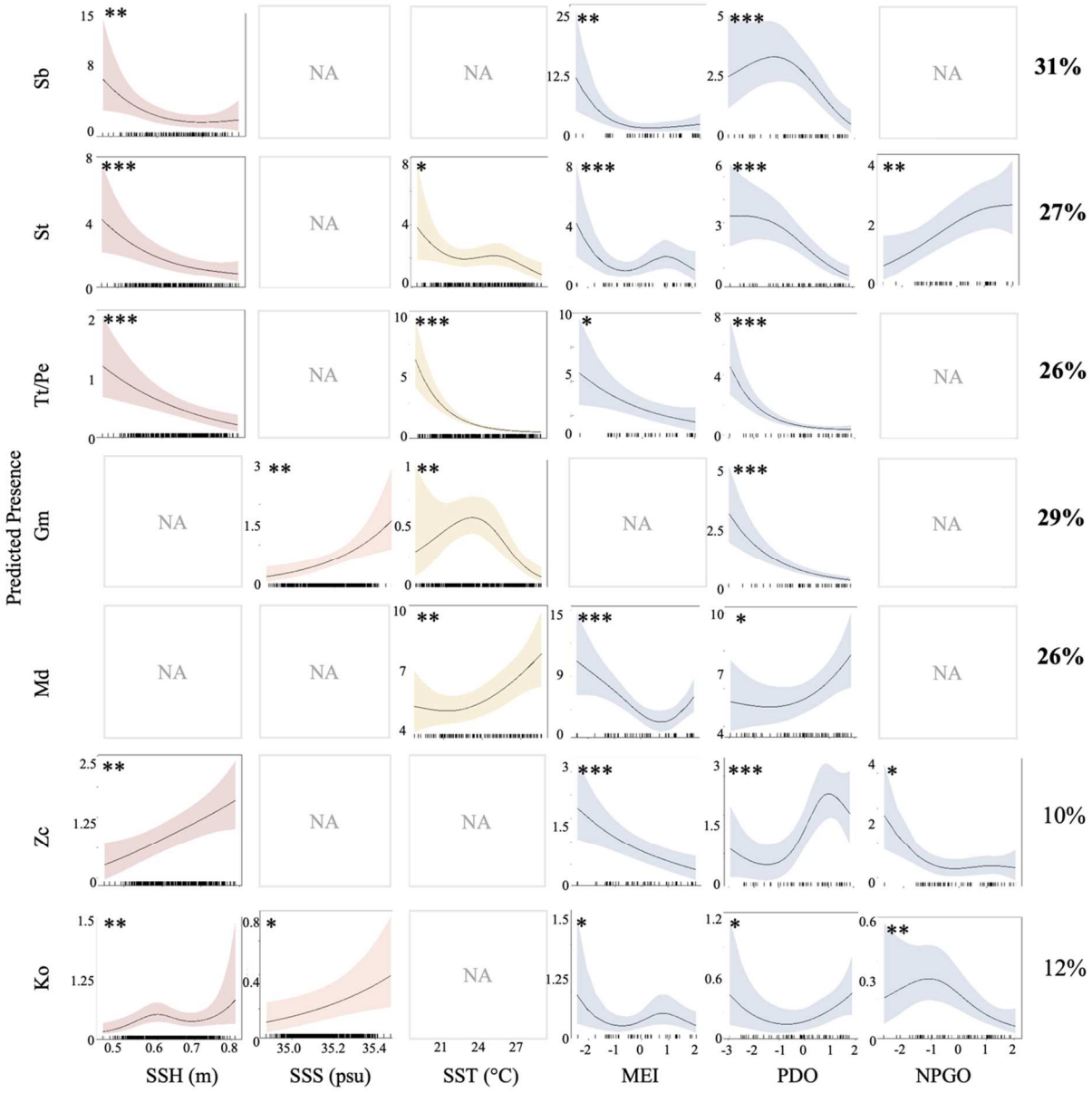

Figure 4.7. Model results for Manawai. Partial fit smooths for all variables considered at Manawai (columns) for each species considered (rows). Predicted detections is shown on y-axes in counts of 5-minute bins per day. Significance level is given by o = $p<0.01$, * = $p<0.05$, ** = $p<0.001$, *** = $p<0.0001$. Column on the right shows explained deviance for each model, with values greater than 15% in bold. Species codes are Sb = rough-toothed dolphin, St = stenellids, Tt/Pe = bottlenose dolphin and melon-headed whale, Gm = short-finned pilot whale, Md = Blainville's beaked whale, Zc = Cuvier's beaked whale, and Ko = *Kogia* spp.

Table 4.1. Model results. Results of final models for each species (column) and site (row) detailing significance levels of included variables. For each variable, p-value (p), degrees of freedom (df), and Chi-squared value (χ^2) is given if the variable was included in the final model for that species and site. Gray boxes denote species for which modelling was not possible due to low detections. Species codes are Pc = false killer whale, Sb = rough-toothed dolphin, Gm = short-finned pilot whale, Tt/Pe = bottlenose dolphin and melon-headed whale, Md = Blainville's beaked whale, Zc = Cuvier's beaked whale, St = stenellids, and Ko = *Kogia* spp.

Model Results (p-value, df, χ^2)		Type							
		False killer whale	**Rough-toothed dolphin**	**Short-finned pilot whale**	**Bottlenose d./ Melon-headed w.**	**Blainville's beaked whale**	**Cuvier's beaked whale**	**Stenellids**	***Kogia* spp.**
Hawai'i	**SSH**			0.093, 1.15, 3.89	0.013, 1.64, 8.73		0.031, 1, 4.64		0.026, 1.01, 5.03
	SSS		0.021, 2.68, 12.3		0.006, 1.62, 9.60	0.011, 1.70, 9.24			0.005, 1.00, 7.95
	SST						<0.001, 1, 19.9	0.001, 1.09, 12.4	<0.001, 2.51, 15.5
	MEI		<0.001, 2.83, 25.6	0.004, 2.50, 16.0		<0.001, 1.29, 29.6	<0.001, 2.81, 36.1		0.003, 2.62, 12.7
	PDO		0.001, 2.85, 15.2						<0.001, 2.73, 60.0
	NPGO				0.005 2.59, 15.3				
Kaua'i	**SSH**	<0.001, 2.85, 31.5	0.071, 1.95, 5.50			0.003, 1.02, 8.64		0.001, 1, 10.4	
	SSS	0.065, 1, 3.40							
	SST	<0.001, 2.91, 29.3		0.058, 2.28, 9.05					0.016, 2.30, 9.38
	MEI	<0.001, 2.11, 39.0	<0.001, 2.17, 62.4		<0.001, 2.34, 33.6	<0.001, 2.78, 32.9		<0.001, 1, 37.9	<0.001, 2.87, 19.7
	PDO	<0.001, 1, 13.8		<0.001, 1.00, 18.9	<0.001, 2.83, 34.0				
	NPGO	0.016, 1, 5.86		0.044, 2.70, 8.90					
Manawai	**SSH**		0.005, 1.98, 11.3		<0.001, 1, 13.1		0.001, 1.29, 12.2	<0.001, 1.60, 15.5	0.004, 2.73, 8.71
	SSS			0.002, 1.03, 10.2					0.015, 1, 5.88
	SST			<0.001, 2.46, 24.8	<0.001, 1, 98.3	0.002, 1.97, 14.5		0.024, 2.62, 9.01	
	MEI		0.001, 2.45, 17.5		0.015, 1.32, 7.08	<0.001, 2.74, 16.4	<0.001, 1.29, 14.4	<0.001, 2.79, 19.7	0.031, 2.74, 7.97
	PDO		<0.001, 2.37, 20.2	<0.001, 1, 41.4	<0.001, 2.16, 53.4	0.025, 1.98, 7.93	<0.001, 2.72, 17.2	<0.001, 2.19, 27.9	0.037, 2.25, 9.74
	NPGO			<0.001, 1, 19.3			0.025, 2.35, 13.4	0.005, 1.78, 11.6	0.001, 2.13, 14.9

Table 4.2. Model metrics. Evaluation metrics and information about final habitat models for each species (columns) and each site (rows). Metrics given are number of days with detections (nPresDays), number of days binned to account for autocorrelation (ACbin), deviance explained by the final model (percentage), and adjusted R^2. Deviance explained greater than 15% has been bolded. Gray boxes denote species for which modelling was not possible based on low detections.

Model Metrics		Type							
		False killer whale	Rough-toothed dolphin	Short-finned pilot whale	Bottlenose d./ Melon-headed w.	Blainville's beaked whale	Cuvier's beaked whale	Stenellids	*Kogia* spp.
Hawai'i	nPresDays, AC bin	85	555, 4	1277, 11	416, 3	789, 14	193, 2	1840, 28	723, 3
	Deviance explained (%)	--	13.1	10.8	5.12	**17.4**	9.11	11	15.1
	Adjusted R^2	--	0.118	0.175	0.0262	0.134	0.0398	0.2	0.115
Kaua'i	nPresDays, AC bin	191, 4	571, 4	288, 2	233, 2	190, 3	0	551, 5	132, 2
	Deviance explained (%)	**47.8**	**23.9**	10.7	**16.2**	**27.7**	--	**22.6**	8.34
	Adjusted R^2	0.305	0.212	0.0995	0.106	0.181	--	0.284	0.0104
Manawai	nPresDays, AC bin	33	583, 8	225, 2	400, 3	1268, 8	642, 3	617, 4	142, 2
	Deviance explained (%)	--	**30.8**	**28.8**	**26.1**	**25.7**	10.4	**27.2**	11.8
	Adjusted R^2	--	0.349	0.129	0.0668	0.212	0.117	0.215	0.0575

Future Recommendations

There are many questions still to be answered in this dataset. Future work using the existing classifications might consider exploring classification error more, particularly how it varies with duty cycle, ambient noise conditions, and seasonal changes in distributions of various species. Classifier performance itself might be improved by developing a tiered

method to classify clicks, as mentioned in Chapter 2, or incorporate multiple types of vocalizations into the classification scheme. This would have the added benefit of more holistically representing acoustic presence. Special attention to the stenellid and combined bottlenose dolphin and melon-headed whale class might be able to tease out species makeup, which was not possible over the course of the dissertation. Inclusion of whistles might aid in this, as well as additional tagging or sighting data that could help attribute these signals to species. While it was generally assumed that detectability of species was within a 5 km (maximum) radius from HARP locations, actual detectability at each site likely varies, and additionally varies amongst species. Detection probability can be modelled, and this could be an interesting avenue for further study, particularly as it relates to species' density estimation using this dataset.

As mentioned in Chapter 3, lunar illumination and phase were considered as a temporal parameter but were removed from analysis due to lack of compelling relationships. Further teasing apart these factors, including considerations of cloud cover and interactions between multiple temporal parameters, might reveal patterns that were not seen in the current analysis. For Chapters 3 and 4, data from part of the Manawai timeseries was removed from analysis due to low detections, which were presumed to be due to equipment errors. As additional data from this site becomes available, it would be interesting to see whether these low detection numbers persist; this would help determine whether or not the decrease is truly due to lower presence.

Longer timeseries from all considered sites may also be the key to solidifying findings from Chapter 4. The climate indices considered vary over long time scales, and

while we've captured some of this variability, having a longer dataset would be hugely advantageous in truly understanding species' relationships to differing oceanographic states. In addition to this, there are many environmental variables that we removed from Chapter 4 to simplify analyses that could provide further avenues for research, including temperature and salinity at depth, anthropogenic noise, chlorophyll-a concentration, and many others. Fisheries data and active acoustic monitoring of prey species were not readily available, but would also be highly useful in further defining species' relationships to environmental factors in the Hawaiian Islands.

Outside of the chapters included here, there are many more interesting phenomena that could be further investigated. For example, there is some specific patterning in stenellid detections (which I affectionately call 'rainbow detections') that appear at Hawai'i and not the other sites. The reason for this may be related to the way species approach this site or other behavioral considerations, and might be interesting to study further. In addition to this, I've observed a number of acoustic mixed species assemblages (i.e., times when multiple species are present concurrently in the acoustic data) that could prove very interesting if studied further. Mixed species groups are seen across the animal kingdom, and have a variety of functionalities. Acoustic study of these groups has mostly not been attempted, and will likely be complicated, but might provide some really interesting insights into interspecific interactions.

References

1. Calil PHR, Richards KJ. Transient upwelling hot spots in the oligotrophic North Pacific. Journal of Geophysical Research: Oceans. 2010;115(2).

2. Polovina JJ, Mitchum GT, Evans GT. Decadal and basin-scale variation in mixed layer depth and the impact on biological production in the Central and North Pacific, 1960-88. Deep-Sea Research Part I. 1995;42(10):1701–16.

3. Baird RW, Webster DL, Aschettino JM, Schorr GS, McSweeney DJ. Odontocete cetaceans around the main Hawaiian Islands: Habitat use and relative abundance from small-boat sighting surveys. Aquatic Mammals. 2013;39(3):253–69.

4. Carretta J V, Forney KA, Oleson EM, Weller DW, Lang AR, Baker J, et al. U.S. Pacific marine mammal stock assessments: 2016. NOAA technical memorandum NOAA-TM-NMFS-SWFSC-577. 2017;(August).

5. Baumann-Pickering S, Roch MA, Brownell RL, Simonis AE, McDonald MA, Solsona-Berga A, et al. Spatio-temporal patterns of beaked whale echolocation signals in the North Pacific. PLoS ONE. 2014 Jan 22;9(1).

6. Baumann-Pickering S, Simonis AE, Oleson EM, Baird RW, Roch MA, Wiggins SM. False killer whale and short-finned pilot whale acoustic identification. Endangered Species Research. 2015;28(2):97–108.

7. Merkens KP, Simonis AE, Oleson EM. Geographic and temporal patterns in the acoustic detection of sperm whales Physeter macrocephalus in the central and western North Pacific Ocean. Endangered Species Research. 2019;39:115–33.

8. Gilmartin M. THE "ISLAND MASS" EFFECT ON THE PHYTOPLANKTON AND PRIMARY PRODUCTION OF THE HAWAIIAN ISLANDS. Vol. 16, mar. Biol. Ecol. @ North-Holland Publishing Company; 1974.

9. Baird RW, Gorgone AM, McSweeney DJ, Webster DL, Salden DR, Deakos MH, et al. False killer whales (Pseudorca crassidens) around the main Hawaiian Islands: Long-term site fidelity, inter-island movements, and association patterns. Marine Mammal Science. 2008 Jul;24(3):591–612.

10. Bibby TS, Gorbunov MY, Wyman KW, Falkowski PG. Photosynthetic community responses to upwelling in mesoscale eddies in the subtropical North Atlantic and Pacific Oceans. Deep-Sea Research Part II: Topical Studies in Oceanography. 2008 May;55(10–13):1310–20.

11. Seki MP, Polovina JJ, Brainard RE, Bidigare RR, Leonard CL, Foley DG. Biological enhancement at cyclonic eddies tracked with GOES thermal imagery in Hawaiian waters. Geophysical Research Letters. 2001 Apr 15;28(8):1583–6.

12. Woodworth PA, Schorr GS, Baird RW, Webster DL, Mcsweeney DJ, Hanson MB, et al. Eddies as offshore foraging grounds for melon-headed whales (Peponocephala electra). Vol. 28, Marine Mammal Science. 2012. p. 638–47.

13. Baird RW, Schorr GS, Webster DL, McSweeney DJ, Hanson MB, Andrews RD. Movements and habitat use of satellite-tagged false killer whales around the main Hawaiian Islands. Endangered Species Research. 2010;10(1):107–21.

14. Schmelzer I. Seals and seascapes: Covariation in Hawaiian monk seal subpopulations and the oceanic landscape of the Hawaiian Archipelago. Journal of Biogeography. 2000;

15. Baumann-Pickering S, Roch MA, Brownell RL, Simonis AE, McDonald MA, Solsona-Berga A, et al. Spatio-temporal patterns of beaked whale echolocation signals in the North Pacific. PLoS ONE. 2014;

16. Au WWL, Giorli G. Studying the Biosonar Activities of Deep Diving Odontocetes in Hawaii and Other Western Pacific Locations. In 2016. p. 83–115. Available from: http://link.springer.com/10.1007/978-1-4939-3176-7_5

17. Hildebrand JA, Frasier KE, Baumann-Pickering S, Wiggins SM, Merkens KP, Garrison LP, et al. Assessing seasonality and density from passive acoustic monitoring of signals presumed to be from pygmy and dwarf sperm whales in the gulf of Mexico. Frontiers in Marine Science. 2019;6(FEB).

18. Rice A, Deecke VB, Ford JKB, Pilkington JF, Oleson EM, Hildebrand JA, et al. Spatial and temporal occurrence of killer whale ecotypes off the outer coast of Washington State, USA. Marine Ecology Progress Series. 2017;

19. Wiggins SM, Hildebrand JA. High-frequency Acoustic Recording Package (HARP) for broad-band, long-term marine mammal monitoring. In: International Symposium on Underwater Technology, UT 2007 - International Workshop on Scientific Use of Submarine Cables and Related Technologies 2007 [Internet]. 2007. p. 551–7. Available from: http://www.motorola.com

20. Ziegenhorn MA, Frasier KE, Hildebrand JA, Oleson EM, Baird RW, Wiggins SM, et al. Discriminating and classifying odontocete echolocation clicks in the Hawaiian Islands using machine learning methods. Plos One [Internet]. 2022;17(4):e0266424. Available from: http://dx.doi.org/10.1371/journal.pone.0266424

21. Frasier KE, Roch MA, Soldevilla MS, Wiggins SM, Garrison LP, Hildebrand JA. Automated classification of dolphin echolocation click types from the Gulf of Mexico. PLoS Computational Biology. 2017 Dec 1;13(12).

22. Cohen RE, Frasier KE, Baumann-Pickering S, Wiggins SM, Rafter MA, Hildebrand JA. Identification of western North Atlantic odontocete echolocation click types

using machine learning and spatiotemporal correlates. PLoS ONE. 2022;

23. Reyes Reyes MV, Iñíguez MA, Hevia M, Hildebrand JA, Melcón ML. Description and clustering of echolocation signals of Commerson's dolphins (*Cephalorhynchus commersonii*) in Bahía San Julián, Argentina. The Journal of the Acoustical Society of America [Internet]. 2015 Oct;138(4):2046–53. Available from: http://asa.scitation.org/doi/10.1121/1.4929899

24. Baird RW. The lives of Hawai`i's Dolphins and Whales: natural history and conservation. University of Hawai`i Press, Honolulu, Hawai`i; 2016.

25. Carretta J V, Oleson EM, Forney KA, Muto MM, Weller DW, Lang AR, et al. U.S. Pacific Marine Mammal Stock Assessments: 2020 [Internet]. (U.S.) SFSC, editor. 2021. (NOAA technical memorandum NMFS). Available from: https://repository.library.noaa.gov/view/noaa/31436

26. Lin TH, Yu HY, Chen CF, Chou LS. Passive acoustic monitoring of the temporal variability of odontocete tonal sounds from a long-term marine observatory. PLoS ONE. 2015;10(4):1–16.

27. Castellote M, Small RJ, Lammers MO, Jenniges JJ, Mondragon J, Atkinson S. Dual instrument passive acoustic monitoring of belugas in Cook Inlet, Alaska. The Journal of the Acoustical Society of America [Internet]. 2016 May;139(5):2697–707. Available from: http://asa.scitation.org/doi/10.1121/1.4947427

28. Seger KD, Miksis-Olds JL. Acoustic documentation of temperate odontocetes in the Bering and Chukchi Seas. Marine Mammal Science. 2019;35(3):1099–111.

29. Charif RA, Shiu Y, Muirhead CA, Clark CW, Parks SE, Rice AN. Phenological changes in North Atlantic right whale habitat use in Massachusetts Bay. Global Change Biology [Internet]. 2020 Feb 1;26(2):734–45. Available from: https://doi.org/10.1111/gcb.14867

30. Oswald JN, Rankin S, Barlow J. To whistle or not to whistle? Geographic variation in the whistling behavior of small odontocetes. Aquatic Mammals. 2008;34(3):288–302.

31. Smith HR, Zitterbart DP, Norris TF, Flau M, Ferguson EL, Jones CG, et al. A field comparison of marine mammal detections via visual, acoustic, and infrared (IR) imaging methods offshore Atlantic Canada. Marine Pollution Bulletin [Internet]. 2020;154(February):111026. Available from: https://doi.org/10.1016/j.marpolbul.2020.111026

32. Panicker D, Baumgartner M, Stafford K. Fine-scale spatial and temporal acoustic occurrence of island-associated odontocetes near a mid-oceanic atoll in the northern Indian Ocean. Marine Ecology Progress Series [Internet]. 2022;683:195–208.

Available from: http://dx.doi.org/10.3354/meps13947

33. Macaulay J, Kingston A, Coram A, Oswald M, Swift R, Gillespie D, et al. Passive acoustic tracking of the three□dimensional movements and acoustic behaviour of toothed whales in close proximity to static nets. Methods in Ecology and Evolution. 2022;0–3.

34. DeAngelis AI, Stanistreet JE, Baumann-Pickering S, Cholewiak DM. A description of echolocation clicks recorded in the presence of True's beaked whale (*Mesoplodon mirus*). The Journal of the Acoustical Society of America [Internet]. 2018 Nov;144(5):2691–700. Available from: http://asa.scitation.org/doi/10.1121/1.5067379

35. Baumann-Pickering S, McDonald MA, Simonis AE, Solsona Berga A, Merkens KPB, Oleson EM, et al. Species-specific beaked whale echolocation signals. The Journal of the Acoustical Society of America. 2013;

36. Giorli G, Au WWL. Spatio-temporal variation and seasonality of Odontocetes' foraging activity in the leeward side of the island of Hawaii. Deep-Sea Research Part I: Oceanographic Research Papers. 2017 Mar 1;121:202–9.

37. Henderson EE, Martin SW, Manzano-Roth R, Matsuyama BM. Occurrence and habitat use of foraging Blainville's beaked whales (Mesoplodon densirostris) on a U.S. Navy range in Hawaii. Aquatic Mammals. 2016;42(4):549–62.

38. McCullough JLK, Wren JLK, Oleson EM, Allen AN, Siders ZA, Norris ES. An Acoustic Survey of Beaked Whales and Kogia spp. in the Mariana Archipelago Using Drifting Recorders. Frontiers in Marine Science [Internet]. 2021;8:761. Available from: https://www.frontiersin.org/article/10.3389/fmars.2021.664292

39. Palmer KJ, Brookes KL, Davies IM, Edwards E, Rendell L. Habitat use of a coastal delphinid population investigated using passive acoustic monitoring. Aquatic Conservation: Marine and Freshwater Ecosystems. 2019;29:254–70.

40. Poupard M, Ferrari M, Best P, Glotin H. Passive acoustic monitoring of sperm whales and anthropogenic noise using stereophonic recordings in the Mediterranean Sea, North West Pelagos Sanctuary. Scientific Reports [Internet]. 2022;12(1):1–13. Available from: https://doi.org/10.1038/s41598-022-05917-1

41. McCullough JLK, Simonis AE, Sakai T, Oleson EM. Acoustic classification of false killer whales in the Hawaiian islands based on comprehensive vocal repertoire. JASA Express Letters [Internet]. 2021 Jul;1(7):071201. Available from: https://asa.scitation.org/doi/10.1121/10.0005512

42. Buchanan C, Bi Y, Xue B, Vennell R, Childerhouse S, Pine MK, et al. Deep Convolutional Neural Networks for Detecting Dolphin Echolocation Clicks. In:

2021 36th International Conference on Image and Vision Computing New Zealand (IVCNZ). IEEE; 2021. p. 1–6.

43. Shiu Y, Palmer KJ, Roch MA, Fleishman E, Liu X, Nosal EM, et al. Deep neural networks for automated detection of marine mammal species. Scientific Reports. 2020;10(1):1–12.

44. Zhang L, Wang D, Bao C, Wang Y, Xu K. Large-scale whale-call classification by transfer learning on multi-scale waveforms and time-frequency features. Applied Sciences (Switzerland). 2019;9(5):1–11.

45. Yang L, Sharpe M, Temple AJ, Jiddawi N, Xu X, Berggren P. Description and classification of echolocation clicks of Indian Ocean humpback (Sousa plumbea) and Indo-Pacific bottlenose (Tursiops aduncus) dolphins from Menai Bay, Zanzibar, East Africa. PLoS ONE [Internet]. 2020;15(3):1–13. Available from: http://dx.doi.org/10.1371/journal.pone.0230319

46. Schall E, Roca I, Van Opzeeland I. Acoustic metrics to assess humpback whale song unit structure from the Atlantic sector of the Southern ocean. The Journal of the Acoustical Society of America. 2021;149(6):4649–58.

47. Li K, Sidorovskaia NA, Tiemann CO. Model-based unsupervised clustering for distinguishing Cuvier's and Gervais' beaked whales in acoustic data. Ecological Informatics [Internet]. 2020;58:101094. Available from: https://www.sciencedirect.com/science/article/pii/S1574954120300443

48. Pace F, Benard F, Glotin H, Adam O, White P. Subunit definition and analysis for humpback whale call classification. Applied Acoustics [Internet]. 2010;71(11):1107–12. Available from: http://dx.doi.org/10.1016/j.apacoust.2010.05.016

49. Frasier KE. A machine learning pipeline for classification of cetacean echolocation clicks in large underwater acoustic datasets. PLoS Computational Biology [Internet]. 2021;17(12):1–26. Available from: http://dx.doi.org/10.1371/journal.pcbi.1009613

50. Kowarski K, Delarue J, Martin B, O'Brien J, Meade R, Cadhla O, et al. Signals from the deep: Spatial and temporal acoustic occurrence of beaked whales off western Ireland. PLoS ONE. 2018;13(6):1–26.

51. Hazen EL, Nowacek DP, Laurent St L, Halpin PN, Moretti DJ. The relationship among oceanography, prey fields, and beaked whale foraging habitat in the tongue of the ocean. PLoS ONE. 2011;6(4).

52. Wiggins SM, Roch MA, Hildebrand JA. TRITON software package: Analyzing large passive acoustic monitoring data sets using MATLAB. The Journal of the

Acoustical Society of America. 2010;

53. Székely GJ, Rizzo ML, Bakirov NK. Measuring and testing dependence by correlation of distances. Annals of Statistics. 2007;35(6):2769–94.

54. Biemann C. Chinese whispers - An efficient graph clustering algorithm and its application to natural language processing problems. Proceedings of TextGraphs: The 1st Workshop on Graph-Based Methods for Natural Language Processing. 2006;(June):73–80.

55. Fred ALN, Jain AK. Combining Multiple Clusterings Using Evidence Accumulation. IEEE Transactions on Pattern Analysis and Machine Intelligence. 2005;27(6):835–50.

56. Ziegenhorn MA. LabelVis [Internet]. 2020. Available from: https://github.com/MarineBioAcousticsRC/Triton/wiki/LabelVis

57. Merkens KP, Baumann-Pickering S, Ziegenhorn MA, Trickey JS, Allen AN, Oleson EM. Characterizing the Long-Term, Wind-Band, Deep-Water Soundscape off Hawaii. Frontiers in Marine Science. 2021;

58. Solsona-Berga A, Frasier KE, Baumann-Pickering S, Wiggins SM, Hildebrand JA. Detedit: A graphical user interface for annotating and editing events detected in long-term acoustic monitoring data. PLoS Computational Biology. 2020;

59. Yano KM, Oleson EM, Keating JL, Ballance LT, Hill MC, Bradford AL, et al. Cetacean and Seabird Data Collected During the Hawaiian Islands Cetacean and Ecosystem Assessment Survey (HICEAS), July-December 2017. 2018; Available from: https://doi.org/10.25923/7avn-gw82

60. Frasier KE, Debich AJ, Pickering SB-, Širović A, Kerosky SM, Roche LK, et al. Passive Acoustic Monitoring for Marine Mammals in the Jacksonville Range Complex Augst 2014 - May 2015. Marine Physical Laboratory. 2016;(August 2014).

61. Rafter MA, Trickey JS, Rice AC, Merrifield M, Thayre BJ, Neill O, et al. Passive Acoustic Monitoring for Marine Mammals offshore of Cape Hatteras June 2018 – September 2019. 2020;(September 2019).

62. Rice AC, Baumann-Pickering S, Širović A, Hildebrand JA, Rafter M, Thayre BJ, et al. Passive Acoustic Monitoring for Marine Mammals in the SOCAL Range Complex April 2016 - June 2017. MPL Technical Memorandum #636 [Internet]. 2018;(January). Available from: http://cetus.ucsd.edu/Publications/Reports/RiceMPLTM636-2019.pdf

63. Rankin S, Oswald JN, Simonis AE, Barlow J. Vocalizations of the rough-toothed

dolphin, Steno bredanensis, in the Pacific Ocean. Marine Mammal Science. 2015.

64. Bradford AL, Oleson EM, Forney KA, Moore JE, Barlow J. Line-transect Abundance Estimates of Cetaceans in U.S. Waters around the Hawaiian Islands in 2002, 2010, and 2017 [Internet]. Service. USNMF, (U.S.) PIFSC, (U.S.) SFSC, Region PI, editors. 2021. (NOAA technical memorandum NMFS-PIFSC ; 115). Available from: https://repository.library.noaa.gov/view/noaa/29004

65. Becker EA, Forney KA, Oleson EM, Bradford AL, Moore JE, Barlow J. Habitat-Based Density Estimates for Cetaceans within the Waters of the U.S. Exclusive Economic Zone around the Hawaiian Archipelago. 2021; Available from: https://doi.org/10.25923/x9q9-rd73

66. Shaff JF, Baird RW. Diel and lunar variation in diving behavior of rough-toothed dolphins (Steno bredanensis) off Kauaʻi, Hawaiʻi. Marine Mammal Science [Internet]. 2021 Oct 1;37(4):1261–76. Available from: https://doi.org/10.1111/mms.12811

67. Baird RW, Schorr GS, Webster DL, Mcsweeney DJ, Hanson MB, Andrews RD. Movements of two satellite-tagged pygmy killer whales (Feresa attenuata) off the island of Hawai'i. Vol. 27, Marine Mammal Science. 2011.

68. Soldevilla MS, Baumann-Pickering S, Cholewiak D, Hodge LEW, Oleson EM, Rankin S. Geographic variation in Risso's dolphin echolocation click spectra. The Journal of the Acoustical Society of America. 2017;

69. Soldevilla MS, Wiggins SM, Hildebrand JA. Spatio-temporal comparison of Pacific white-sided dolphin echolocation click types. Aquatic Biology. 2010;9(1):49–62.

70. Norris KS. The Hawaiian spinner dolphin. Choice Reviews Online. 1995;32(06):32-3310-32–3310.

71. Baird RW, Ligon AD, Hooker SK, Gorgone AM. Subsurface and nighttime behaviour of pantropical spotted dolphins in Hawai'i. Canadian Journal of Zoology. 2001;79(6):988–96.

72. Baird RW. Behavior and Ecology of Not-So-Social Odontocetes: Cuvier's and Blainville's Beaked Whales. In: Würsig B, editor. Ethology and Behavioral Ecology of Odontocetes [Internet]. Cham: Springer International Publishing; 2019. p. 305–29. Available from: https://doi.org/10.1007/978-3-030-16663-2_14

73. Baird RW, Webster DL, Schorr GS, McSweeney DJ, Barlow J. Diel variation in beaked whale diving behavior. Marine Mammal Science. 2008 Jul;24(3):630–42.

74. Owen K, Andrews RD, Baird RW, Schorr GS, Webster DL. Lunar cycles influence the diving behavior and habitat use of short-finned pilot whales around the main

Hawaiian Islands. Marine Ecology Progress Series. 2019 Oct 24;629:193–206.

75. Merkens KP, Oleson EM. Comparison of High-frequency Echolocation Clicks (likely Kogia) in Two Simultaneously Collected Passive Acoustic Data Sets Sampled at 200 kHz and 320 kHz. 2018;(September). Available from: https://doi.org/10.25923/jjss-er34

76. Baird RW, Oleson EM, Barlow J, Ligon AD, Gorgone AM, Mahaffy SD. Evidence of an Island-Associated Population of False Killer Whales (Pseudorca crassidens) in the Northwestern Hawaiian Islands . Pacific Science. 2013 Oct;67(4):513–21.

77. Baird R, Hanson M, Schorr G, Webster D, McSweeney D, Gorgone A, et al. Range and primary habitats of Hawaiian insular false killer whales: informing determination of critical habitat. Endangered Species Research. 2012;

78. Baird R, Hanson M, Schorr G, Webster D, McSweeney D, Gorgone A, et al. Range and primary habitats of Hawaiian insular false killer whales: informing determination of critical habitat. Endangered Species Research. 2012;

79. Sequeira AMM, Rodríguez JP, Eguíluz VM, Harcourt R, Hindell M, Sims DW, et al. Convergence of marine megafauna movement patterns in coastal and open oceans. Proceedings of the National Academy of Sciences of the United States of America. 2018;115(12):3072–7.

80. Forney KA, Kobayashi DR, Johnston DW, Marchetti JA, Marsik MG. What's the catch? Patterns of cetacean bycatch and depredation in Hawaii-based pelagic longline fisheries. Marine Ecology. 2011 Sep;32(3):380–91.

81. Soldevilla MS, Wiggins SM, Hildebrand JA, Oleson EM, Ferguson MC. Risso's and Pacific white-sided dolphin habitat modeling from passive acoustic monitoring. Marine Ecology Progress Series. 2011;423:247–60.

82. Kanaji Y, Okazaki M, Miyashita T. Spatial patterns of distribution, abundance, and species diversity of small odontocetes estimated using density surface modeling with line transect sampling. Deep-Sea Research Part II: Topical Studies in Oceanography. 2017 Jun 1;140:151–62.

83. Seger KD, Miksis-Olds JL. A decade of marine mammal acoustical presence and habitat preference in the Bering Sea. Polar Biology [Internet]. 2020;43(10):1549–69. Available from: https://doi.org/10.1007/s00300-020-02727-x

84. Schmelzer I. Seals and seascapes: covariation in Hawaiian monk seal subpopulations and the oceanic landscape of the Hawaiian Archipelago. Vol. 27, Journal of Biogeography. 2000.

85. Abecassis M, Polovina J, Baird RW, Copeland A, Drazen JC, Domokos R, et al.

Characterizing a foraging hotspot for short-finned pilot whales and blainville's beaked whales located off the west side of Hawai'i island by using tagging and oceanographic data. PLoS ONE. 2015 Nov 1;10(11).

86. Thorne LH, Johnston DW, Urban DL, Tyne J, Bejder L, Baird RW, et al. Predictive modeling of spinner dolphin (Stenella longirostris) resting habitat in the main Hawaiian Islands. PLoS ONE. 2012 Aug 24;7(8).

87. Squires N, Hodgson Ball K, Bennett K, Votier S, Ingram S. Using Passive Acoustics and Shore-Based Surveys to Investigate te Distribution of Small Odontocetes. Journal of the Lundy Field Society. 2014;39–56.

88. Wang ZT, Nachtigall PE, Akamatsu T, Wang KX, Wu YP, Liu JC, et al. Passive acoustic monitoring the diel, lunar, seasonal and tidal patterns in the biosonar activity of the Indo-Pacific humpback dolphins (Sousa chinensis) in the Pearl River Estuary, China. PLoS ONE. 2015;10(11):1–24.

89. Wirth C, Warren J. Passive acoustic monitoring finds concurrent use of an artificial reef in the New York Bight by foraging humans and odontocetes (Tursiops truncatus). The Journal of the Acoustical Society of America. 2017;141(5):3943.

90. Baird RW, Mahaffy SD, Lerma JK. Site fidelity, spatial use, and behavior of dwarf sperm whales in Hawaiian waters: using small□boat surveys, photo□identification, and unmanned aerial systems to study a difficult□to□study species. Marine Mammal Science [Internet]. 2021 Aug 24;mms.12861. Available from: https://onlinelibrary.wiley.com/doi/10.1111/mms.12861

91. Lu Y, Mellinger D, Klinck H. Joint classification of whistles and echolocation clicks from odontocetes. In: Proceedings of Meetings on Acoustics. 2013.

92. Stanistreet JE, Nowacek DP, Read AJ, Baumann-Pickering S, Moors-Murphy HB, Van Parijs SM. Effects of duty-cycled passive acoustic recordings on detecting the presence of beaked whales in the northwest Atlantic. The Journal of the Acoustical Society of America [Internet]. 2016;140(1):EL31–7. Available from: http://dx.doi.org/10.1121/1.4955009

93. Thieurmel B, Achraf E. suncalc: Compute Sun Sunlight Phases, Moon Position and Lunar Phase. R package version 0.5.0 [Internet]. 2019. Available from: https://cran.r-project.org/package=suncalc

94. Bray JR, Curtis JT. An ordination of the upland forest communities of Southern Wisconsin. Ecol Monogr. 1957 Jan 1;50:131–51.

95. R Core. R: A language and environment for statistical computing [Internet]. R Foundation for Statistical Computing, Vienna, Austria; 2021. Available from: https://www.r-project.org/

96. Bailey H, Corkrey R, Cheney B, Thompson PM. Analyzing temporally correlated dolphin sightings data using generalized estimating equations. Marine Mammal Science. 2013;

97. Pirotta E, Matthiopoulos J, MacKenzie M, Scott-Hayward L, Rendell L. Modelling sperm whale habitat preference: A novel approach combining transect and follow data. Marine Ecology Progress Series. 2011;436(Whitehead 2003):257–72.

98. Pan W. Akaike's Information Criterion in Generalized Estimating Equations. Biometrics [Internet]. 2001 Mar 1;57(1):120–5. Available from: https://doi.org/10.1111/j.0006-341X.2001.00120.x

99. Wang W, Yan J. splines2: Regression Spline Functions and Classes. R package ,; 2021.

100. Lüdecke D, Ben-Shachar MS, Patil I, Waggoner P, Makowski D. performance: An R package for assessment, comparison and testing of statistical models. Journal of Open Source Software. 2021;6(60).

101. Gelman A, Hill J. Data analysis using regression and multilevel/hierarchical models. Cambridge university press; 2006.

102. Tjur T. Coefficients of determination in logistic regression models—A new proposal: The coefficient of discrimination. The American Statistician. 2009;63(4):366–72.

103. McSweeney DJ, Baird RW, Mahaffy SD, Webster DL, Schorr GS. Site fidelity and association patterns of a rare species: Pygmy killer whales (Feresa attenuata) in the main Hawaiian Islands. Marine Mammal Science. 2009 Jul;25(3):557–72.

104. Baird RW. Pygmy Killer Whale. Encyclopedia of Marine Mammals. 2018;788–90.

105. Madsen PT, Kerr I, Payne R. Source parameter estimates of echolocation clicks from wild pygmy killer whales (*Feresa attenuata*) (L). The Journal of the Acoustical Society of America. 2004;

106. Manzano-roth R, Alongi GC, Matsuyama B, Henderson EE, Martin CR, Martin SW. Dive characteristics of Cross Seamount beaked whales from long-term passive acoustic monitoring at the Pacific Missile Range Facility , Kaua ' i. 2022;(June 2021):1–20.

107. Polovina JJ, Howell EA, Kobayashi DR, Seki MP. The transition zone chlorophyll front updated: advances from a decade of research. Progress in Oceanography. 2017;150:79–85.

108. Baird RW, Webster DL, Mahaffy SD, McSweeney DJ, Schorr GS, Ligon AD. Site

fidelity and association patterns in a deep-water dolphin: Rough-toothed dolphins (Steno bredanensis) in the Hawaiian Archipelago. Marine Mammal Science. 2008 Jul;24(3):535–53.

109. Baird RW, Webster DL. Using dolphins to catch tuna: Assessment of associations between pantropical spotted dolphins and yellowfin tuna hook and line fisheries in Hawai‘i. Fisheries Research [Internet]. 2020;230(May):105652. Available from: https://doi.org/10.1016/j.fishres.2020.105652

110. Simonis AE. By the light of the moon: North Pacific dolphins optimize foraging with the lunar cycle. Vol. 79. 2018. p. No Pagination Specified-No Pagination Specified.

111. Baumann-Pickering S, Roch MA, Wiggins SM, Schnitzler HU, Hildebrand JA. Acoustic behavior of melon-headed whales varies on a diel cycle. Behavioral Ecology and Sociobiology. 2015 Sep 18;69(9):1553–63.

112. West KL, Walker WA, Baird RW, Webster DL, Schorr GS. Stomach contents and diel diving behavior of melon-headed whales (Peponocephala electra) in Hawaiian waters. Marine Mammal Science. 2018;34(4):1082–96.

113. Baird RW. Behavior and Ecology of Not-So-Social Odontocetes: Cuvier’s and Blainville’s Beaked Whales. In 2019. p. 305–29.

114. Jacobson EK, Henderson EE, Miller DL, Oedekoven CS, Moretti DJ, Thomas L. Quantifying the response of Blainville’s beaked whales to U.S. naval sonar exercises in Hawaii. Marine Mammal Science. 2022;(May):1–17.

115. Baird RW, Anderson DB, Kratofil MA, Webster DL, Mahaffy SD. Cooperative conservation and long-term management of false killer whales in Hawai‘i: geospatial analyses of fisheries and satellite tag data to understand fishery interactions. 2019;(67703):48.

116. Bradford AL, Oleson EM, Baird RW, Boggs CH, Forney KA, Young NC. Revised Stock Boundaries for False Killer Whales (Pseudorca crassidens) in Hawaiian Waters. NOAA Technical Memorandum NMFS-PIFSC-47. 2015;(September):29.

117. Simon Pittman CJ, Winship AJ, Poti M, Kinlan BP, Leirness JB, Baird RW, et al. Bureau of Ocean Energy Management and National Oceanic and Atmospheric Administration. Vol. 359. 2016.

118. Au WWL, Giorli G, Chen J, Copeland A, Lammers MO, Richlen M, et al. Presence and seasonal variation of deep diving foraging odontocetes around Kauai, Hawaii using remote autonomous acoustic recorders. The Journal of the Acoustical Society of America. 2014 Jan;135(1):521–30.

119. McSweeney DJ, Baird RW, Mahaffy SD. Site fidelity, associations, and movements of Cuvier's (Ziphius cavirostris) and Blainville's (Mesoplodon densirostris) beaked whales off the island of Hawai'i. Marine Mammal Science. 2007 Jul;23(3):666–87.

120. Allen AN, Harvey M, Harrell L, Jansen A, Merkens KP, Wall CC, et al. A Convolutional Neural Network for Automated Detection of Humpback Whale Song in a Diverse, Long-Term Passive Acoustic Dataset. Frontiers in Marine Science. 2021 Mar 17;8.

121. Polovina JJ, Howell EA, Abecassis M. Ocean's least productive waters are expanding. Geophysical Research Letters. 2008 Feb 16;35(3).

122. Baird RW, Schorr GS, Webster DL, McSweeney DJ, Hanson MB, Andrews RD. Movements and habitat use of satellite-tagged false killer whales around the main Hawaiian Islands. Endangered Species Research. 2010;10(1):107–21.

123. Baird RW, Webster DL, Aschettino JM, Schorr GS, McSweeney DJ. Odontocete cetaceans around the main Hawaiian Islands: Habitat use and relative abundance from small-boat sighting surveys. Aquatic Mammals. 2013;39(3):253–69.

124. Holbrook NJ, Claar DC, Hobday AJ, McInnes KL, Oliver ECJ, Gupta A Sen, et al. ENSO□driven ocean extremes and their ecosystem impacts. El Niño southern oscillation in a changing climate. 2020;409–28.

125. Howell EA, Kobayashi DR. El Niño effects in the Palmyra Atoll region: Oceanographic changes and bigeye tuna (Thunnus obesus) catch rate variability. Fisheries Oceanography. 2006 Nov;15(6):477–89.

126. Brönnimann S. Impact of El Niño-Southern Oscillation on European climate. Reviews of Geophysics. 2007;45(3).

127. Mantua NJ, Hare SR. The Pacific decadal oscillation. Journal of oceanography. 2002;58(1):35–44.

128. Di Lorenzo E, Schneider N, Cobb KM, Franks PJS, Chhak K, Miller AJ, et al. North Pacific Gyre Oscillation links ocean climate and ecosystem change. Geophysical Research Letters. 2008;35(8).

129. Kavanaugh MT, Church MJ, Davis CO, Karl DM, Letelier RM, Doney SC. ALOHA from the edge: Reconciling three decades of in situ eulerian observations and geographic variability in the North Pacific subtropical Gyre. Frontiers in Marine Science. 2018;5(APR):1–14.

130. Polovina JJ, Howell E, Kobayashi DR, Seki MP. The transition zone chlorophyll front, a dynamic global feature defining migration and forage habitat for marine resources. Progress in oceanography. 2001;49(1–4):469–83.

131. Polovina JJ, Howell EA, Kobayashi DR, Seki MP. The Transition Zone Chlorophyll Front updated: Advances from a decade of research. Progress in Oceanography [Internet]. 2017;150:79–85. Available from: http://dx.doi.org/10.1016/j.pocean.2015.01.006

132. Bograd SJ, Foley DG, Schwing FB, Wilson C, Laurs RM, Polovina JJ, et al. On the seasonal and interannual migrations of the transition zone chlorophyll front. Geophysical Research Letters. 2004;31(17).

133. Wren JLK, Shaffer SA, Polovina JJ. Variations in black-footed albatross sightings in a North Pacific transitional area due to changes in fleet dynamics and oceanography 2006–2017. Deep-Sea Research Part II: Topical Studies in Oceanography [Internet]. 2019;169–170(June):104605. Available from: https://doi.org/10.1016/j.dsr2.2019.06.013

134. Verdon DC, Franks SW. Long□term behaviour of ENSO: Interactions with the PDO over the past 400 years inferred from paleoclimate records. Geophysical Research Letters. 2006;33(6).

135. Gove JM, Lecky J, Walsh WJ, Ingram RJ, Leong K, Williams I, et al. West Hawai‘i integrated ecosystem assessment ecosystem status report. 2019;46.

136. Redfern J V., Barlow J, Bailance LT, Gerrodette T, Becker EA. Absence of scale dependence in dolphin-habitat models for the eastern tropical Pacific Ocean. Marine Ecology Progress Series. 2008 Jul 15;363:1–14.

137. Forney KA, Becker EA, Foley DG, Barlow J, Oleson EM. Habitat-based models of cetacean density and distribution in the central North Pacific. Endangered Species Research. 2015;27(1):1–20.

138. Virgili A, Racine M, Authier M, Monestiez P, Ridoux V. Comparison of habitat models for scarcely detected species. Ecological Modelling. 2017 Feb 24;346:88–98.

139. Thorne LH, Foley HJ, Baird RW, Webster DL, Swaim ZT, Read AJ. Movement and foraging behavior of short-finned pilot whales in the Mid-Atlantic Bight: Importance of bathymetric features and implications for management. Marine Ecology Progress Series. 2017 Dec 7;584:245–57.

140. Azzellino A, Panigada S, Lanfredi C, Zanardelli M, Airoldi S, Notarbartolo di Sciara G. Predictive habitat models for managing marine areas: Spatial and temporal distribution of marine mammals within the Pelagos Sanctuary (Northwestern Mediterranean sea). Ocean and Coastal Management. 2012 Oct;67:63–74.

141. Tepsich P, Rosso M, Halpin PN, Moulins A. Habitat preferences of two deep-diving cetacean species in the northern Ligurian Sea. Marine Ecology Progress Series.

2014 Aug 4;508:247–60.

142. Abecassis M, Polovina J, Baird RW, Copeland A, Drazen JC, Domokos R, et al. Characterizing a foraging hotspot for short-finned pilot whales and blainville's beaked whales located off the west side of Hawai'i island by using tagging and oceanographic data. PLoS ONE. 2015 Nov 1;10(11).

143. Frasier KE, Garrison LP, Soldevilla MS, Wiggins SM, Hildebrand JA. Cetacean distribution models based on visual and passive acoustic data. Scientific reports. 2021;11(1):1–16.

144. Roberts JJ, Best BD, Mannocci L, Fujioka EI, Halpin PN, Palka DL, et al. Habitat-based cetacean density models for the US Atlantic and Gulf of Mexico. Scientific reports. 2016;6(1):1–12.

145. Fader JE, Baird RW, Bradford AL, Dunn DC, Forney KA, Read AJ. Patterns of depredation in the Hawai 'i deep□set longline fishery informed by fishery and false killer whale behavior. Ecosphere. 2021;12(8):e03682.

146. Barlow J, Gerrodette T. Predicting Cuvier's (Ziphius cavirostris) and Mesoplodon beaked whale population density from habitat characteristics in the eastern tropical Pacific Ocean [Internet]. 2006. Available from: https://www.researchgate.net/publication/284925131

147. Panigada S, Zanardelli M, MacKenzie M, Donovan C, Mélin F, Hammond PS. Modelling habitat preferences for fin whales and striped dolphins in the Pelagos Sanctuary (Western Mediterranean Sea) with physiographic and remote sensing variables. Remote Sensing of Environment. 2008 Aug 15;112(8):3400–12.

148. Carlucci R, Fanizza C, Cipriano G, Paoli C, Russo T, Vassallo P. Modeling the spatial distribution of the striped dolphin (Stenella coeruleoalba) and common bottlenose dolphin (Tursiops truncatus) in the Gulf of Taranto (Northern Ionian Sea, Central-eastern Mediterranean Sea). Ecological Indicators. 2016 Oct 1;69:707–21.

149. Andrews KR, Karczmarski L, Au WWL, Rickards SH, Vanderlip CA, Bowen BW, et al. Rolling stones and stable homes: Social structure, habitat diversity and population genetics of the Hawaiian spinner dolphin (Stenella longirostris). Molecular Ecology. 2010 Feb;19(4):732–48.

150. Aschettino JM, Baird RW, Mcsweeney DJ, Webster DL, Schorr GS, Huggins JL, et al. Population structure of melon-headed whales (Peponocephala electra) in the Hawaiian Archipelago: Evidence of multiple populations based on photo identification. Marine Mammal Science. 2012 Oct;28(4):666–89.

151. Manzano-Roth R, Henderson EE, Martin SW, Martin C, Matsuyama BM. Impacts of U.S. Navy training events on Blainville's beaked whale (Mesoplodon

densirostris) foraging dives in hawaiian waters. Aquatic Mammals. 2016;42(4):507–18.

152. Ruzicka JJ, Steele JH, Ballerini T, Gaichas SK, Ainley DG. Dividing up the pie: Whales, fish, and humans as competitors. Progress in Oceanography. 2013 Sep;116:207–19.

153. Frasier KE. A machine learning pipeline for classification of cetacean echolocation clicks in large underwater acoustic datasets. 2021;

154. Wood SN. Generalized additive models: an introduction with R. chapman and hall/CRC; 2006.

155. MuMIn BK. Multi-Model Inference. R package version 1.15. 1. 2015. 2015.

156. Akaike H. Information theory and an extension of the maximum likelihood principle. In: Selected papers of hirotugu akaike. Springer; 1998. p. 199–213.

157. Lüdecke D. ggeffects: Tidy data frames of marginal effects from regression models. Journal of Open Source Software. 2018;3(26):772.

158. Wentz FJ, Gentemann C, Smith D, Chelton D. Satellite measurements of sea surface temperature through clouds. Science. 2000;288(5467):847–50.

159. Yoshida S, Qiu B, Hacker P. Wind-generated eddy characteristics in the lee of the island of Hawaii. Journal of Geophysical Research: Oceans. 2010;115(3):1–15.

160. Courbis S, Baird RW, Cipriano F, Duffield D. Multiple populations of pantropical spotted dolphins in Hawaiian waters. Journal of Heredity. 2014;105(5):627–41.

161. Baird RW, Schorr GS, Webster DL, Mahaffy SD, McSweeney DJ, Hanson MB, et al. Open-ocean movements of a satellite-tagged Blainville's beaked whale (Mesoplodon densirostris): Evidence for an offshore population in Hawai'i? Vol. 37, Aquatic Mammals. 2011. p. 506–11.

162. Tyack PL, Johnson M, Soto NA, Sturlese A, Madsen PT. Extreme diving of beaked whales. Journal of Experimental Biology. 2006;209(21):4238–53.

163. Becker EA, Forney KA, Oleson EM, Bradford AL, Moore JE, Barlow J. Habitat-Based Density Estimates for Cetaceans within the Waters of the U.S. Exclusive Economic Zone around the Hawaiian Archipelago. 2021; Available from: https://doi.org/10.25923/x9q9-rd73

164. Kanaji Y, Okazaki M, Miyashita T. Spatial patterns of distribution, abundance, and species diversity of small odontocetes estimated using density surface modeling with line transect sampling. Deep-Sea Research Part II: Topical Studies in

Oceanography [Internet]. 2017;140:151–62. Available from: http://dx.doi.org/10.1016/j.dsr2.2016.05.014

165. Baumann□Pickering S, Trickey JS, Wiggins SM, Oleson EM. Odontocete occurrence in relation to changes in oceanography at a remote equatorial Pacific seamount. Marine Mammal Science. 2016;32(3):805–25.

166. Ramírez-León MR, García-Aguilar MC, Romo-Curiel AE, Ramírez-Mendoza Z, Fajardo-Yamamoto A, Sosa-Nishizaki O. Habitat suitability of cetaceans in the Gulf of Mexico using an ecological niche modeling approach. PeerJ. 2021;9:e10834.

167. Chavez-Rosales S, Palka DL, Garrison LP, Josephson EA. Environmental predictors of habitat suitability and occurrence of cetaceans in the western North Atlantic Ocean. Scientific Reports. 2019;9(1):1–11.

168. Ruiz-Cooley RI, Gerrodette T, Fiedler PC, Chivers SJ, Danil K, Ballance LT. Temporal variation in pelagic food chain length in response to environmental change. Science advances. 2017;3(10):e1701140.

169. Chhak K, Di Lorenzo E. Decadal variations in the California Current upwelling cells. Geophysical Research Letters. 2007;34(14).

170. Silva TL, Mooney TA, Sayigh LS, Tyack PL, Baird RW, Oswald JN. Whistle characteristics and daytime dive behavior in pantropical spotted dolphins (Stenella attenuata) in Hawai‘i measured using digital acoustic recording tags (DTAGs) . The Journal of the Acoustical Society of America. 2016 Jul;140(1):421–9.

171. West KL, Walker WA, Baird RW, White W, Levine G, Brown E, et al. Diet of pygmy sperm whales (Kogia breviceps) in the Hawaiian Archipelago. Marine Mammal Science. 2009 Oct;25(4):931–43.

172. Lehodey P, ANDRE J, Bertignac M, Hampton J, Stoens A, Menkes C, et al. Predicting skipjack tuna forage distributions in the equatorial Pacific using a coupled dynamical bio□geochemical model. Fisheries Oceanography. 1998;7(3□4):317–25.

173. Wu Y-L, Lan K-W, Tian Y. Determining the effect of multiscale climate indices on the global yellowfin tuna (Thunnus albacares) population using a time series analysis. Deep Sea Research Part II: Topical Studies in Oceanography. 2020;175:104808.

174. Baird RW, Anderson DB, Kratofil MA, Webster DL, Mahaffy SD. Cooperative conservation and long-term management of false killer whales in Hawai‘i: geospatial analyses of fisheries and satellite tag data to understand fishery interactions. 2019;

175. Díaz-Torres ER, Marín-Enríquez E, Corgos A, Olivos-Ortiz A, Ortega-Ortiz CD. Influence of environmental variability on the distribution and abundance of the pantropical spotted dolphin (Stenella attenuata) in the Mexican Central Pacific. Ciencias Marinas. 2022;

176. Diogou N, Palacios DM, Nystuen JA, Papathanassiou E, Katsanevakis S, Klinck H. Sperm whale (Physeter macrocephalus) acoustic ecology at Ocean Station PAPA in the Gulf of Alaska–Part 2: oceanographic drivers of interannual variability. Deep Sea Research Part I: Oceanographic Research Papers. 2019;150:103044.

177. Llapapasca MA, Pacheco AS, Fiedler P, Goya E, Ledesma J, Peña C, et al. Modeling the potential habitats of dusky, commons and bottlenose dolphins in the Humboldt Current System off Peru: The influence of non-El Niño vs. El Niño 1997-98 conditions and potential prey availability. Progress in Oceanography. 2018;168:169–81.